The Role of NFAT Family Transcription Factors in Diabetic Retinopathy

By

Colin Andrew Bretz

Dissertation

Submitted to the Faculty of the

Graduate School of Vanderbilt University

in partial fulfillment of the requirements

for the degree of

DOCTOR OF PHILOSOPHY

in

Cell and Developmental Biology

May 2015

Nashville, Tennessee

Approved:

Professor Chin Chiang

Professor David M Miller

Professor Douglas G McMahon

Professor John S Penn

ACKNOWLEDGEMENTS

This work was made possible through financial support from the National Institute of Health Mechanisms in Vascular Disease training grant (T32-HL07751), multiple grants from the National Eye Institute (R01-EY07533, R01-EY023639, P30-EY08126), and an unrestricted grant from Research to Prevent Blindness Inc.

Likewise, this project would not have been possible without the support and direction of my dissertation advisor Dr. John Penn, and I owe him a debt of gratitude for the opportunity and freedom to pursue my research interests over the last 5 years. I also owe a great deal of thanks to the other members of the Penn Lab, especially Sara Savage, who has been a constant collaborator and sounding board for much of this work. Additionally, I'd like to thank the members of my dissertation committee, Dr. Chin Chiang, Dr. David Miller, Dr. Douglas McMahon, and Dr. Laurie Lee who have provided advice and counsel along the way.

Lastly, I'd like to thank my parents, Debra and Vance, who have always supported me in whatever I chose to do, and without whom I would not be the person I am today.

LIST OF PAPERS

This dissertation includes work from the following manuscripts:

Bretz CA, Savage S, Suarez S, Capozzi M, Penn JS. *NFAT-isoforms play distinct roles in TNFα-induced retinal leukostasis.* In Prep

Savage S*, Bretz CA*, Penn JS. *RNA-seq reveals a role for NFAT-signaling in human retinal microvascular endothelial cells treated with TNFα*. PLOS one. 2015;10(1):e0116941. PMCID: PMC4305319
*Co-first authors

Bretz CA, Savage S, Capozzi M, Penn JS. *The role of the NFAT signaling pathway in retinal neovascularization*. Investigative Ophthalmology & Visual Science. 2013;54(10):7020-7. PMCID: PMC3809948

TABLE OF CONTENTS

Page

Appendix

LIST OF TABLES

LIST OF FIGURES

LIST OF ABBREVIATIONS

AAV ..... adeno-associated virus

AMD ..... age-related macular degeneration

ANOVA..... analysis of variance

Brdu..... bromodeoxyuridine

CAT ..... Ca^{2+}/CN-dependent translocation

CK1 ..... casein kinase 1

CN ..... calcineurin

COX..... cyclooxygenase

CX3CL1..... chemokine (C-X3-C) motif) ligand 1

CX3CR1 ..... CX3C chemokine receptor 1

CXCL10..... chemokine (C-X-C) motif) ligand 10

CXCL11..... chemokine (C-X-C) motif) ligand 11

DME ..... diabetic macular edema

DR ..... diabetic retinopathy

DYRK1 ..... dual-specificity tyrosine-(Y)-phosphorylation regulated kinase 1

ELISA ..... enzyme-linked immunosorbant assay

GSK-3..... glycogen synthase kinase 3

HBA_{1c} ..... hemoglobin A_{1c}

HRMEC ..... human retinal microvascular endothelial cells

ICAM1 ..... intercellular adhesion molecule 1

IL-6 ..... interleukin-6

INCA-6..... inhibitor of NFAT-calcineurin association-6

MCP-1 ..... monocyte chemoattractant protein 1

NCX..... Na^{+}-Ca^{2+} exchanger

NFAT ..... nuclear factor of activated T-cells

NES ..... nuclear export sequence

NLS ..... nuclear localization sequence

NPDR ..... non-proliferative retinopathy

OIR ..... oxygen-induced retinopathy

PBMC ..... peripheral blood mononuclear cells

PDR..... proliferative retinopathy

PLC ..... phospholipase C

PPFC..... parallel plate flow chamber

qRT-PCR..... quantitative reverse transcriptase-polymerase chain reaction

ROP..... retinopathy of prematurity

RNA..... ribonucleic acid

SEM..... standard error of the mean

SMOC..... second messenger-operated channels

SOC..... store-operated channels

TNFα ..... tumor necrosis factor alpha

VCAM1 ..... vascular cell adhesion molecule 1

VEGF..... vascular endothelial growth factor

VOC..... voltage-operated channels

VSMC ..... vascular smooth muscle cell

CHAPTER I

INTRODUCTION

1.1 Diabetic Retinopathy

1.1.1 Prevalence & Risk

Diabetes mellitus is a set of metabolic diseases in which the body experiences high levels of blood glucose, or hyperglycemia, for long periods of time, stemming from a defect in insulin signaling.[1] There are two primary types of diabetes, Type I is an autoimmune disease in which the body's immune response damages the pancreas and impairs its ability to produce insulin.[2] Where as in Type II diabetes, which accounts for nearly 95% of diabetic cases, the body is able to make insulin, but either makes an insufficient amount or has become resistant to the effects. Recent estimates place the total worldwide diabetic population at roughly 387 million, with approximately 38.8 million patients in North America alone.[3]

Both clinical and pre-clinical studies indicate that hyperglycemia is a causative factor in the development of microvascular complications associated with diabetes and can lead to a number of serious complications that include heart disease, stroke, kidney failure, and vision loss. In this context, the primary cause of vision loss is diabetic retinopathy (DR), which is damage to the retinal microvasculature caused by diabetes. A pooled meta-analysis compiling 35 population-based studies from around the world estimated that roughly 34.6% of diabetic patients aged 20-79 had some form of DR, and that the condition was vision threatening in 10.2% of those cases.[4] This finding applied to current estimates of the worldwide diabetic population suggests that there are roughly 13.4 million cases of DR in North America, and 133.9 million worldwide.

	Diabetic Retinopathy	Vision Threatening Retinopathy
Type of Diabetes		
Type I	77.31%	38.48%
Type 2	25.15%	6.92%
Duration of Diabetes		
< 10 years	21.09%	3.53%
10 to < 20 years	54.22%	17.78%
≥ 20 years	76.32%	40.87%
HBA1c Levels		
≤ 7.0%	17.99%	5.4%
7.1 – 8.0%	33.13%	10.82%
8.1 – 9.0%	43.1%	13.64%
> 9.0%	51.2%	18.35%

Table 1. Age standardized prevalence of DR in diabetic subjects aged 20-79 years. Vision threatening retinopathy refers to classifications of either PDR or DME. Adapted from Yau et al. 2012.

Incidence of DR in diabetic populations has been shown to correlate with a number of key factors (**Table 1**).[4] DR occurs in both Type I and Type II patients, although the prevalence of DR is significantly higher in Type I populations (77.31%) than in Type II populations (25.16%). This may in part be a result of increased duration of disease in Type I versus Type II patients as the onset of Type I typically occurs at a much younger age then Type II. In fact, duration of diabetes is the strongest risk factor for DR, with the prevalence increasing from 21.09% during the first 10 years of disease, to 54.22% in years 10 through 20, and climbing to 76.32% in cases of longer than 20 years. Blood glucose control is another major risk factor, and in clinical settings is typically evaluated by measuring hemoglobin A_{1c} (HBA_{1c}) levels. Increased HBA_{1c} levels coincide to an increased prevalence of DR, with levels of ≤7% and >9% yielding

prevalence rates of 17.99% and 51.2% respectively. Studies have shown that instituting increased blood glucose control can slow the progression of DR pathology, but does not reverse existing pathology.[5,6]

1.1.2 Clinical Classification & Treatment

Clinically DR falls into two main classifications, non-proliferative diabetic retinopathy (NPDR) and proliferative diabetic retinopathy (PDR), based on the absence or presence of retinal neovascularization. NPDR occurs early in disease progression and is initially characterized by microvascular complications such as microaneurysms and small hemorrhages.[7,8] These initial pathologic features of NPDR are not vision threatening in and of themselves, but increases in their presence and severity are predictive of disease progression.[7,9] In later more severe stages of NPDR, capillary degeneration and nonperfusion become more prominent pathologic features of the diseased vasculature, and over time lead to localized retinal ischemia.[10] Retinal ischemia results in tissue hypoxia that, while not measured or evaluated clinically, is believed to drive the retinal neovascularization that defines PDR. The newly formed blood vessels that comprise neovascular tufts found in PDR are leaky and fragile and can easily rupture leading to vitreous hemorrhages and sudden vision loss.[10,11] In addition, if left untreated these aberrant vessels can intertwine with the vitreous collagen fibers and detach the retina resulting in severe, and often irreversible, vision loss.[11]

While retinal neovascularization and detachment are serious vision threatening complications of DR, the most common cause of vision loss in diabetic patients is diabetic macular edema (DME). DME can occur in both NPDR and PDR, and is a result of blood retinal barrier (BRB) breakdown and fluid leaking out of the compromised

vasculature into the macula, the area of the retina responsible for high acuity vision, causing it to swell and blurring vision.[10,12]

A number of therapeutic treatments for addressing DR pathology have been developed, of which retinal photocoagulation was for many years the gold standard. In this procedure a focused laser is used to energize and denature cellular proteins resulting in localized necrosis and tissue coagulation. In cases of DME, laser treatment is applied around the macula and typically focuses on sites of retinal hemorrhaging and vascular damage, preventing further leakage and allowing the eye to clear built up fluid. Focal laser treatment can also be used in cases of NPDR and PDR to cauterize specific sites of vascular leakage and neovascularization before the occurrence of DME. In cases of early and developing PDR, pan-retinal photocoagulation can be used to ablate large portions of the peripheral retina, which serves the dual purpose of both reducing tissue hypoxia by killing off oxygen utilizing neurons and killing the glial cells that produce pro-angiogenic growth factors in response to tissue hypoxia.[13] Unfortunately, this form of treatment also results in reduced peripheral and night vision, which has lead to the development of therapies that target specific inflammatory cytokines and growth factors known to contribute to DR pathology.[14]

Targeting retinal inflammation and inflammatory cytokines in diabetes extends back as early as 1964, when it was reported that diabetic patients taking anti-inflammatory medication for rheumatoid arthritis had a lower than expected incidence of DR.[15] More recently, nonsteroidal anti-inflammatory drugs such as aspirin and other cyclooxygenase (COX) inhibitors have been investigated as potential treatments. So far, high doses of aspirin (900mg/day) have been shown to minimize the development of

retinal microaneurysms in patients with early NPDR, and topical administration of COX-2 inhibitors have been shown to have a similar benefit, while avoiding the deleterious effects of systemic COX-2 inhibition.[16-18] Several therapies targeting the pro-inflammatory cytokine tumor necrosis factor alpha (TNFα) are also currently being evaluated for the treatment of DR, with early trials of the monoclonal antibody Infliximab (Remicade®) proving efficacious in the treatment of DME.[19-21]

To date, the most successful therapy for the treatment of DR pathology has been a class of vascular endothelial growth factor (VEGF) antagonists, which includes pegaptanib (Macugen®, Pfizer), bevacizumab (Avastin®, Genentech), and ranibizumab (Lucentis®, Genentech). Originally developed to address neovascular pathology associated with age-related macular degeneration (AMD), these compounds have proven efficacious in treating both pathologic retinal edema and neovascularization, and become established clinical treatments for DME and PDR.[22-27] VEGF plays a prominent role in retinal neovascular pathology, and as such anti-VEGF therapies have proven particularly efficacious in the treatment of PDR. However, studies in patients with DME have shown that nearly 50% present with persistent retinal edema even after multiple treatments.[28] Add to this, concerns that chronic administration of anti-VEGF therapies may cause adverse effects in the neural retina, and there is a clear need for additional therapeutic options to address DR pathology.[29,30]

1.1.3 Retinal Inflammation & Resulting Pathology

The temporal and spatial relationships between retinal inflammation and the onset of microvascular complications is tightly correlated and this underlies subsequent pathology.[31-34] Inflammation is the body's defense against pathogens, and a critical step

in the response to tissue damage. Although there are no pathogens associated with DR, hyperglycemia has been linked with increased formation of advanced glycation end products, overproduction of reactive oxygen species, and accumulation of polyols, all of which are known to increase the production of inflammatory cytokines.[35-38] TNFα, chemokine (C-X-C) motif) ligand 10 (CXCL10), chemokine (C-X-C) motif) ligand 11 (CXCL11), Interleukin-6 (IL-6), monocyte chemoattractant protein 1 (MCP-1), and VEGF are just some of a host of cytokines found to be increased in vitreous samples taken from DR patients, and increased levels of TNFα, IL-6, and VEGF have been shown to correlate with increased progression and severity of DR.[39-46] Together, these cytokines activate a number of signaling pathways that contribute to DR related pathologies.[47,48]

The earliest and most direct way in which inflammatory cytokines drive DR pathology is through modulation of the BRB. As it does in the brain, the BRB tightly regulates the flow of fluids and solutes between the vasculature and surrounding retinal tissues, and BRB breakdown results in the increased vascular permeability endemic to DR pathology. Upregulated inflammatory cytokines including TNFα, IL-6, and VEGF have all been identified as factors capable of inducing changes in the tight junctions that regulate BRB resistance and directly increase vascular permeability.[12,49-52]

Another important aspect of the inflammatory response is the recruitment of leukocytes to infected and damaged tissue. Increased numbers of leukocytes have been observed in both the retinal and choroidal vessels of diabetic patients and monkeys.[53-55] There is also a sustained increase in the number and adherence of retinal leukocytes in rodent models of diabetes that is correlated with the progression of pathology such as BRB breakdown and endothelial cell death.[56] The adhesion of

leukocytes or other myeloid derived cells to the vascular endothelium is termed leukostasis, and this interaction is facilitated by a number of inflammatory cytokines and adhesion molecules.

During leukostasis, adhesion molecules expressed by vascular endothelial cells interact with ligands expressed on the surface of circulating leukocytes in a well-defined process that includes tethering, adhesion, and transmigration (**Figure 1**). The various steps of this leukocyte recruitment cascade are mediated by different sets of adhesion molecules. The selectin family of adhesion molecules, P-selectin and E-selectin, mediate the initial contact and tethering of circulating leukocytes to the vascular endothelium through binding to sialyl-Lewis X ligands on the leukocyte cell surface.[57-60] After the selectins initiate contact with the leukocytes, immunoglobulin superfamily molecules such as intercellular adhesion molecule 1 (ICAM1) and vascular cell adhesion molecule 1 (VCAM1) are involved in reducing the rolling velocity of captured leukocytes and firmly adhering them to the endothelium.[60-62] Endothelial ICAM1 and VCAM1 interact with integrins such as LFA-1, Mac-1, and VLA-4 expressed by leukocytes in order to facilitate this adhesion.[62] Chemokine (C-X3-C motif) ligand 1 (CX3CL1), which is also known as fractalkine, is a membrane bound chemokine that participates in the firm adhesion of leukocytes by binding to the CX3CR1 receptor on the leukocyte cell surface, and also contributes to the next phase of the cascade by stimulating leukocyte transmigration.[63-66] During transmigration, activated leukocytes can extravasate into the surrounding tissue along cell-cell junctions. This process is facilitated by adhesion molecules such as platelet endothelial cell adhesion molecule 1 (PECAM1) and vascular adhesion protein 1 (VAP1).[60,67]

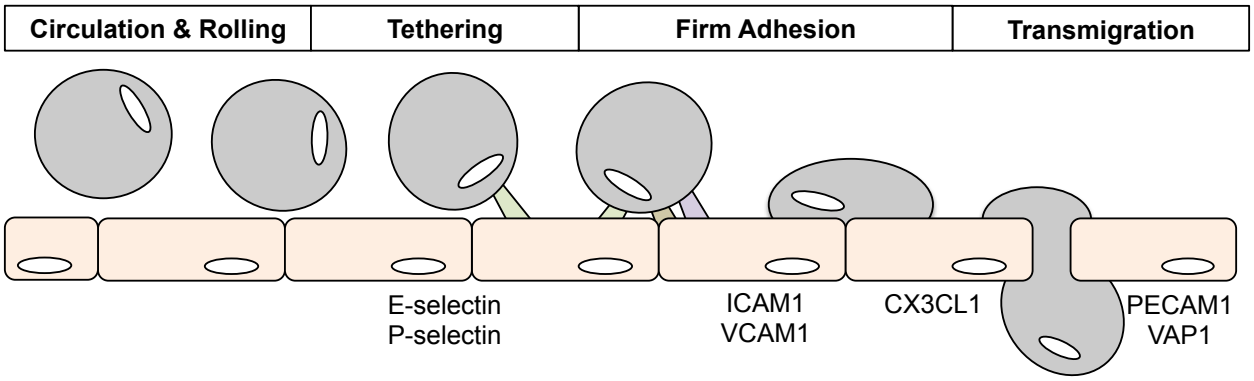

Figure 1. Leukocyte capture and adhesion to the vascular endothelium. Selectin family adhesion molecules E-selectin and P-selectin are involved in the initial association of circulating leukocytes with the luminal surface of EC. Once they begin to associate with the EC surface, ICAM1 and VCAM1 further slow the movement of leukocytes and firmly adhere them to the endothelial surface. CX3CL1 contributes to firm adhesion of the captured leukocytes and helps stimulate transmigration. This extravasation through cell-cell junctions is mediated by PECAM1 and VAP1.

Many of the cell adhesion molecules involved in leukostasis have been implicated in the progression of DR pathology, either through increased expression or increased levels of the cleaved protein in serum and vitreous samples. For instance, cleaved E-selectin levels were increased in serum from diabetic patients, and increased vitreous levels were seen in patients with PDR, suggesting that increased E-selectin correlates with DR progression.[68-71] ICAM1 is the adhesion molecule most closely tied to DR pathology, as it is known to be highly expressed in retinal blood vessels of diabetic patients, and its expression correlates with increased leukocytes in the retinas of these patients.[69-72] Furthermore, inhibition of ICAM1 in animal models of DR attenuates not only retinal leukostasis but also subsequent endothelial cell death and vascular leakage.[56,73] Similarly, VCAM1 is also upregulated in retinal vessels of diabetic animals while inhibition of the VCAM1 and VLA-4 interaction has been shown to reduce leukocyte adhesion, vascular leakage, and inflammatory cytokine production.[74] This combined with increased levels of soluble VCAM1 in patients with DR suggests a clear contribution of VCAM1 to DR pathology.[68-71] CX3CL1 is also known to be increased in

the vitreous of patients with PDR, and in addition to its function as an adhesion protein, the cleaved form is known to serve as a leukocyte chemoattractant.[75-77]

Increased expression and production of a number of inflammatory cytokines and leukocyte chemoattractants is another feature of retinal inflammation that contributes to retinal leukostasis and other microvascular complications.[34,48,78] TNFα and VEGF are two such inflammatory cytokines that are found to be elevated early on in the pathogenesis of DR, and correlate with increased progression of pathology.[42,44-47] In addition to their influence on vascular permeability, both cytokines have been shown to induce adhesion protein expression in vascular endothelial cells as well as induce production of chemokines such as CXCL10, CXCL11, and MCP-1.[52] These chemokines, in addition to being found increased in vitreous of patients with DR, have well defined roles as leukocyte chemoattractants.[79-84]

The increased retinal leukostasis that results from activation of the leukocyte recruitment cascade is an important pathogenic feature of DR and can contribute to pathology associated with NPDR, PDR, and DME.[48,78,85] This contribution is typically attributed to either tissue inflammation or retinal capillary occlusion (**Figure 2**). In the context of tissue inflammation, leukocytes are recruited and adhere to sites of initial inflammation and vascular damage. Once there, the leukocytes induce further inflammation and vascular damage by secreting inflammatory cytokines, growth factors and proteases that result in endothelial cell damage, increased vascular permeability, and recruitment of more leukocytes.[56,73,85] This activity becomes a perpetuating cycle of tissue inflammation and vascular damage that eventually leads to more significant vascular complications such as BRB breakdown, microaneurysms, and ultimately retinal

edema. Another way that retinal leukostasis contributes to the progression of DR pathology is through capillary occlusion, in which adherent leukocytes block or impede blood flow in smaller capillaries leading to tissue ischemia, endothelial cell death, and the development of acellular capillaries downstream.[78] The loss of healthy and patent blood vessels to a given area results in focal ischemia and tissue hypoxia which give rise to retinal neovascularization through well-established mechanisms.

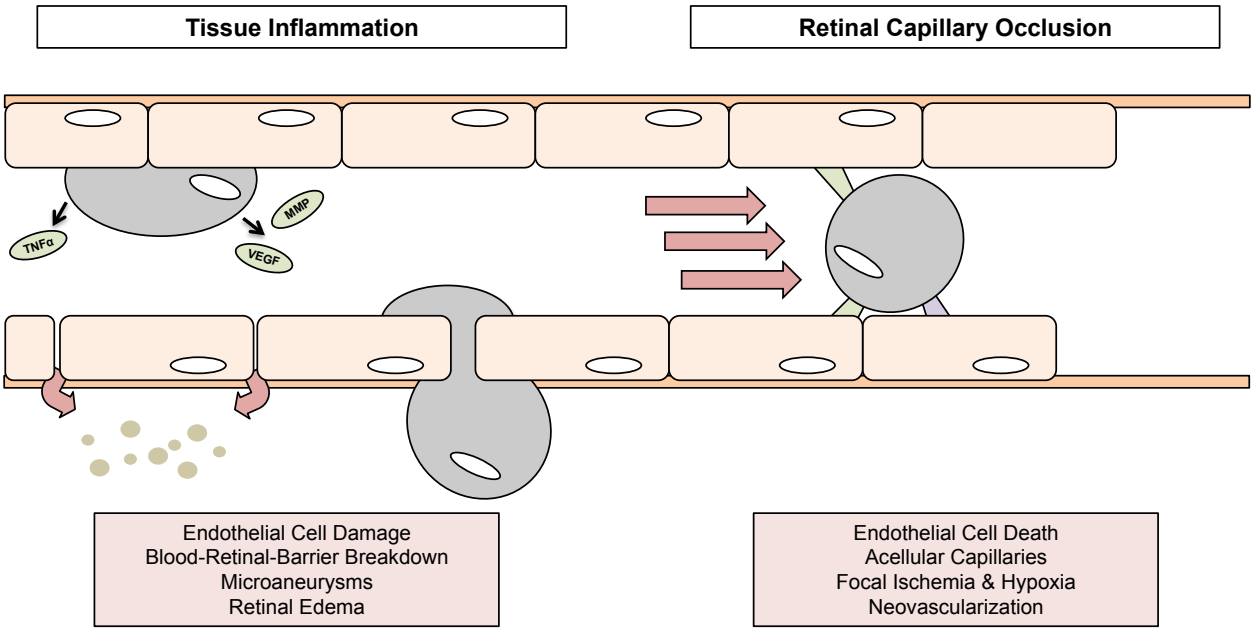

Figure 2. Contributions of leukostasis to DR pathology. Leukostasis can help drive DR pathology through either increased tissue inflammation or retinal capillary occlusion. Adherent and extravasated leukocytes secrete a number of inflammatory cytokines and proteases that act on nearby endothelium to induce endothelial cell damage, BRB breakdown, microaneurysms, and retinal edema, compounding the inflammation that originally induced leukostasis. In addition, adherent leukocytes can block or disrupt blood flow in smaller capillaries, leading to acellular capillaries, focal ischemia, increased growth factor production, and ultimately neovascularization downstream of the obstruction.

Neovascularization is the defining pathology associated with PDR and is a common pathologic feature of other retinal diseases such as retinopathy of prematurity (ROP) and AMD. In all of these, neovascularization represents a common outcome from multifaceted and disparate processes, but is broadly the result of ischemia and resulting tissue hypoxia. In response to retinal hypoxia, numerous growth factors are produced which stimulate angiogenesis in the surrounding tissue, though VEGF is commonly

accepted as the most critical regulator in this context.[86,87] In addition to its effects as a pro-inflammatory cytokine, VEGF is also a powerful driver of angiogenesis and stimulates pro-angiogenic cell activities such as proliferation, migration, and tube formation. Retinal hypoxia, which occurs in DR as a result of focal ischemia due to reduced vascular function or capillary occlusion, is known to regulate VEGF on multiple levels including transcription, mRNA stability, translation, and secretion, and increased VEGF levels have been tied to the transition between NPDR and PDR.[88,89]

1.2 Nuclear Factor of Activated T-cells

1.2.1 NFAT Family Transcription Factors

The nuclear factor of activated T-cells (NFAT) family of transcription factors are a set of five proteins grouped together for their similarity to Rel/NF-kB family transcription factors.[90] Four of the protein isoforms are regulated by the serine phosphatase calcineurin (CN) and as such are denoted as NFATc1, NFATc2, NFATc3, and NFATc4.[91] The fifth isoform, NFAT5 (also known as TonEBP), is involved in regulating cellular tonicity, and although it shares a conserved DNA-binding domain with other NFAT isoforms, it lacks the CN-binding domain essential for activation of NFATc1-4.[91,92] CN activation of NFATc1-4 is regulated by the phosphorylation status of a conserved Ca^{2+}/CN-dependent translocation (CAT) domain, consisting of a 300 amino acid region located at the N-terminal of the DNA binding domain, and encoded by a single exon in all four proteins (**Figure 3**).[93,94] In a static state, the CAT-domain is heavily phosphorylated, but activated CN dephosphorylates this domain to reveal a nuclear localization sequence (NLS) that leads to increased nuclear accumulation and increased affinity of NFAT for target DNA sites.[95,96] CN binding to and dephosphorylation

of NFAT further serves to mask a nuclear export sequence (NES) within the CAT domain that helps direct NFAT back to the cytosol when revealed.[96]

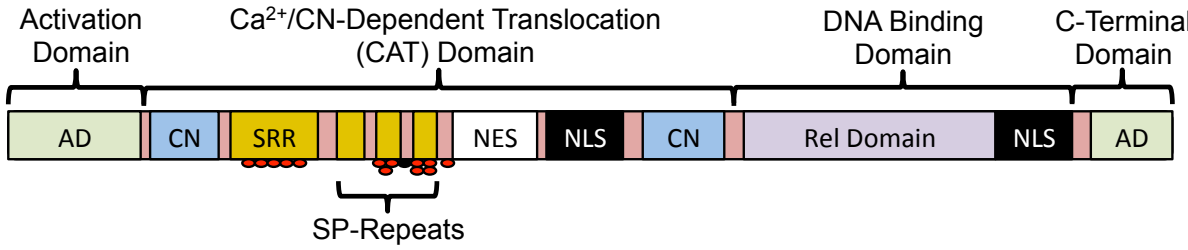

Figure 3. Conserved domains present in all CN-dependent NFAT proteins. The CAT domain is conserved between all NFAT forms. Red dots represent sites of phosphorylation altered by CN activity.

1.2.2 NFAT signaling Pathway

The canonical NFAT signaling pathway is triggered by an initial rise in intracellular Ca^{2+} levels from either extracellular sources or intracellular stores (**Figure 4**). Increased Ca^{2+} is bound by both calmodulin and CN which then complex to activate CN. Once active, CN binds NFAT proteins via a discrete NFAT-specific binding site, dephosphorylating the transcription factor and causing it to translocate to the nucleus.[96,97] Once in the nucleus, NFAT dimerizes with a variety of DNA binding partners to regulate target gene transcription.[96] NFAT kinases eventually rephosphorylate the NFAT proteins leading to their export from the nucleus.[97]

There are a number of well-established ways for Ca^{2+} to enter the cell, and common mechanisms of cell entry include ion channels such as voltage-operated channels (VOC), second messenger-operated channels (SMOC), and store-operated channels (SOC), as well as the Na^{+}-Ca^{2+} exchanger (NCX).[98,99] In addition to these mechanisms, G-protein-coupled receptor and tyrosine kinase receptor signaling can stimulate NFAT activity through second messenger activation of $InsP_3$ which binds to $InsP_3$ receptors on the endoplasmic reticulum causing Ca^{2+} dumping and increased cytosolic Ca^{2+}.[100,101] NFAT signaling has been shown to be exquisitely sensitive to both

the mode of entry and the localization of the resulting Ca^{2+}. For instance, in immune cells SOC mediate Ca^{2+} entry into the cell and a sustained low amplitude increase in Ca^{2+} is important for effective NFAT activation, however in neuronal cell populations VOC play a more prominent role in Ca^{2+} entry and the transient spikes in ion concentration are sufficient for NFAT activation.[98,99] Calcium release from intracellular stores, and mediated by G-protein-coupled receptor and tyrosine kinase receptor signaling is an inducer of NFAT activity in both vascular smooth muscle cells (VSMC) and endothelial cells.[100,102-106]

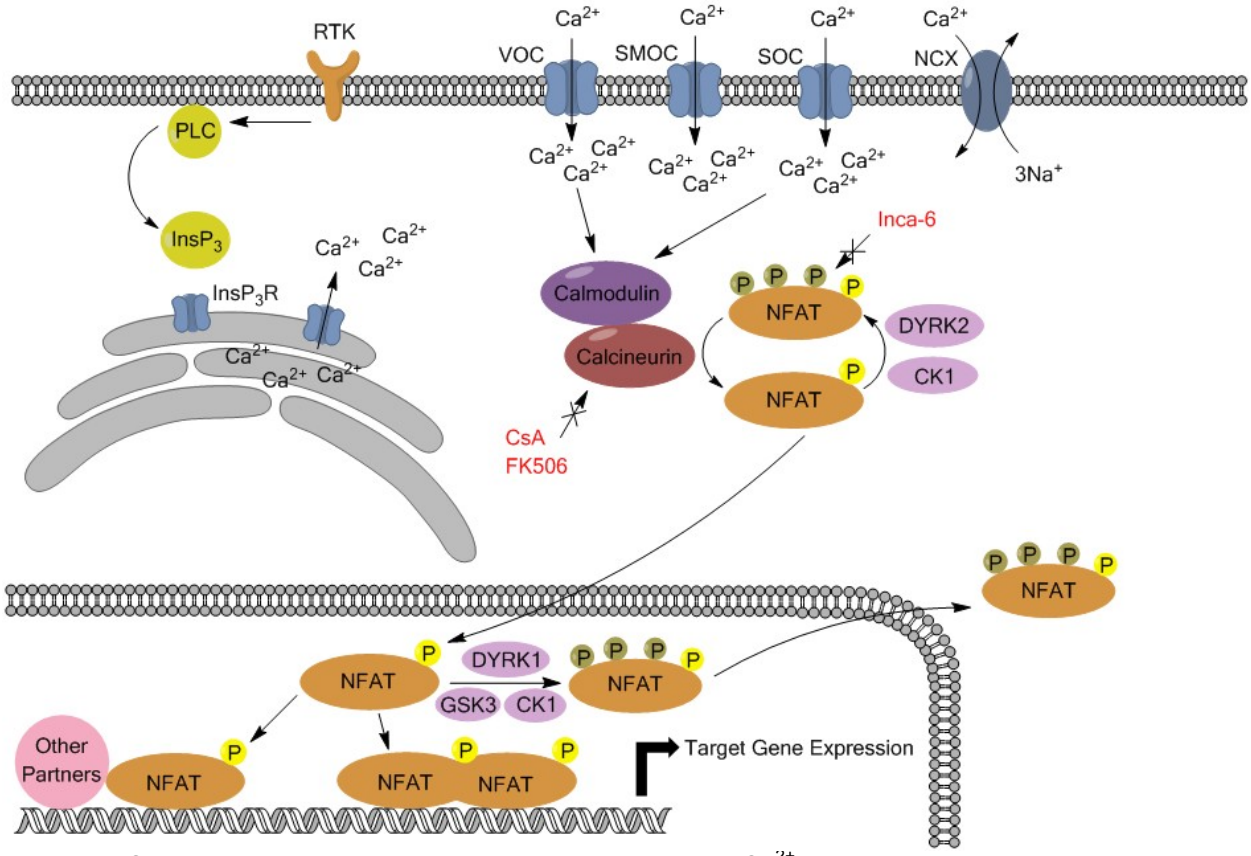

Figure 4. Canonical NFAT signaling pathway. Intracellular Ca^{2+} levels rise in the cell, either by import through various ion channels or as a result of dumping from intracellular stores, and activate the calmodulin/CN enzyme complex. CN dephosphorylates and activates NFAT transcription factors, which then translocate to the nucleus, where they can cooperate with multiple transcriptional partners to regulate gene expression. NFAT proteins are rephosphorylated by NFAT kinases and exported from the nucleus. This pathway can be pharmacologically inhibited using the CN inhibitors CsA and FK-506 and the NFAT-specific inhibitor INCA-6.

Increased cytosolic Ca^{2+} is bound by the calcium-dependent protein calmodulin, which undergoes a conformational change that enables it to complex with CN and form a calcium-regulated enzyme complex.[96,107] CN is itself also a heterodimer of two CN subunits, a catalytic phosphatase subunit (CNa) and a regulatory subunit (CNb), and bound Ca^{2+} is critical for proper activation of both.[96,108] CN complexes with phosphorylated NFAT proteins pre and post Ca^{2+} activation, which is believed to account for the rapid speed of NFAT dephosphorylation and translocation in response to Ca^{2+} flux.[108,109] Efficient dephosphorylation of NFAT has been shown to require a direct docking interaction with CN, and the protein is quickly rephosphorylated by NFAT kinases in the nucleus when this interaction is disrupted.[96] As a result, pharmacologic disruption of the CN/NFAT signaling pathway, can be achieved using the small molecule inhibitors Tacrolimus (FK-506) and inhibitor of NFAT-calcineurin association-6 (INCA-6). FK-506 is an FDA-approved and widely used small molecule immuno-modulator that complexes with immunophilin FKBP12 to bind CN and block its activation by Ca^{2+}/calmodulin, where as INCA-6 is a small organic molecule that competitively binds to the discrete NFAT-binding site on CN, effectively blocking NFATc1-c4 without disrupting additional CN phosphatase activities.[110-115]

Once in the nucleus, NFAT proteins can elicit target gene expression through a number of different interactions. Depending on the context, NFAT isoforms can act as homodimers, heterodimers, or can complex with other transcription factors to induce target gene expression. Identified NFAT binding partners include AP-1 in immune cells, GATA4 in cardiac muscle cells, MEF2 in skeletal muscle cells, and NF-κB in cardiomyocytes.[116-119] NFAT kinases such as glycogen synthase kinase 3 (GSK-3), dual-

specificity tyrosine-(Y)-phosphorylation regulated kinase 1 (DYRK1), and casein kinase 1 (CK1), also interact with NFAT in the nucleus, phosphorylating the protein and promoting its export to the cytosol.[97,109,120,121]

1.2.3 NFAT in Ocular Disease

NFAT was first identified in immune cells as an inducer of early T-lymphocyte activation genes.[122] Subsequently its role has been well defined in the context of immune cell signaling and differentiation, and there is also considerable literature on the role of NFAT in the vasculature, with critical roles identified in vasculogenesis, valve development, and hypertrophy.[91,93,123-126]

Comparatively, the role of NFAT in ocular disease is considerably less well defined, though CN/NFAT signaling is already an established therapeutic target in this context. The CN-inhibitor FK-506 (also known as Tacrolimus and marketed as Prograf® and Advagraf®) is used both as an immunosuppressant to prevent tissue rejection in corneal transplants, and as a therapy for patients with severe refractory uveitis.[127-130] These current applications relate more to the role of NFAT in immune cell signaling and activation, then to any ocular tissue specific feature of NFAT signaling. Recently though, studies have identified roles for NFAT related to both retinal ganglion cell apoptosis in retinal degeneration and myocilin expression in glaucoma, and there is growing evidence that NFAT may be a valuable therapeutic target for the treatment of DR.[131-134]

Hyperglycemia is a critical feature leading to the microvascular complications of DR pathology, and has been tied to NFAT signaling in other tissues. In VSMC, elevated glucose stimulates increased production of extracellular nucleotides, which signal through GPCR to induce Ca^{2+} flux and stimulate NFAT translocation.[104] Ca^{2+} entering

the cell through the SOC channel, TRPC1, also activates NFAT transcription in VSMC, and high glucose has been shown to increase expression of TRPC1 expression in bovine aortic endothelial cells.[135] Glucose is also known to induce NFAT-dependent gene transcription in pancreatic β cells, as well as inhibit the expression of nuclear kinase GSK-3.[104,136] Thus, hyperglycemia may set the stage for unrestricted NFAT transcriptional activity, both by increasing NFAT activation and reducing its deactivation.

NFAT activation has also been tied to inflammatory cytokines critical to DR pathology and progression, particularly TNFα and VEGF. TNFα is known to activate NFAT signaling in macrophages, as well as induce intracellular calcium flux in endothelial cells through receptor signaling and phospholipase C (PLC).[137-139] VEGF also induces intracellular Ca^{2+} flux through receptor activation of PLC and serves as an additional driver of NFAT-dependent transcription.[105,106,140-143] Notably, VEGF stimulates NFAT translocation in human pulmonary valve endothelial cells, intestinal microvascular endothelial cells, and HUVEC.[140,144,145] NFAT-dependent gene transcription has been shown to occur in endothelial cells, and identified NFAT gene targets include *GM-CSF, TF, SELE, IL6, VCAM1, ICAM1, CCL2,* and *CXCL2*.[141,142,146-153] This group of genes regulates tissue inflammation and related processes that may drive the progression of retinopathy.[103,140,152,154-158]

CHAPTER II

The Effects of Pharmacologic NFAT inhibition on TNFα-Treated Human Retinal Microvascular Endothelial Cells

2.1 Overview

TNFα has been identified as playing an important role in pathologic complications associated with diabetic retinopathy, such as retinal inflammation and leukostasis. However, the transcriptional effects of TNFα on retinal microvascular endothelial cells and the different signaling pathways involved are not yet fully understood. In the present study, RNA-seq was used to initially profile the transcriptome of human retinal microvascular endothelial cells (HRMEC) treated with TNFα in the presence or absence of the NFAT-specific inhibitor INCA-6, in order to gain insight into the effects of TNFα on HRMEC and identify any involvement of NFAT signaling.

Differential expression and pathway analyses revealed that TNFα treatment significantly upregulated the expression of transcripts associated with cytokine-cytokine receptor interactions, cell adhesion molecules, and leukocyte transendothelial migration. Additional analysis comparing TNFα-treated samples to those co-treated with INCA-6, highlighted a small subset of transcripts whose expression were significantly reduced by NFAT inhibition, and more then half of which encode for proteins involved in leukocyte recruitment and adhesion.

Based on these initial findings, the functional effects of pharmacologic NFAT inhibition were further evaluated *in vitro* using a parallel plate flow chamber (PPFC) assay, as well as *in vivo* using a mouse model of retinal leukostasis. In both cases, NFAT blockade reduced TNFα-induced cell adhesion to retinal endothelial cells, highlighting a functional role for NFAT signaling in TNFα-induced retinal leukostasis.

2.2 Results

2.2.1 RNA-seq analysis of TNFα treatment and pharmacologic NFAT inhibition in HRMEC

RNA-seq quality, alignment, and differential expression

In order to profile the transcriptional effects of TNFα in HRMEC, and determine what role NFAT signaling might play in this context, we conducted an RNA-seq using HRMEC treated with vehicle, TNFα (1ng/ml) plus vehicle, or TNFα plus INCA-6 (1μM). Each treatment group contained 3 independent samples, and there was no statistical difference between the number of sequence reads in each group (p=0.21). Total reads among the 9 samples varied between 24,038,972 and 35,171,982 over a total of 33,240 unique transcripts, and between 2,119 and 5,365 reads were removed from each sample due to low quality. The remaining reads from each sample were mapped using TopHat to align the transcripts, and roughly 97% of the transcripts mapped to the UCSC human genome hg19. This data is summarized in **Table 2**.

	Control				**TNFα**				**TNFα + INCA-6**			
	1	2	3	Avg	1	2	3	Avg	1	2	3	Avg
Total Reads (m)	36.4	39.0	33.0	36.2	43.0	34.3	38.4	38.6	29.0	36.9	29.5	31.8
Reads Removed	2328	5365	2161	3285	3089	2701	3006	2932	2085	2724	2119	2309
% Mapped	96.1	97.8	96.0	97.0	96.6	98.1	97.1	97.0	97.9	97.9	97.9	98.0

Table 2. Summary of reads mapping to the human genome. Analysis was done using TopHat v2.0.9

After alignment, differential expression was determined using three different algorithms: DESeq, edgeR, and baySeq. Comparisons were made between the TNFα-treated and control samples, and the TNFα-treated and TNFα plus INCA-6 treated samples, and the differentially expressed transcript lists were restricted to those considered significantly changed (false discovery rate (FDR) <0.05) by all three

algorithms. Compared to control, TNFα treatment changed the expression of 744 transcripts, of which 579 were upregulated, and over 50% of those were upregulated by more than 2-fold (**Figure 5**). Comparison of the TNFα plus INCA-6 and TNFα-treated samples revealed only 18 genes that were differentially expressed. A summary of this data is provided in **Table 3.**

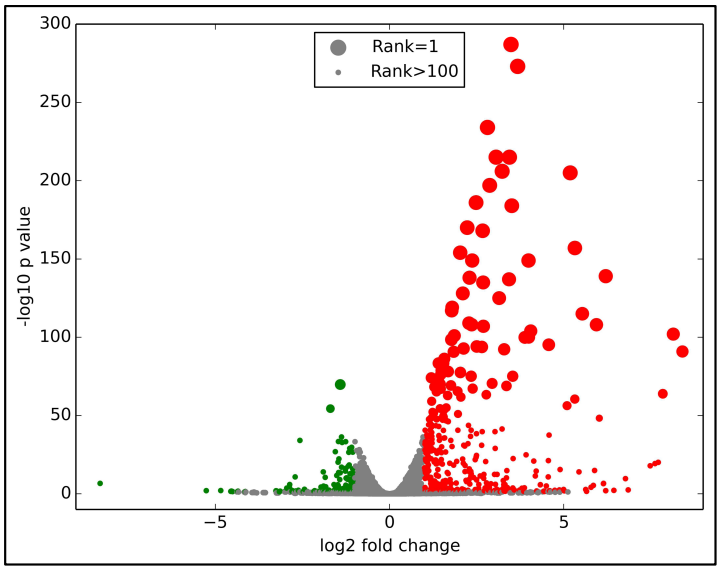

Figure 5. Volcano plot of transcripts induced by TNFα. Red circles indicate upregulated genes while green circles indicate downregulated genes. Circle size indicates gene rank using MultiRankSeq.

	Transcripts with FDR < 0.05	Upregulated Transcripts	Downregulated Transcripts
TNFα vs Control	744	579	165
TNFα + INCA-6 vs TNFα	18	5	13

Table 3. Summary of RNA-seq differential expression analysis.

The effect of TNFα treatment on HRMEC gene expression

The top 10 transcripts upregulated and downregulated by TNFα treatment of HRMEC are summarized in **Table 4**. The products of several of these genes have well characterized roles in leukostasis. Notably *VCAM1*, *ICAM1*, *and CXCL10*, genes known for their roles in vascular adhesion, were three of the highest expressed genes in the

TNFα-treated samples, and the gene with the lowest expression was *KCNK2*, a potassium channel that negatively regulates leukocyte transmigration.[159]

Ensembl Gene ID	Gene Symbol	Log2 Fold Change	p-Value	FDR
Upregulated Transcripts				
ENSG00000162692	VCAM1	9.052	<0.00001	<0.00001
ENSG00000169245	CXCL10	8.405	1.83E-94	1.17E-91
ENSG00000049249	TNFRSF9	8.143	1.04E-105	8.28E-103
ENSG00000237988	OR2I1P	7.842	3.18E-67	1.37E-64
ENSG00000173391	OLR1	7.711	5.57E-23	7.71E-21
ENSG00000213886	UBD	7.619	3.41E-22	4.51E-20
ENSG00000267607	CTD-2369P2.8	7.481	1.05E-20	1.30E-18
ENSG00000023445	BIRC3	7.101	<0.00001	<0.00001
ENSG00000235947	EGOT	6.770	2.96E-12	2.03E-10
ENSG00000090339	ICAM1	6.670	<0.00001	<0.00001
Downregulated Transcripts				
ENSG00000250961	CTD-2023N9.1	-1.848	3.59E-06	0.000115
ENSG00000107562	CXCL12	-1.894	3.26E-07	1.26E-05
ENSG00000171227	TMEM37	-1.902	1.14E-16	1.12E-14
ENSG00000226808	LINC00840	-1.966	1.36E-06	4.79E-05
ENSG00000164089	ETNPPL	-2.442	5.27E-05	0.001298
ENSG00000003137	CYP26B1	-2.572	3.28E-37	7.89E-35
ENSG00000162009	SSTR5	-2.709	2.12E-13	1.63E-11
ENSG00000187513	GJA4	-2.865	2.62E-08	1.21E-06
ENSG00000232259	RP11-4C20.3	-2.868	5.51E-06	0.000172
ENSG00000082482	KCNK2	-2.950	7.59E-06	0.00023

Table 4. Top 10 upregulated and downregulated transcripts by TNFα in HRMEC. Fold changes and p-values reported were calculated by the edgeR algorithm.

In order to further characterize the differentially expressed genes, pathway analysis was conducted using the database for annotation, visualization and integrated

discovery (DAVID) annotation tool and the Kyoto Encyclopedia of Genes and Genomes (KEGG) database, to identify pathways which were significantly enriched ($p<0.05$). According to the KEGG database, 19 pathways were enriched by TNFα-treatment, several of which are related to retinal inflammation and leukostasis, including cytokine-cytokine receptor interaction (44 transcripts), chemokine signaling (27 transcripts), cell adhesion molecules (19 transcripts), and leukocyte transendothelial migration (13 transcripts; **Figure 6**).

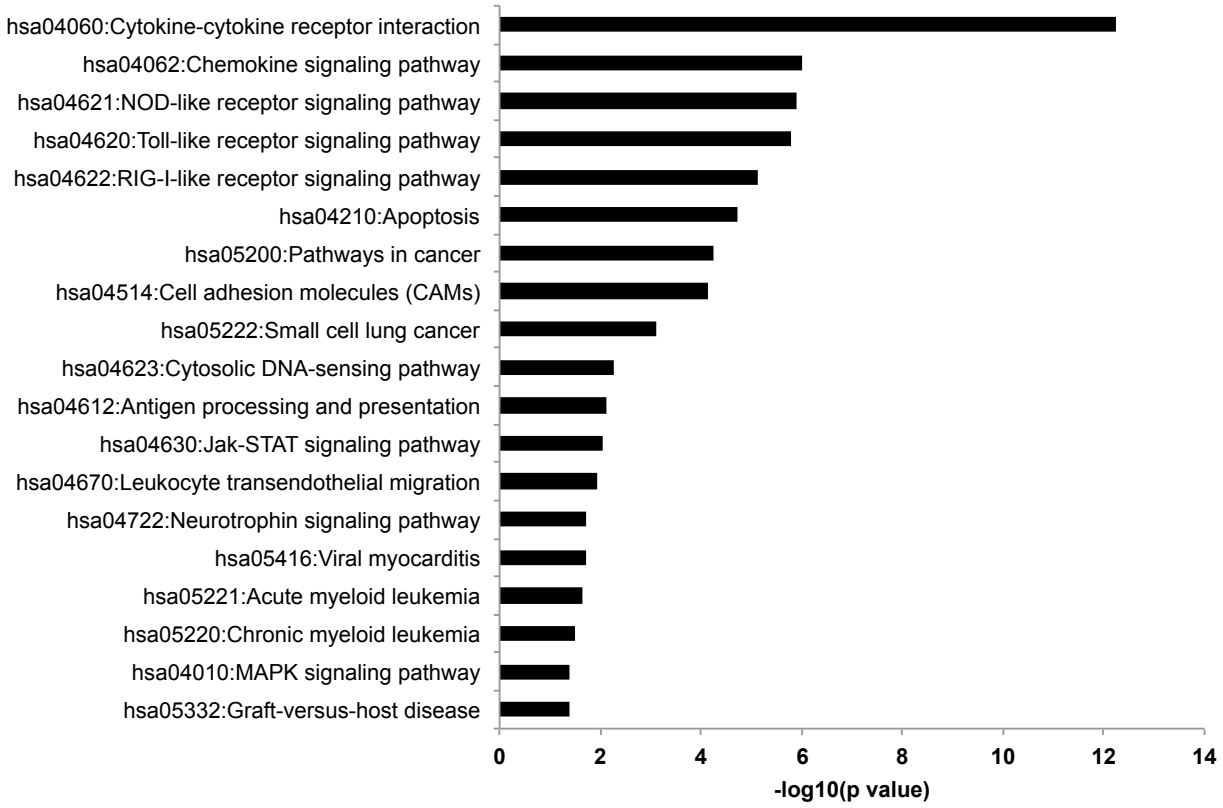

Figure 6. KEGG pathway enrichment in TNFα-treated HRMEC. Pathway enrichment was determined using DAVID and a $p<0.05$.

The effect of INCA-6 on TNFα-treated HRMEC

As previously mentioned, co-treatment with INCA-6 changed the expression of 18 genes compared to HRMEC treated with TNFα alone. Of those 18 genes, 13 were

also differentially expressed in TNFα-treated cells compared to control. INCA-6 exacerbated the effects of TNFα on three of these genes (*FRY*, *TNIP3*, *SQSTM1*), and INCA-6 counteracted the TNFα-induced expression of the other 10 genes (**Table 5**).

Ensembl Gene ID	Gene Symbol	Log2 Fold Change Control vs TNFα	Log2 Fold Change TNFα vs INCA-6	p-Value	FDR
ENSG00000006210	CX3CL1	6.438	-1.177	1.64E-19	7.43E-16
ENSG00000169245	CXCL10	8.405	-0.983	2.95E-09	4.26E-06
ENSG00000169248	CXCL11	3.988	-0.765	3.10E-14	1.09E-10
ENSG00000227507	LTB	4.569	-0.732	1.65E-07	0.000145
ENSG00000102934	PLLP	1.757	-0.716	8.91E-09	1.01E-05
ENSG00000162692	VCAM1	9.052	-0.624	4.59E-22	2.43E-18
ENSG00000121858	TNFSF10	1.627	-0.616	4.93E-11	1.20E-07
ENSG00000146374	RSPO3	1.144	-0.597	5.70E-11	1.29E-07
ENSG00000188015	S100A3	4.052	-0.581	8.14E-07	0.000549
ENSG00000143387	CTSK	1.681	-0.548	8.57E-08	7.99E-05

Table 5. Genes that were significantly upregulated by TNFα and downregulated by INCA-6. Fold changes and p-values reported were calculated by the edgeR algorithm.

Figure 7. KEGG pathways enrichment in INCA-6 treated HRMEC. Pathway enrichment was determined using DAVID and a $p<0.05$.

Notably, four of the genes significantly inhibited by INCA-6 treatment, *CX3CL1*, *CXCL10*, *CXCL11*, and *VCAM1* have established roles in the recruitment and adhesion of leukocytes to vascular endothelium, suggesting that NFAT signaling plays a role in TNFα-induced leukostasis. This assertion is further supported by KEGG pathway enrichment analysis, which identified involvement of the INCA-6 inhibited genes in both cytokine-cytokine receptor interaction (5 transcripts) and chemokine signaling pathways (3 transcripts; **Figure 7**).

qRT- PCR validation of RNA-seq

In order to confirm the RNA-seq findings, five different genes were validated by performing qRT-PCR on the sequenced samples as well as samples from a second biologically independent experiment (**Figure 8**). qRT-PCR analysis showed that TNFα treatment caused upregulation of *CXCL10*, *CXCL11*, *SELE*, *ICAM1*, and *VCAM1* in HRMEC ($p<0.0001$), and INCA-6 significantly reduced expression of *CXCL10*, *CXCL11*, and *VCAM1*, but not *SELE* or *ICAM1* compared to TNFα-treated cells ($p<0.0001$). This qRT-PCR data is consistent with the RNA-seq findings, showing similar patterns for both TNFα-induced changes and the effect of NFAT inhibition.

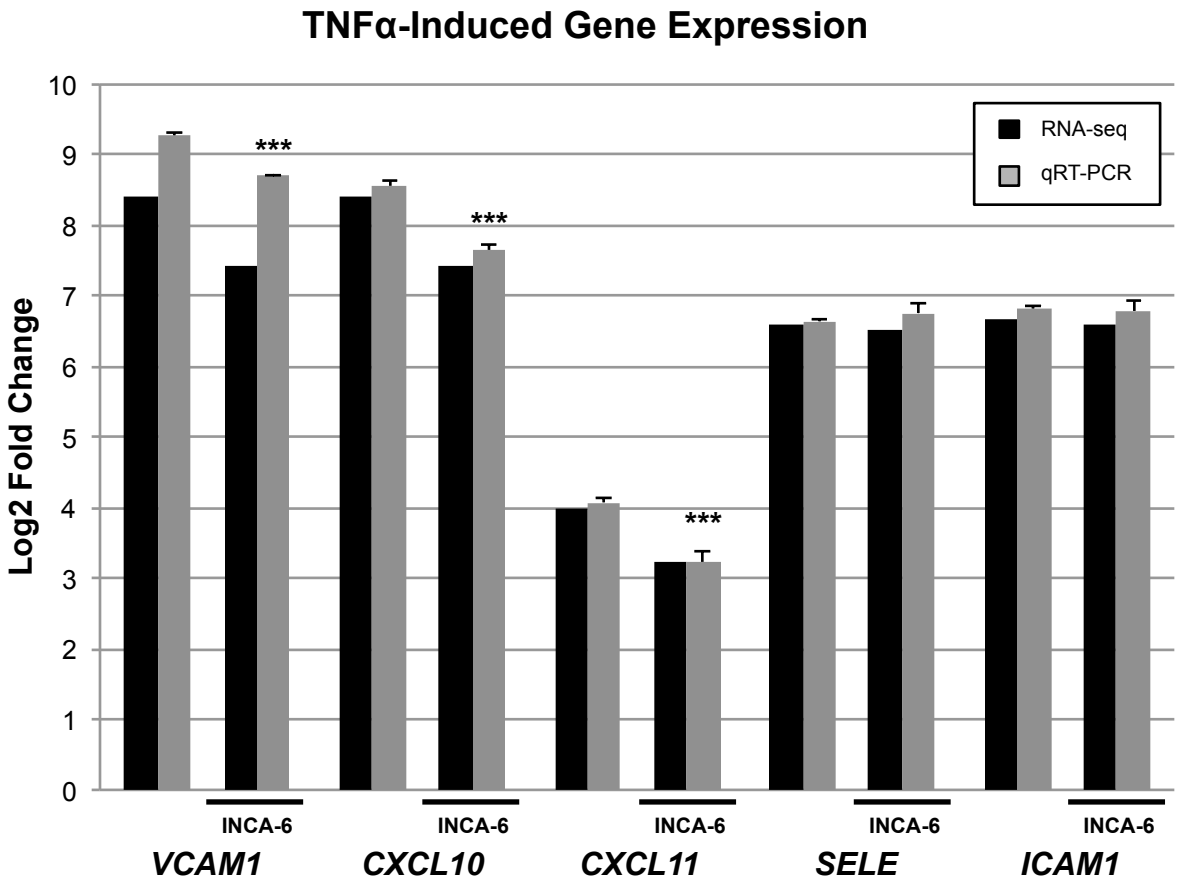

Figure 8. qRT-PCR validation of differentially expressed RNA-seq genes. Black bars indicate fold change from the RNA-seq data calculated by edgeR. Fold change for qRT-PCR (gray bars) was determined by the relative Ct method normalized to β-actin (*** $p<0.001$).

2.2.2 Effect of pharmacologic NFAT inhibition on TNFα-induced PPFC cell adhesion

Based on the RNA-seq findings that pharmacologic NFAT inhibition reduced the TNFα-induced expression of proteins heavily involved in leukocyte recruitment and adhesion, PPFC was used to determine whether these changes manifested in a functional effect on TNFα-induced leukostasis. In the PPFC assay PBMCs are flown over a treated endothelial monolayer in a context designed to mirror physiologic conditions, after which the number of adherent PBMCs are counted and serve as an *in vitro* measure of leukostasis.

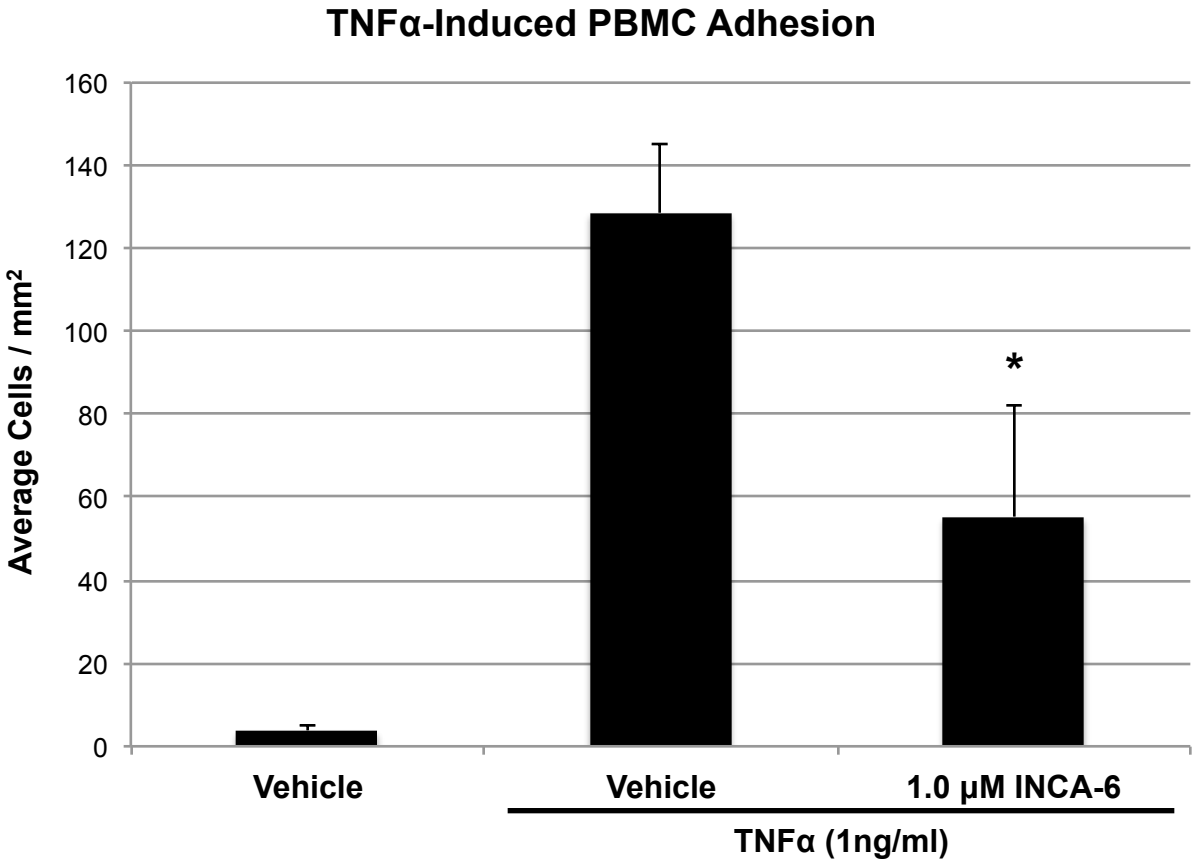

Figure 9. Effect of INCA-6 treatment on TNFα-induced PBMC adhesion. HRMEC monolayers were treated with TNFα (1ng/ml) in the presence or absence of the NFAT-inhibitor INCA-6 (1μM) for 4hrs. Monolayers were placed in a parallel plate flow chamber and PBMCs were flown over the monolayer for 7min. Non-adherent cells were then washed off and the remaining adherent cells counted. Co-treatment with INCA-6 significantly reduced TNFα-induced PBMC adhesion. Each bar represents the mean ± SEM (n=4). * = $p<0.05$

HRMEC monolayers were treated with vehicle, TNFα (1ng/ml), or TNFα plus INCA-6 (1μM) for 4hrs prior to being assayed in the flow chamber. TNFα treatment induced a 37-fold increase in PBMC adhesion compared to non-stimulated controls, and co-treatment with INCA-6 reduced this effect by 58.9% ($p<0.0001$ and $p=0.0222$, **Figure 9**). This finding highlights a functional role for NFAT signaling in TNFα-induced PBMC adhesion in HRMEC.

2.2.3 Effect of pharmacologic NFAT inhibition on TNFα-induced retinal leukostasis

Given the identified involvement of NFAT signaling in both TNFα-induced expression of leukocyte recruitment and adhesion proteins, and the adhesion of PBMCs to HRMEC monolayers, a proof of principal study was conducted to determine whether these effects translated to pathologic changes in a mouse model of TNFα-induced retinal leukostasis. In this study, injection of TNFα (50ng/ml) induced a 2.1-fold increase in retinal leukocyte adhesion after 6hrs compared to control ($p=0.0023$), and co-injection of INCA-6 (25μM) reduced this effect by 79.2% ($p=0.0089$, **Figure 10**).

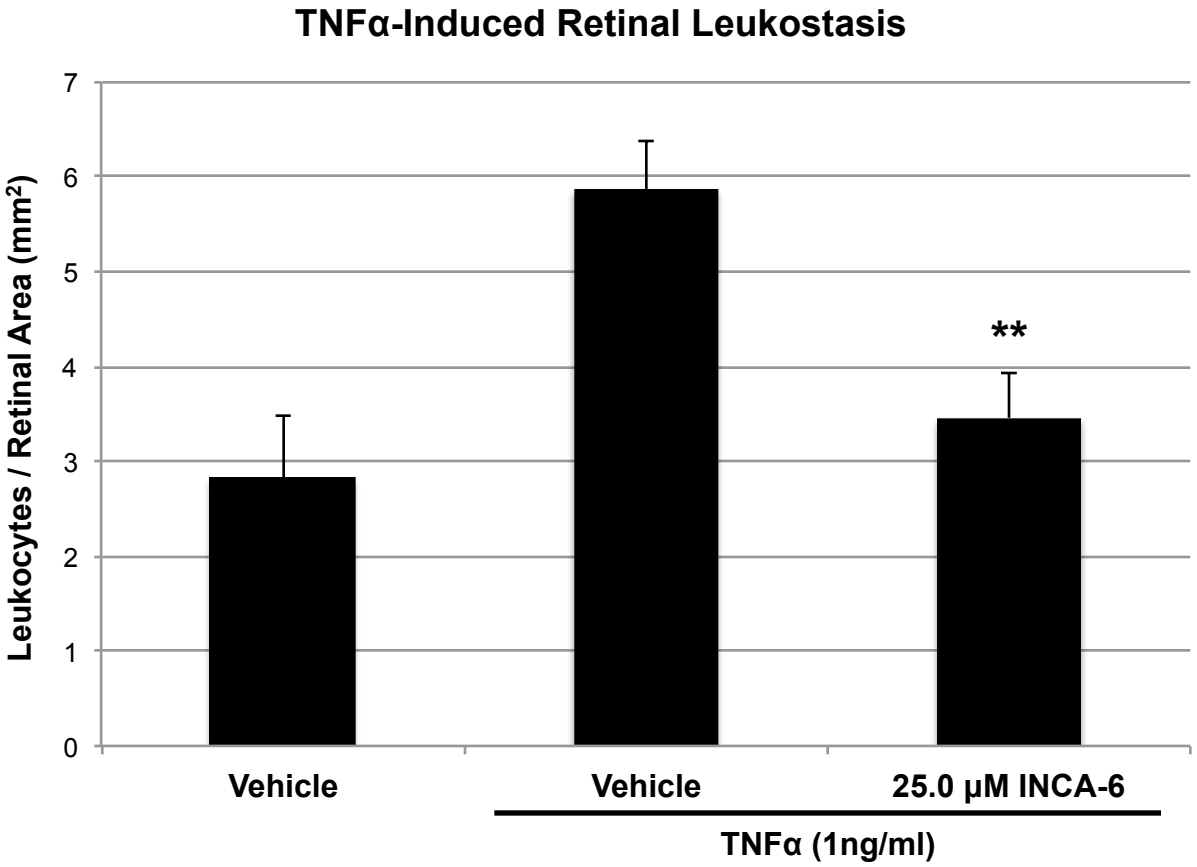

Figure 10. Effect of INCA-6 treatment on TNFα-induced retinal leukocyte adhesion. C57BL/6 mice received intravitreal injections of vehicle (0.1% DMSO in PBS), TNFα (50ng/mL) or TNFα plus INCA-6 (25μM) 6hrs prior to perfusion with saline and concanavalin A. Adherent leukocytes were then counted in flat-mounted retinas. Co-injection of INCA-6 significantly reduced TNFα-induced retinal leukocyte adhesion. Each bar represents the mean ± SEM (For Vehicle, n=5; for TNFα + Vehicle, n=9; for TNFα + INCA-6, n=6). ** = $p<0.01$

2.3 Conclusions

This study provides a characterization of the effect of TNFα on retinal microvascular endothelial cells. Furthermore, it elucidates a role for pharmacologic NFAT inhibition in both TNFα-induced expression of leukocyte recruitment and adhesion proteins, and TNFα-induced leukocyte adhesion.

RNA-seq analysis revealed that TNFα stimulated the differential expression of a number of genes, particularly those related to cytokine-cytokine receptor interaction, cell adhesion, and leukocyte transendothelial migration. Three of the genes most highly upregulated by TNFα were *ICAM1, VCAM1,* and *SELE*, which code for adhesion proteins ICAM1, VCAM1, and E-Selectin. These proteins are known to be regulated by TNFα and have been shown to mediate the effect of TNFα on leukocyte adhesion in other endothelial cell types.[160,161] Genes coding for the cytokines CXCL10, CXCL11, and MCP-1, were also all notably upregulated by TNFα, and these proteins play well-defined roles in the recruitment of leukocytes to inflamed or damaged endothelium.[79-81,162] Additionally, the gene with the largest reduction in expression by TNFα was *KCNK2*, which encodes the TWIK-related potassium channel-1 (TREK1). Blockade of TREK1 channel activity or reduced expression of *KCNK2* has been shown to increase leukocyte transmigration across brain endothelial cells.[159]

In addition to characterizing the effect of TNFα on RMEC, this study also provides the first insight into how NFAT family transcription factors modulate TNFα signaling in the retinal endothelium. TNFα is known to activate NFAT signaling in macrophages, and a number of studies have shown a role for NFAT-induced TNFα expression, but to date none have looked at a role for NFAT downstream of TNFα in

endothelial cells.[137,163,164] Our study found that INCA-6 reduced expression of a small subset of genes that were upregulated by TNFα. Interestingly, this subset included the previously discussed *VCAM1*, *CXCL10*, and *CXCL11*, as well as *CX3CL1* and *TNFSF10*. CX3CL1 is an inflammatory cytokine that, in its soluble form, assists in recruitment of leukocytes to areas of inflammation and in its membrane-bound form aids in leukocyte tethering and adhesion, while *TNFSF10* is the gene encoding TNF-related apoptosis-inducing ligand (TRAIL), a cytokine that promotes endothelial cell apoptosis in addition to leukocyte adhesion.[165,166] These initial findings suggested that TNFα regulates leukostasis at least partially through NFAT signaling.

In order to test whether the observed changes in TNFα-induced gene expression have a functional impact on TNFα-induced leukocyte adhesion, the effect of NFAT inhibition on TNFα-stimulated HRMEC was evaluated using a PPFC assay. In this assay, TNFα-stimulation increases the capacity of endothelial monolayers to capture and firmly adhere PBMC flowing over the monolayer under physiologic conditions. Previous studies using this technique have shown that siRNA and pharmacologic treatments that directly target leukocyte adhesion proteins CX3CL1 and VCAM1, two of the NFAT regulated gene targets identified via RNA-seq, reduce the ability of leukocytes to adhere to the monolayer. Accordingly, treatment with INCA-6 significantly reduced TNFα-induced PBMC adhesion to the treated monolayers, indicating a functional impact of NFAT signaling on TNFα-induced cell adhesion.

As a final proof of concept we evaluated the effect of pharmacologic NFAT inhibition, in a mouse model of TNFα-induced retinal leukostasis. Intraocular injection of TNFα leads to increased leukocyte adhesion to the vascular endothelium, and provides

an acute way to model a chronic pathology that may take months or years to develop in diabetics. Co-injection of INCA-6 significantly reduced TNFα-induced leukocyte adhesion to the retinal endothelium, and confirmed a functional role for NFAT signaling in TNFα-induced retinal leukostasis.

CHAPTER III

Analysis of NFAT Isoform-Specific Roles in TNFα-Treated Human Retinal Microvascular Endothelial Cells

3.1 Overview

Initial studies using the pharmacologic NFAT inhibitor INCA-6 revealed a role for NFAT signaling in TNFα-induced retinal leukostasis (**Chapter II**). These studies identified NFAT signaling as a regulator of TNFα-induced leukocyte adhesion protein and chemoattractant expression in HRMEC and established a functional role for NFAT signaling in TNFα-induced cell adhesion. However, as INCA-6 is a general inhibitor of all four CN-dependent NFAT isoforms it remained to be seen what role individual isoforms play in this context.

In order to investigate this, the present study required development of a protocol for the effective transfection of HRMEC and identification of siRNA oligonucleotides capable of targeting the individual NFAT isoforms. With this accomplished, the contribution of individual-isoforms in TNFα-induced expression of known NFAT gene targets was systematically evaluated, as were the isoform-specific contributions to TNFα-induced cytokine production. This evaluation revealed distinct and at times counteractive roles for the individual isoforms in TNFα-treated HRMEC, and identified NFATc2 and NFATc4 as important regulators of TNFα-induced leukocyte adhesion protein expression and cytokine production. Lastly, transfected monolayers were assayed under flow conditions to confirm that the observed isoform-specific effects resulted in functional changes in TNFα-induced cell adhesion. Accordingly, NFATc2 and NFATc4 knockdown reduced TNFα-induced PBMC adhesion, highlighting the functional importance of their role in TNFα-stimulated HRMEC.

3.2 Results

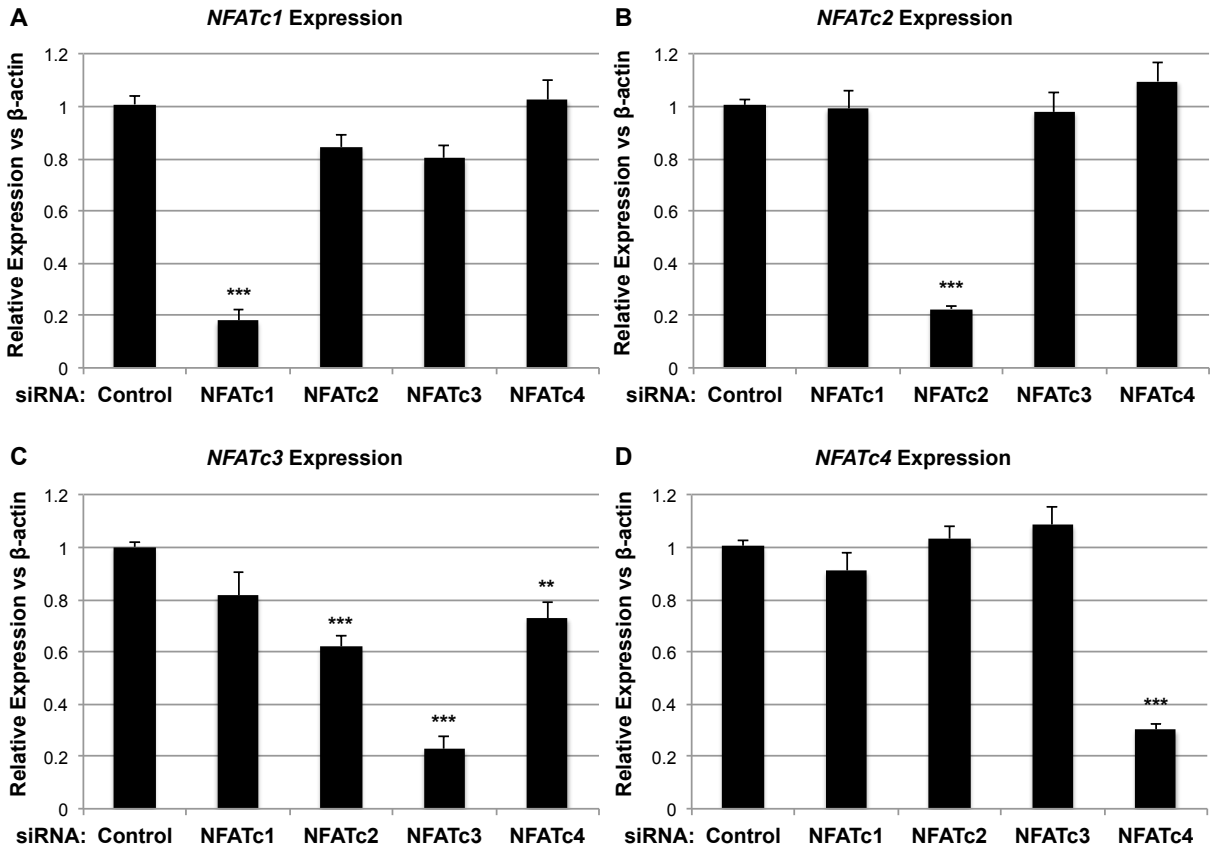

Figure 11. Effect of isoform-specific siRNA on NFAT-isoform expression in HRMEC. HRMEC were transfected with either control or isoform-specific siRNA for 36hrs. Total RNA was then collected and expression was analyzed using qRT-PCR. **A) *NFATc1* Expression**. Transfection with NFATc1 siRNA inhibited *NFATc1* expression by 82%. **B) *NFATc2* Expression.** Transfection with NFATc2 siRNA inhibited *NFATc2* expression by 78%. **C) *NFATc3* Expression.** NFATc3 siRNA inhibited *NFATc3* expression by 77%. NFATc2 and NFATc4 siRNA also inhibited *NFATc3* expression by 37% and 27% respectively. **D) *NFATc4* Expression.** NFATc4 siRNA inhibited *NFATc4* expression by 70%. Each bar represents the mean ± SEM (n=9). ** = $p<0.01$, *** = $p<0.001$

3.2.1 Identification and evaluation of isoform-specific siRNA

In order to evaluate the role of individual NFAT isoforms in signaling pathways first identified via pharmacologic NFAT inhibition, oligos targeting individual isoforms were identified. Commercially available oligos were systematically evaluated individually and in combination, to identify the oligo or oligo cocktail that yielded optimal target knockdown. In total, 4 oligos targeting *NFATc1*, 4 oligos targeting *NFATc2*, 6 oligos targeting *NFATc3*, and 9 oligos targeting *NFATc4* were evaluated before sufficient

knockdown was established. In HRMEC, the selected NFATc1 directed oligos were found to knock down *NFATc1* expression by 82%, while NFATc2, NFATc3, and NFATc4 directed siRNA knockdown expression of their target isoform by 78%, 77%, and 70% respectively (**Figure 11**). NFATc2 and NFATc4 directed siRNA also reduced *NFATc3* expression by 37% and 27%, though this is not due to any overlap in the target sequences. Additionally, the effectiveness of isoform-specific siRNA at 24, 36, and 48hrs post transfection was evaluated and no significant changes in target knockdown were detected over this time course (**Appendix A**).

3.2.2 Effect of NFAT isoform-specific knockdown on TNFα-induced adhesion protein expression

The previous studies using RNA-seq established that TNFα-stimulation of HRMEC resulted in increased expression of the leukocyte adhesion proteins CX3CL1, VCAM1, E-Selectin, and ICAM1, and that NFAT blockade inhibited the induction of both *CX3CL1* and *VCAM1*. In order to determine what role individual NFAT isoforms play in this context, HRMEC were transfected with either control or isoform-specific siRNA, then treated with TNFα (1ng/ml) for 4hrs, and evaluated using qRT-PCR.

TNFα-stimulation of cells transfected with control siRNA resulted in a 266-fold increase of *CX3CL1* expression compared to non-stimulated control siRNA cells ($p<0.0001$, **Figure 12A**). NFATc2 siRNA knockdown reduced this effect by 45.6% ($p=0.0238$), while NFATc3 knockdown increased *CX3CL1* expression by 90.3% ($p<0.0001$). TNFα-stimulation also induced a 56-fold increase in *VCAM1* expression ($p<0.0001$), which NFATc2 knockdown again inhibited by 34.9% ($p=0.0468$, **Figure 12B**).

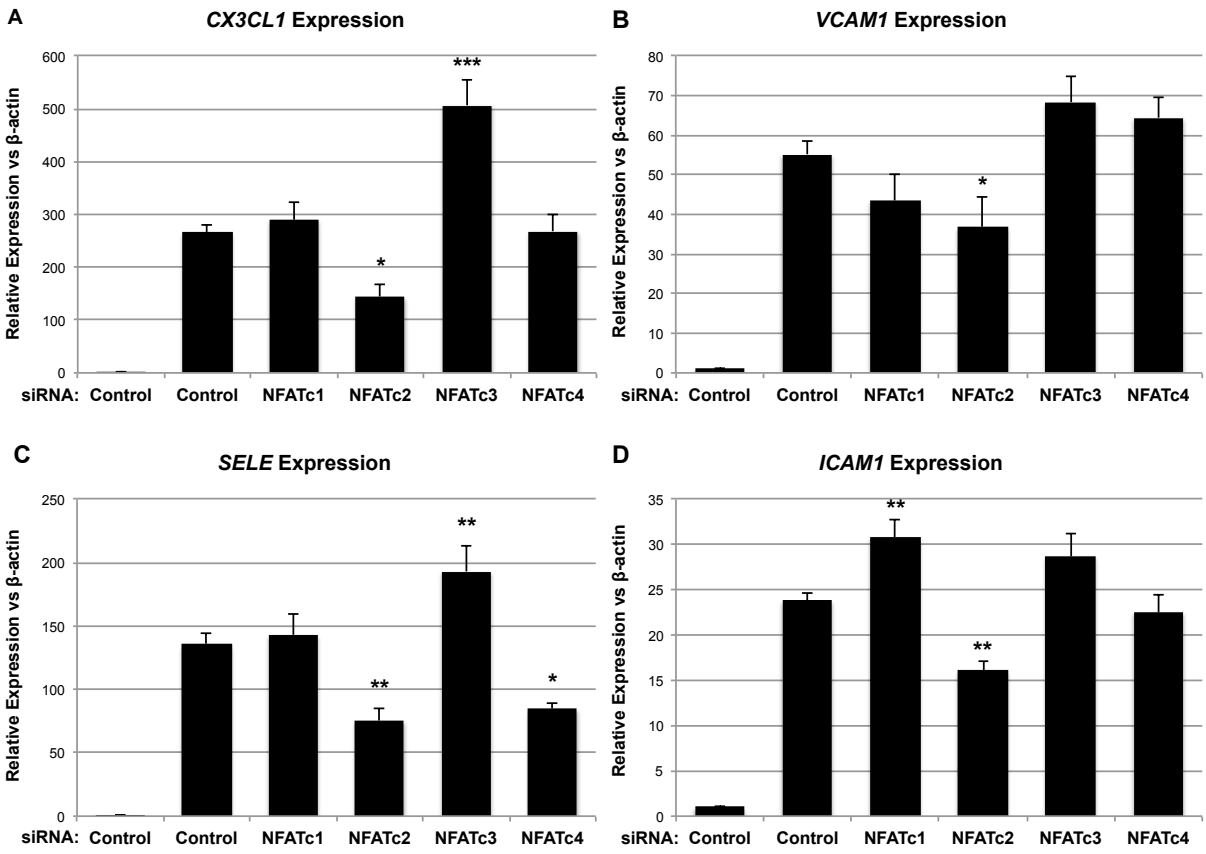

Figure 12. Effect of isoform-specific siRNA knockdown on TNFα-induced leukocyte adhesion protein expression. HRMEC transfected with either control or isoform-specific siRNA were treated with TNFα (1ng/ml) for 4hrs. Total RNA was then collected and expression was analyzed using qRT-PCR. **A) *CX3CL1* Expression**. Transfection with NFATc2 siRNA reduced TNFα-induced expression of *CX3CL1* and NFATc3 siRNA exacerbated the induction. **B) *VCAM1* Expression.** NFATc2 siRNA inhibited TNFα-induced *VCAM1* expression. **C) *SELE* Expression.** NFATc2 and NFATc4 siRNA both inhibited TNFα-induced expression of *SELE*, while NFATc3 siRNA increased the effect. **D) *ICAM1* Expression.** NFATc1 siRNA exacerbated TNFα-induced *ICAM1* expression while NFATc2 siRNA inhibited the induction. Each bar represents the mean ± SEM (n=9). * = $p<0.05$, ** = $p<0.01$, *** = $p<0.001$

INCA-6 treatment had no significant effect on *SELE* or *ICAM1* expression in either the RNA-seq or qRT-PCR validation studies, though both have been identified as NFAT signaling targets in an endothelial cell context. This suggested that either NFAT-regulation of these targets is endothelial cell type specific, or that some aspect of pharmacologic NFAT inhibition masked this effect in previous studies. As a result, the isoform-specific evaluation of TNFα-induced leukocyte adhesion proteins was expanded to include *SELE* and *ICAM1*.

TNFα-stimulation increased *SELE* and *ICAM1* expression by 136- and 24-fold respectively ($p<0.0001$ and $p<0.0001$, **Figure 12C and 12D**). Interestingly, both NFATc2 and NFATc4 knockdown reduced TNFα-induced *SELE* expression, by 44.3% ($p=0.004$) and 37.3% ($p=0.0121$) respectively, while NFATc3 knockdown increased expression by 42.5% ($p=0.0033$). NFATc2 knockdown also reduced ICAM1 expression by 32.6% ($p=0.0077$), while NFATc1 knockdown actually increased expression by 29.3% ($p=0.0091$). These later findings identify an expanded role for NFAT signaling in the expression of TNFα-induced leukocyte adhesion, and suggest that the lack of isoform specificity with pharmacologic NFAT inhibition may mask certain NFAT-dependent effects.

3.2.3 Effect of NFAT isoform-specific knockdown on TNFα-induced cytokine production

TNFα-stimulation of HRMEC also increased expression of numerous soluble inflammatory cytokines, including CXCL10, CXCL11, MCP-1, and IL-6. All of these have been identified as NFAT signaling targets in an endothelial cell context, though only *CXCL10* and *CXCL11* were inhibited by INCA-6 in the previous study. In order to determine what roles individual NFAT isoforms play in the production of these soluble cytokines, transfected HRMEC were treated with TNFα (1ng/ml) for 6hrs and conditioned media were collected and assayed for cytokine production using enzyme-linked immunosorbent assays (ELISA).

TNFα-stimulation induced a 4.1-fold increase of CXCL10 protein in conditioned media ($p<0.0001$), which was inhibited by 58.1% through NFATc4 knockdown ($p=0.0369$, **Figure 13A**). TNFα-stimulation also resulted in a 2.17-fold increase of CXCL11 in conditioned media ($p<0.0001$), which NFATc4 knockdown reduced by

105.7% (p=0.0004), completely inhibiting the effect of TNFα-stimulation (**Figure 13B**). NFATc4 knockdown also inhibited TNFα-induced MCP-1 protein in conditioned media, reducing the 2.4-fold increase by 69.67% (p<0.0001 and p=0.0066, **Figure 13C**). Lastly, TNFα-induced a 3.9-fold increase of IL-6 protein in conditioned media, which was unaffected by transfection with any of the NFAT isoform-specific siRNA (**Figure 13D**).

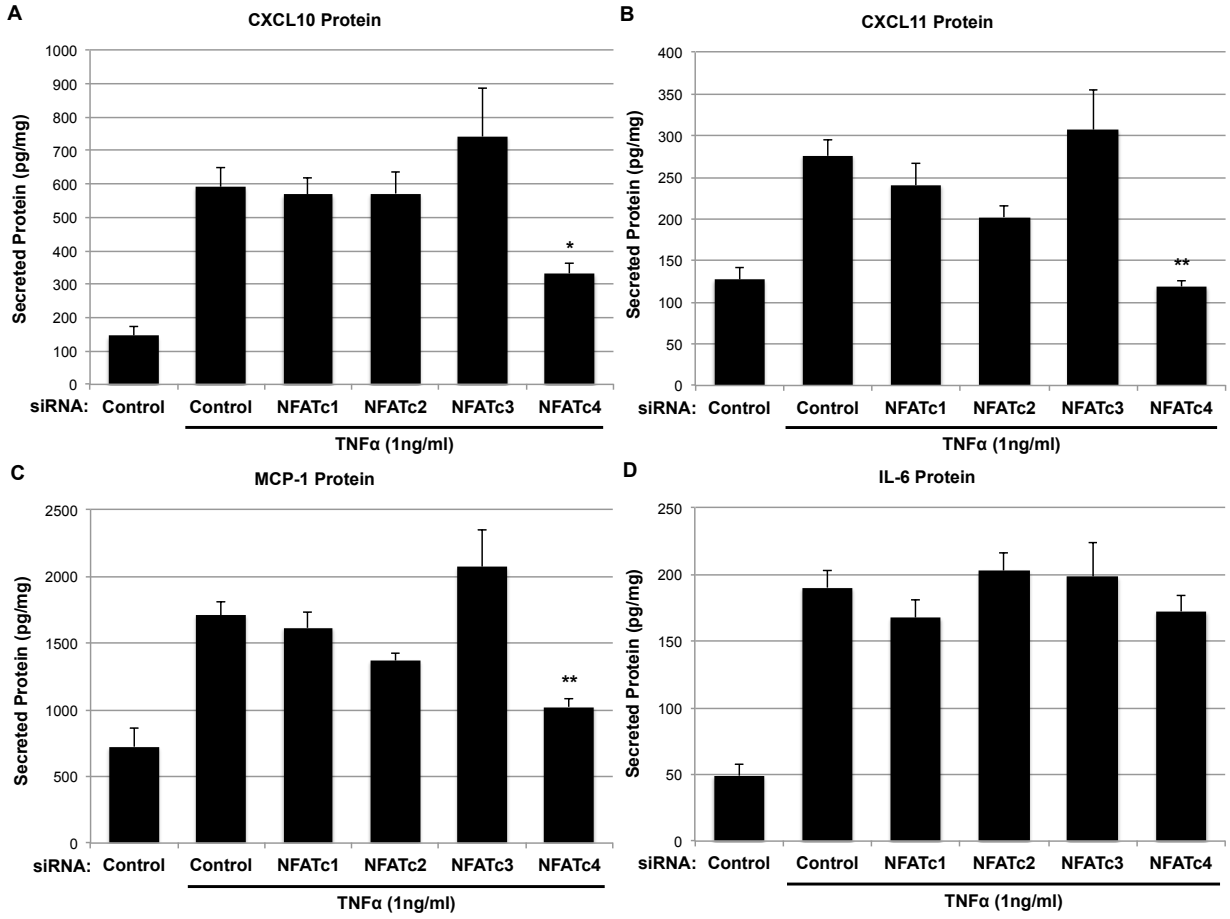

Figure 13. Effect of isoform-specific siRNA knockdown on TNFα-induced cytokine production. HRMEC transfected with either control or isoform-specific siRNA were treated with TNFα (1ng/ml) for 6hrs. Conditioned media was then collected and analyzed for secreted cytokines using ELISA. Transfection with NFATc4 siRNA reduced TNFα-induced levels of **A) CXCL10 B) CXC11** and **C) MCP-1** in conditioned media. **D) IL-6 Protein.** Isoform-specific siRNA did not affect TNFα-induced IL-6 levels in conditioned media. Each bar represents the mean ± SEM (n=9). * = p<0.05, ** = p<0.01

3.2.4 Effect of NFAT isoform-specific knockdown on TNFα-induced PPFC cell adhesion

In order to assess the functional effects of isoform-specific changes in TNFα-induced HRMEC, monolayers were transfected with either control or isoform-specific

siRNA and evaluated using a PPFC cell adhesion assay. TNFα treatment (1ng/ml for 4hrs) of monolayers transfected with control siRNA induced an 11.5-fold increase in PBMC adhesion compared to non-stimulated controls ($p<0.0001$, **Figure 14**). Monolayers transfected with NFATc2 and NFATc4 siRNA reduced TNFα-induced PBMC adhesion by 55% ($p=0.0013$) and 38.4% ($p=0.0289$), respectively, while transfection with NFATc1 and NFATc3 siRNA had no significant effect on TNFα-induced cell adhesion.

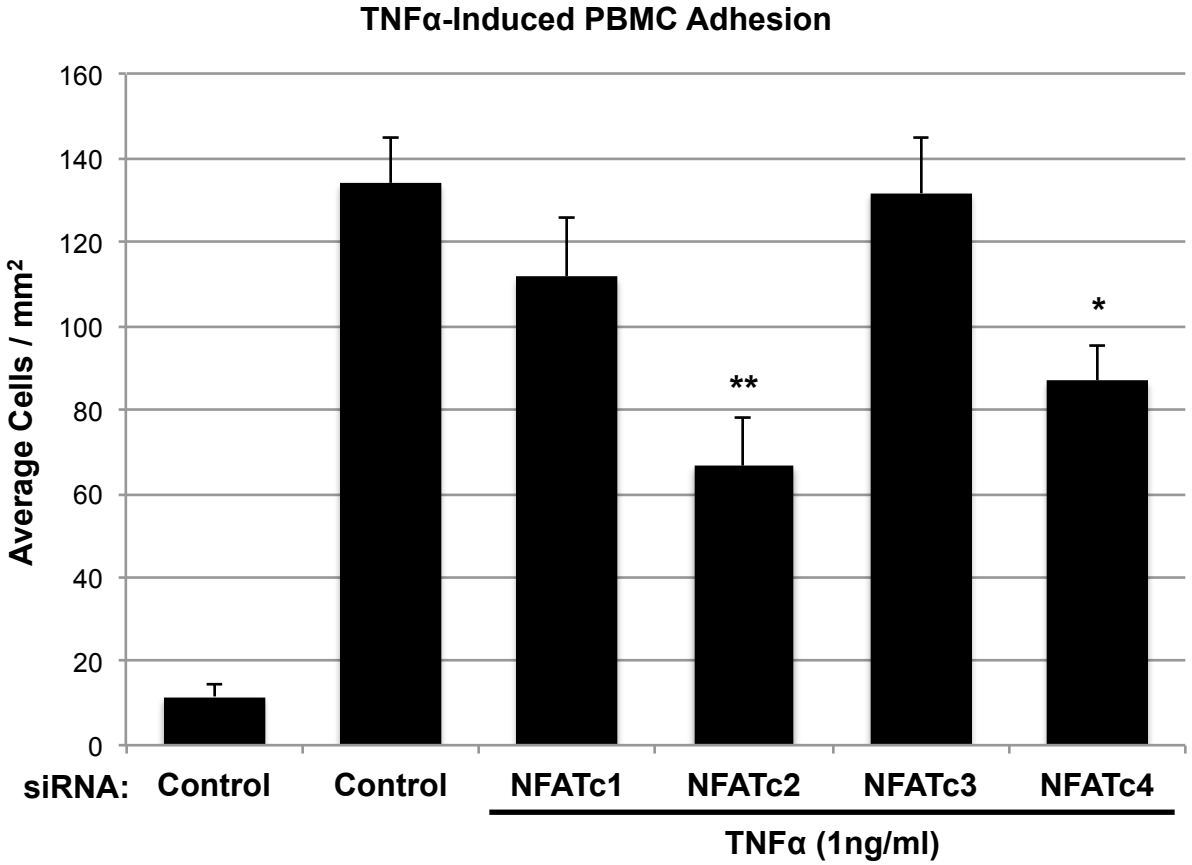

Figure 14. Effect of isoform-specific siRNA knockdown on TNFα-induced PBMC adhesion. HRMEC monolayers transfected with either control or isoform-specific siRNA were treated with TNFα (1ng/ml) for 4hrs. Monolayers transfected with NFATc2 and NFATc4 siRNA significantly reduced TNFα-induced PBMC adhesion. Each bar represents the mean ± SEM (n=5). * = $p<0.05$, ** = $p<0.01$

3.3 Conclusions

The previous study revealed a general role for NFAT signaling in the response of HRMEC to TNFα-stimulation, and identified a functional role in TNFα-induced cell adhesion (**Chapter II**). The present study builds upon those early findings, using isoform-specific siRNA to identify new, discreet, and at times counteractive roles for the individual NFAT isoforms in this context.

The identification and verification of isoform-specific siRNA was a critical first step in being able to evaluate the role of individual NFAT isoforms. At the start of this study, no protocol had been established for the effective transfection of primary human retinal microvascular endothelial cells, and early efforts using Lipofectamine® (Life Technologies; Carlsbad, CA), DharmaFECT (GE Healthcare; Little Chalfont, U.K), and Polyjet™ (SignaGen® Laboratories, Rockville, MD) techniques proved unsuccessful. Eventually, a successful protocol was adapted using a combination of Virofect and Targafect reagents (**6.2.1**), and oligos targeting the individual isoforms could be evaluated.

Considerable effort was put into identifying oligos that could effectively knockdown the target isoform at a low concentration (75nm) and with minimal effect on other isoforms. **Table 8** identifies the oligos identified for each target and used in subsequent studies. In the end, greater than 70% knockdown was achieved for all of the isoforms, and only *NFATc3* expression was affected by siRNA targeting a different isoform. In this instance both NFATc2 and NFATc4 siRNA knocked down expression of NFATc3 by roughly 30%. This was not due to an overlap in the target sequence. NFATc2 has previously been shown to play a role in the expression of other NFAT

isoforms, and this is believed to be responsible for the effect seen here, though there are no reports to date that have evaluated the role of either NFATc2 or NFATc4 in *NFATc3* expression. In both cases, it is believed that this minimal reduction had no effect on the subsequent studies, as NFATc2 and NFATc4 knockdown both caused significant effects that were counter to those seen by the more significant NFATc3 knockdown via NFATc3 siRNA.

Having established the appropriate techniques and reagents to evaluate the roles of individual NFAT isoforms, isoform-specific siRNA was used to further elucidate the contributions of NFAT signaling in TNFα-induced gene expression. The first two targets analyzed were *CX3CL1* and *VCAM1*, which had been identified as NFAT-regulatory targets in the RNA-seq study. Isoform-specific siRNA revealed that NFATc2 knockdown negatively regulated both *CX3CL1* and *VCAM1* expression, and that NFATc3 knockdown increased TNFα-induced upregulation of *CX3CL1*. The latter finding showed that individual NFAT isoforms can play counteractive roles in endothelial cell activities, and highlights the importance of evaluating isoforms individually.

Given these initial findings, the study was expanded to examine the role of NFAT isoforms in TNFα-induced *SELE* and *ICAM1* expression. *SELE* is the gene that codes for E-selectin, and both E-selectin and ICAM1 are adhesion proteins known to mediate TNFα-induced leukocyte adhesion. While the previous study did not find any significant effect of NFAT inhibition on TNFα-induced expression of either target, investigators working in other endothelial cell systems have identified a regulatory role for NFAT in the expression of both.[103,148,155,167] Isoform-specific siRNA knockdown showed that this incongruity was due to counteracting effects of individual isoforms that were masked by

inhibition of all four calcineurin-dependent isoforms with INCA-6. Both NFATc2 and NFATc4 knockdown significantly reduced TNFα-induced expression of *SELE*, while NFATc3 increased its expression. In the case of *ICAM1* expression, NFATc2 again inhibited TNFα-induction and NFATc1 knockdown exacerbated the induction.

The previous analyses using INCA-6 also highlighted a role for NFAT signaling in the regulation of TNFα-induced chemokines CXCL10 and CXCL11. CXCL10 and CXCL11 both serve as ligands for the CXCR3 receptor and are known to play a role in leukocyte recruitment to sites of endothelial inflammation.[79-81] While this activity would not be expected to manifest functionally in an *in vitro* PPFC model for TNFα-induced leukocyte adhesion, leukocyte recruitment is a critical feature of TNFα-induced leukostasis *in vivo*. Accordingly, the effect of isoform-specific siRNA on TNFα-induced protein secretion for each of these cytokines was measured. In this context, NFATc4 siRNA proved to be the most potent regulator of TNFα-induced cytokine secretion, inhibiting both CXCL10 and CXCL11 levels in conditioned media. As was the case with E-selectin and ICAM1, MCP-1 and IL-6 are inflammatory products known to be upregulated by TNFα-stimulation and identified as NFAT-regulatory targets in other endothelial cell populations.[150,167] As such, they were included in this study, and NFATc4 siRNA was again found to reduce TNFα-induced levels in the case of MCP-1, though TNFα-induced secretion of IL-6 was unaffected by all isoforms. Taken together, these findings (summarized in **Table 6**) identify a strong role for NFATc2 in the expression of TNFα-induced leukocyte adhesion proteins, as well as NFATc4 in the production of TNFα-induced leukocyte chemoattractants. Interestingly, a separate study evaluating the role of individual NFAT isoforms in VEGF-induced cytokine production, found that

NFATc1 siRNA reduced VEGF-induced IL-6 levels (**Appendix B**), indicating that not only is the relationship between NFAT and a particular target stimuli dependent, but that the isoforms involved may be as well.

	TNFα-Induced Fold Change	NFATc1 siRNA	NFATc2 siRNA	NFATc3 siRNA	NFATc4 siRNA
Adhesion Protein Expression					
CX3CL1	266	–	↓ 46%	↑ 90%	–
VCAM1	56	–	↓ 35%	–	–
SELE	136	–	↓ 44%	↑ 42%	↓ 37%
ICAM1	24	↑ 29%	↓ 33%	–	–
Secreted Cytokines					
CXCL10	4.1	–	–	–	↓ 58%
CXCL11	2.8	–	–	–	↓ 106%
MCP-1	2.4	–	–	–	↓ 70%
IL-6	3.9	–	–	–	–

Table 6. Summary of the effects of isoform-specific siRNA on TNFα-induced induction in HRMEC.

In order to again test whether the observed findings had a functional impact on TNFα-induced leukocyte adhesion, the effect of isoform-specific siRNA was evaluated in a PPFC assay. The previous study using this technique showed that pharmacologic NFAT inhibition, which reduced both CX3CL1 and VCAM1 expression, significantly reduced TNFα-induced PBMC adhesion, and additional studies have shown that treatments directly targeting E-Selectin and ICAM1 also reduce the ability of leukocytes to adhere to the monolayer. Based on this, it was hypothesized that transfecting monolayers with siRNA specific for NFAT isoforms shown to reduce TNFα-induced expression of these genes would lead to decreases in TNFα-induced PBMC cell adhesion. Accordingly, transfection with NFATc2- and NFATc4-directed siRNA was found to reduce TNFα-induced PBMC cell adhesion. One might expect that conversely,

transfection with NFATc1 and NFATc3 siRNA, which increased TNFα-induced expression of these targets, might increase TNFα-induced PBMC adhesion, but neither NFATc1 nor NFATc3 knockdown had an effect on PBMC adhesion. In the case of NFATc1 siRNA this is likely due to the observed effect on *ICAM1* expression being of minimal influence in the whole of the assay, and in the case of NFATc3, which had significant effects on both *CX3CL1* and *SELE* expression, there being little room at the upper threshold of the assay for significant increases to TNFα-induced PBMC adhesion.

Collectively, these studies show a clear role for NFAT signaling, particularly NFATc2 and NFATc4, in the response of HRMEC to TNFα. Additionally, the isoform-specific effects identified in this study highlight the unique contributions of individual NFAT isoforms, as well as the need to target them individually.

CHAPTER IV

The Role of NFAT signaling in VEGF-Treated Human Retinal Microvascular Endothelial Cells

4.1 Overview

The previous studies examined the role of NFAT signaling in TNFα-induced retinal leukostasis (**Chapter II & III**), a pathogenic feature of early DR that contributes to microvascular complications and disease progression. An important aspect of this disease progression is the development of retinal neovascularization, which defines PDR, and can develop as a result of vascular complications or occlusions caused by leukostasis. VEGF, a powerful regulator of vascular permeability in early NPDR and DME, is also a critical driver of this late neovascular pathology in PDR, and therapeutics targeting the VEGF-signaling pathway have become the primary form of clinical treatment.

VEGF is a known inducer of NFAT activity in endothelial cells, and the present study evaluates the potential contributions of this activity to retinal neovascularization and PDR. Immunocytochemistry was initially used to confirm that VEGF stimulates NFAT nuclear translocation, a surrogate measure of NFAT activity, in HRMEC. After which, the inhibitor INCA-6 was used to evaluate the effect of NFAT blockade on HRMEC proliferation and tube formation *in vitro*. Lastly, the functional effects of pharmacologic NFAT inhibition were evaluated *in vivo* using a rat model of oxygen-induced retinopathy. NFAT inhibition reduced neovascularization in this context, highlighting an additional role for NFAT signaling in retinal neovascularization and PDR pathology.

4.2 Results

4.2.1 VEGF induction of NFATc1 nuclear translocation in HRMEC

NFAT nuclear translocation was used as a surrogate measure to initially determine whether VEGF-induced NFAT activity in HRMEC. Cells were cultured on chamber slides and treated with VEGF (25ng/ml) for 30mins before being fixed and stained for NFAT isoforms c1-c4. All four isoforms were found to be present in cultured HRMEC, however only NFATc1 exhibited clear translocation to the nucleus in response to VEGF treatment (**Figure 15**). This translocation was effectively blocked by co-treatment with the NFAT-specific inhibitor INCA-6 (1.0μM).

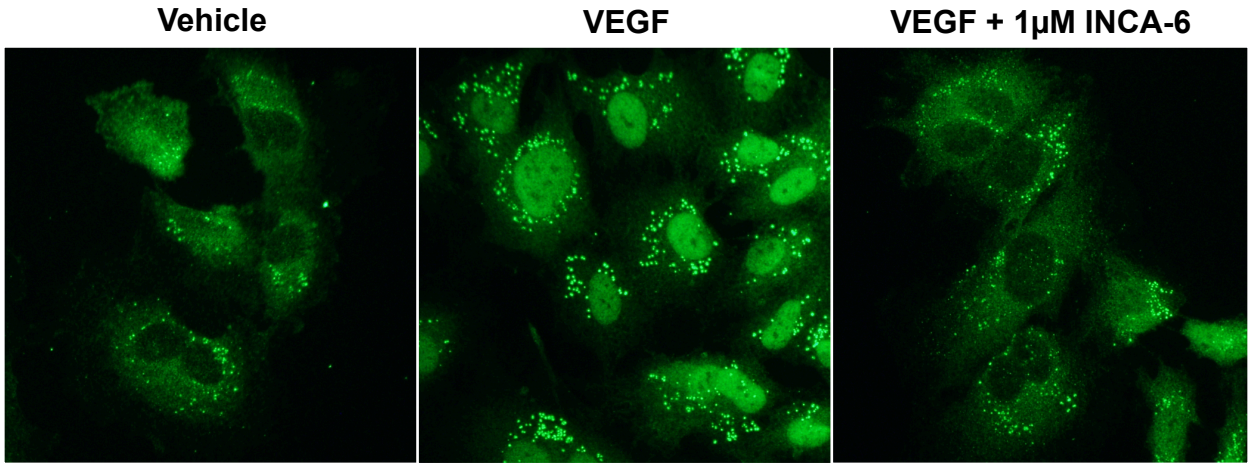

Figure 15. Effect of VEGF treatment on NFATc1 nuclear translocation in HRMEC. VEGF treatment (25ng/ml) resulted in nuclear translocation of NFATc1 after 30mins, and this was effectively inhibited by treatment with INCA-6 (1.0μM).

4.2.2 Effect of pharmacologic NFAT inhibition on *in vitro* angiogenesis

Based on the initial finding that VEGF stimulates NFAT translocation in HRMEC, the contribution of NFAT signaling to *in vitro* models of angiogenesis were evaluated, starting with VEGF-induced HRMEC proliferation. HRMEC were treated with VEGF (25ng/ml) and increasing concentrations of the pharmacologic inhibitor INCA-6, and proliferation was assayed using uptake of bromodeoxyuridine (BrdU). NFAT blockade

was found to significantly inhibit VEGF-induced proliferation at both 1.0 ($p=0.003$) and 2.5μM ($p<0.001$), while also inhibiting serum-stimulated proliferation at 2.5μM ($p<0.003$; **Figure 16**). Notably INCA-6 treatment did not alter baseline proliferation at any of the tested concentrations in the absence of VEGF or serum stimulation.

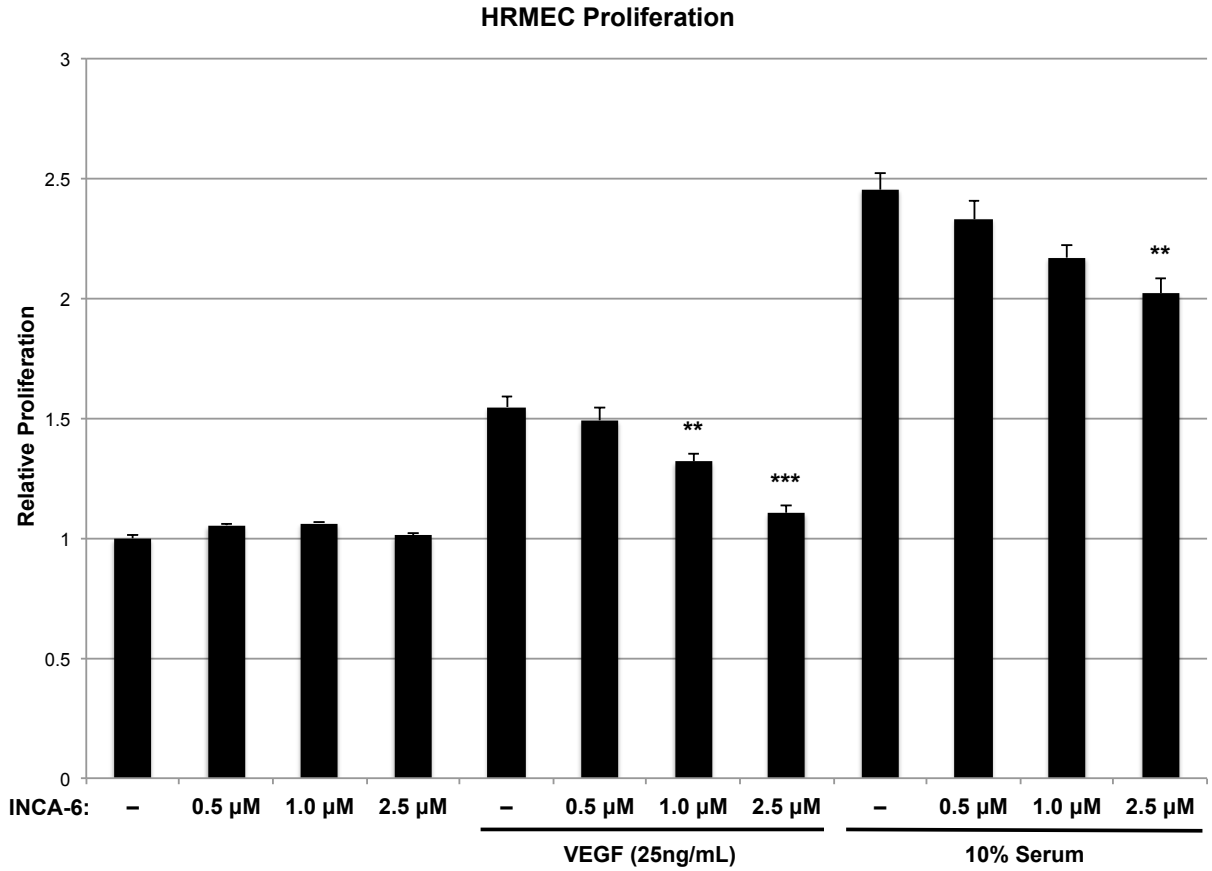

Figure 16. Effect of INCA-6 treatment on HRMEC proliferation. HRMEC proliferation was stimulated with either VEGF (25ng/ml) or 10% serum. INCA-6 treatment significantly decreased both VEGF and serum-induced HRMEC proliferation, but did not affect baseline proliferation. Each bar represents the mean ± SEM (n=21). ** = $p<0.01$. *** = $p<0.001$.

Another *in vitro* assay of angiogenic cell behavior is tube formation, which models the ability of cells to reorganize and form vessels in angiogenesis. When cultured on Matrigel, HRMEC generate capillary-like structures that can be measured and quantified. To investigate whether NFAT signaling also contributes to this angiogenic cell behavior, HRMEC were plated on Matrigel and stimulated with 10%

serum in the presence or absence of the inhibitor INCA-6. Similar to the proliferation studies, INCA-6 significantly inhibited tube formation at 1.0 ($p<0.001$) and 2.5μM ($p<0.0001$; **Figure 17**).

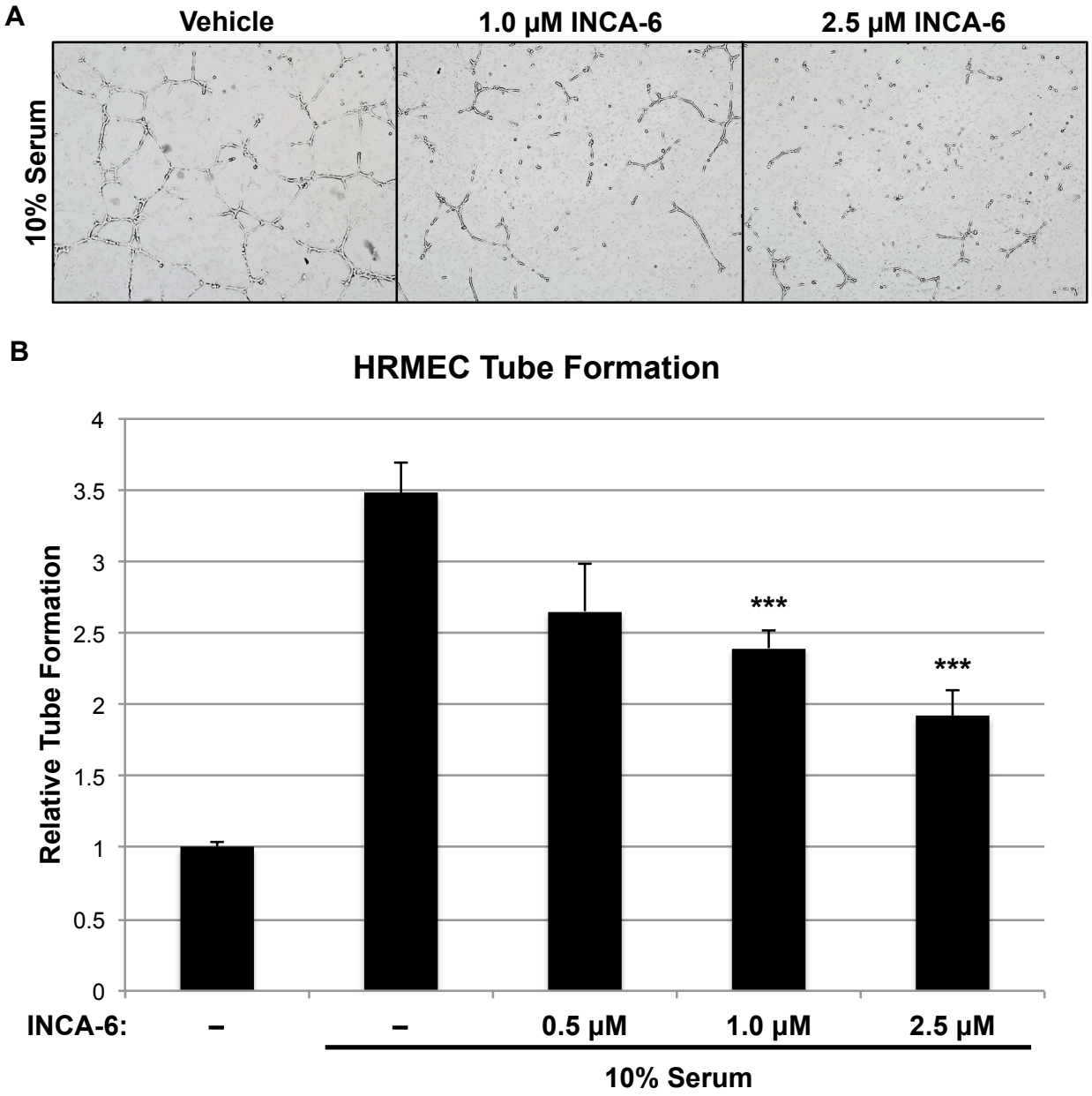

Figure 17. Effect of INCA-6 treatment on HRMEC tube formation. HRMEC tube formation was stimulated with 10% serum. INCA-6 treatment significantly decreased tube formation. **A)** Contrast enhanced representative images from treated wells. **B)** Quantification of tube measurements. Each bar represents the mean ± SEM (n=9). *** = $p<0.001$.

4.2.3 Effect of pharmacologic NFAT inhibition on retinal neovascularization

The proliferation and tube formation studies demonstrate that NFAT inhibition influences the HRMEC response to VEGF and serum stimulation in *in vitro* models of angiogenesis. Accordingly, the efficacy of pharmacologic NFAT inhibition was tested *in vivo* using a rat model of oxygen-induced retinopathy. This model results in the development of pre-retinal neovascular tufts, similar to those seen in PDR, which can be stained and quantified.

In this context, NFAT inhibition via INCA-6 decreased the amount of retinal neovascularization in a dose-dependent manner, with significant inhibition seen at 5.0 and 25.0μM concentrations ($p<0.03$, **Figure 18**). The CN-inhibitor FK-506 was also tested in this model, and a dose-dependent effect of efficacy was again observed, with significant inhibition seen at 5.0 ($p<0.05$) and 25.0μM concentrations ($p<0.02$). In order to determine whether treatment with these inhibitors also had an effect on normal vascular development, the total vascular area of treated retinas was also assessed and no significant changes were observed in any of the treatment groups (**Figure 19A**).

Lastly, the potential toxicity of INCA-6 and FK-506 treatment was assessed by identical treatment of room air animals at the highest concentration of both inhibitors (25.0μM), and no effect was seen on the rate or architecture of early physiologic retinal vascular development (**Figure 19B**).

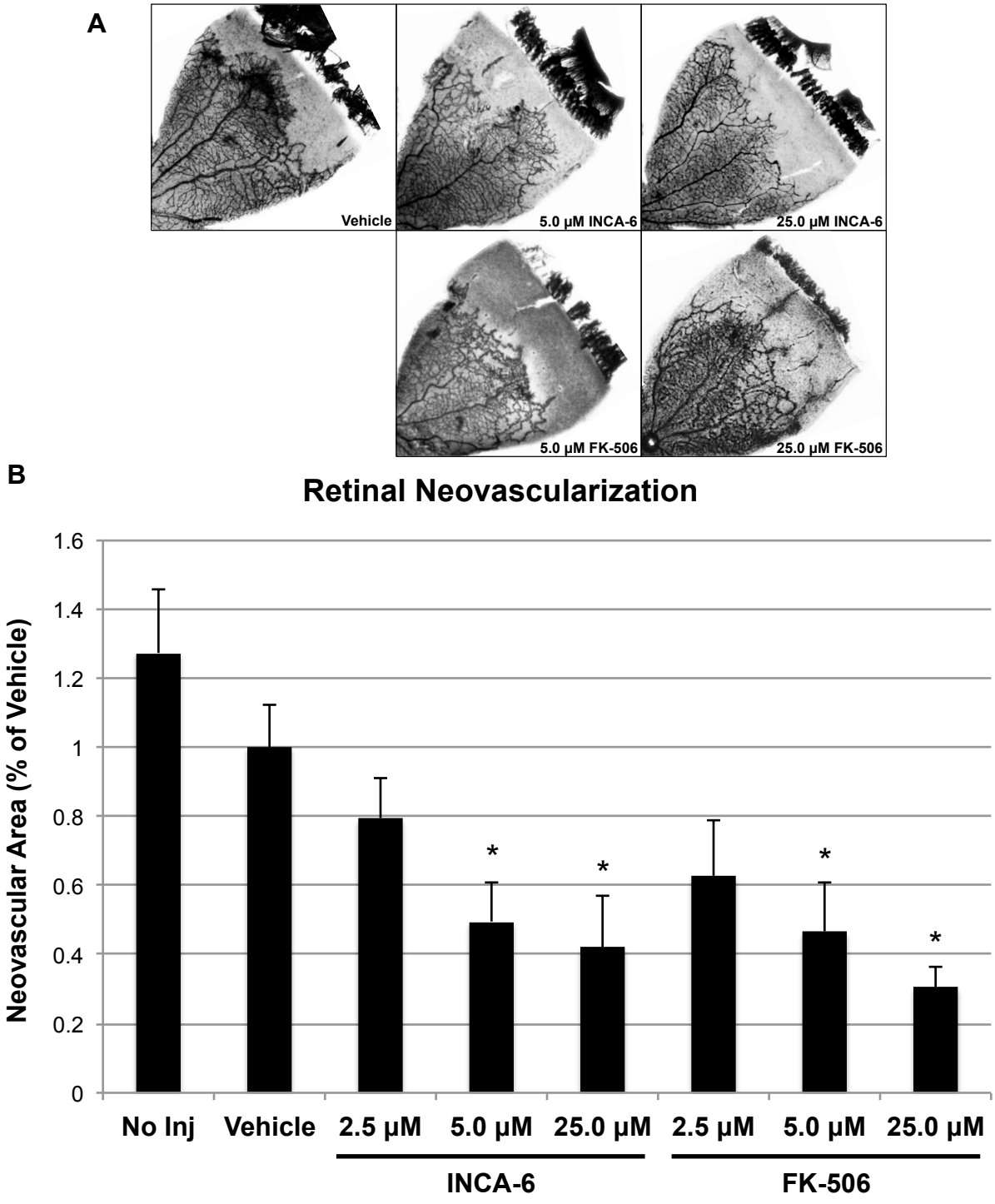

Figure 18. Effect of pharmacologic NFAT inhibition on oxygen-induced retinal neovascularization. INCA-6 and FK-506 significantly inhibited the severity of OIR in a dose-dependent manner. **A)** Representative quadrants from treatment groups. **B)** Quantification of neovascular area, relative to the vehicle injected control. Each bar represents the mean ± SEM (For no injection, n=16; for vehicle n=23; for INCA-6 2.5 µM, n=12; for INCA-6 5.0 µM, n=16; for INCA-6 25.0 µM, n=11; and for FK-506 2.5, 5.0 and 25.0 µM, n=7). * = $p<0.05$.

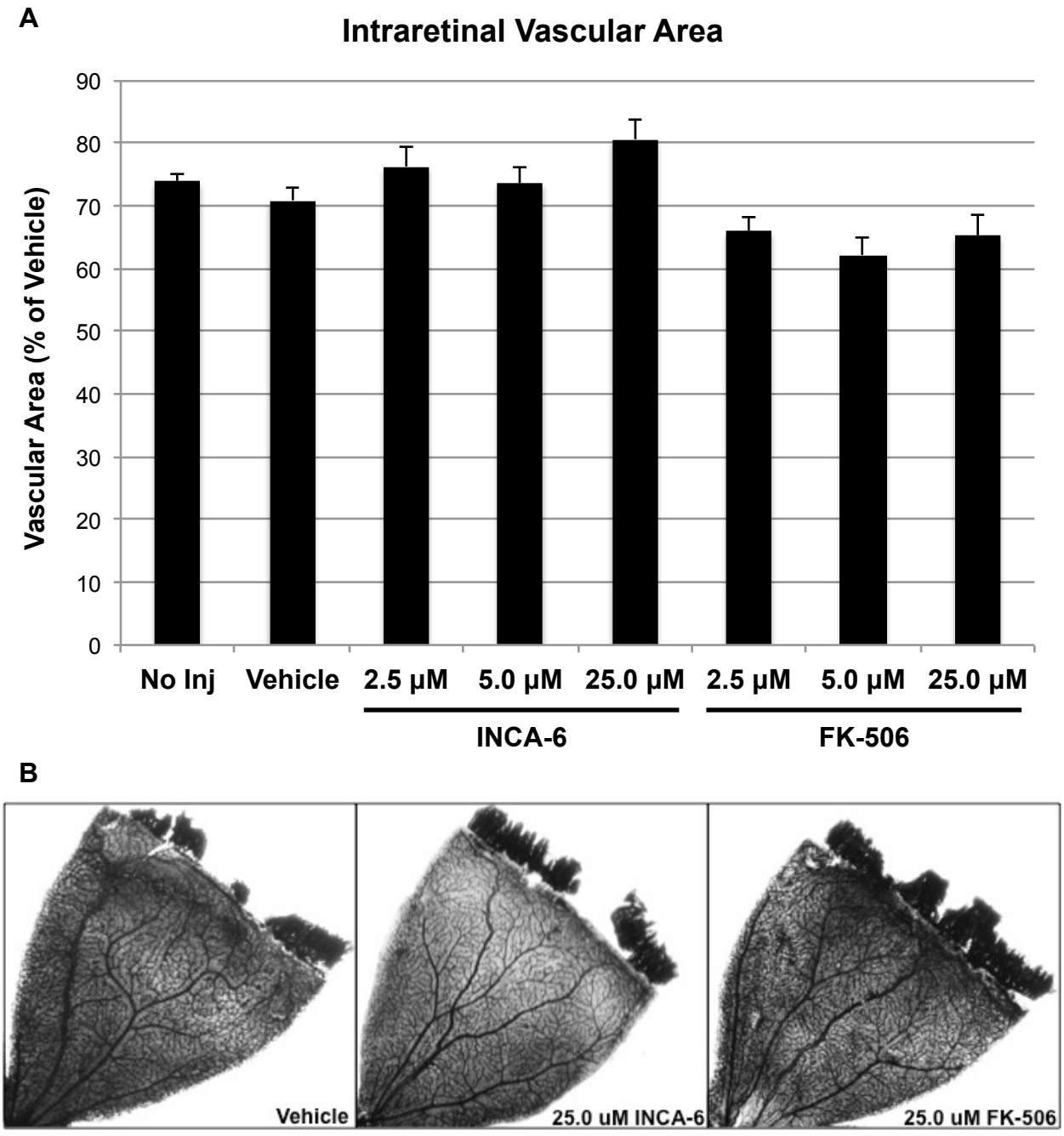

Figure 19. Effect of pharmacologic NFAT inhibition on normal vascular development. A) Effect of inhibitors INCA-6 and FK-506 on intraretinal vascular area in rat OIR. INCA-6 and FK-506 did not significantly affect the intraretinal vascular area of treated retinas. Each bar represents the mean ± SEM (For no injection, n=16; for vehicle n=23; for INCA-6 2.5µM, n=12; for INCA-6 5.0µM, n=16; for INCA-6 25.0µM, n=11; and for FK-506 2.5, 5.0 and 25.0µM, n=7). **B) Effect of inhibitors INCA-6 and FK-506 on retinal vasculature in room air rats.** Treatment with INCA-6 or FK-506 did not significantly alter retinal vascular development in room air animals.

4.3 Conclusions

VEGF is a critical signaling peptide in the development and progression of DR pathology, playing a role in both early microvascular complications and late neovascularization.[44-46,87-89] This study evaluated the contribution of NFAT signaling in the context of this later proliferative feature, and demonstrated that NFAT signaling plays a critical role both in *in vitro* models of retinal angiogenic cell behavior and in an *in vivo* model of retinal neovascularization.

VEGF is an established activator of the NFAT signaling pathway and has been shown to stimulate the translocation of different isoforms in various cellular contexts.[106,143] For instance, VEGF stimulates NFATc1 translocation In human pulmonary valve endothelial cells, and NFATc2 translocation in HUVEC and intestinal microvascular endothelial cells.[140,144,145] As a result, this study began by evaluating the effect of VEGF on NFAT localization, and found that in HRMEC, NFATc1 is the isoform translocated to the nucleus as a result of VEGF treatment (**Figure 15**). This VEGF-induced NFATc1 translocation was abolished by co-treatment with the pharmacologic NFAT-inhibitor INCA-6.

Based on this initial finding, the effect of pharmacologic NFAT inhibition was evaluated *in vitro* using angiogenic cell behavior assays that measure cell proliferation and tube formation. NFAT blockade was found to inhibit both VEGF- and serum-induced cell proliferation (**Figure 16**), as well as serum-induced tube formation (**Figure 17**). Notably, serum includes a number of pro-proliferative factors in addition to VEGF, such as EGF, FGF, and IGF. In the proliferation assays, serum stimulation induced a greater proliferative response than VEGF stimulation. Moreover, optimal INCA-6

treatment completely inhibited VEGF-induced HRMEC proliferation, but was less effective in inhibiting serum-induced proliferation. One explanation for these findings is that the inhibition of serum-stimulated proliferation by INCA-6 was largely or wholly due to inhibition of the contribution of VEGF. Together, these *in vitro* studies indicate that NFAT signaling mediates angiogenic cell behaviors in both a cell type known to contribute to pathological retinal neovascularization and in response to a stimulus known to contribute to retinal neovascularization.

To further evaluate the role of NFAT signaling in retinal neovascularization, the effect of pharmacologic NFAT inhibition was tested *in vivo* using a rat model of oxygen-induced retinopathy. In this context, INCA-6 significantly reduced the severity of pre-retinal neovascularization, as did treatment with the CN inhibitor FK-506 (**Figure 18**). FK-506 inhibits the NFAT signaling pathway upstream from INCA-6 by complexing with FKBP12 to bind CN and prevent its activation and phosphatase activity, and the finding that it caused a similar reduction in neovascularization further confirms the role of NFAT signaling in this pathology.[110-113] Collectively, these studies identify the presence of a VEGF-activated NFAT isoform in HRMEC, show a clear effect of NFAT inhibition in both *in vitro* angiogenic cell behaviors and an *in vivo* model of ocular neovascularization, and suggest that NFAT signaling exerts a pro-angiogenic influence in HRMEC downstream of VEGF.

CHAPTER V

DISCUSSION

5.1 The role of NFAT signaling in TNFα-induced retinal leukostasis

TNFα is a powerful inducer of vascular inflammation and a well-established contributor to the development of DR. Not only is it found elevated in the vitreous fluid of patients with PDR, but it is known to help regulate vascular permeability, induce vascular inflammation and damage, and promote leukostasis, all of which are important features of DR progression.[34,40,47] For these reasons TNFα has garnered growing attention as a potential therapeutic target for the treatment of DR pathology, and multiple clinical trials have been conducted evaluating the efficacy of FDA-approved TNFα-directed therapies in this context. Thus far the results of these trials have been mixed. The recombinant fusion protein Etanercept (approved to treat psoriasis) showed no significant benefit in patients with DME, though systemic treatment with the TNFα-antagonist Infliximab (approved to treat Crohn's disease) proved initially efficacious and administration by intravitreal injection is currently being evaluated.[19,20] This latter study highlights the potential of TNFα-directed therapies in the treatment of DR, while the former makes it clear that there is a need for improved treatments that target the pathogenic features of TNFα-signaling in this context.

With this backdrop, the two initial studies described herein focus on the role of NFAT signaling downstream of TNFα-stimulation in HRMEC. HRMEC are a main component of the retinal microvasculature and serve as the primary cell type throughout these studies, because DR is first and foremost, a disease of microvascular complications. Prior to these studies, the role of NFAT signaling had not been evaluated

in HRMEC, though it had been studied in other endothelial cell populations including HUVEC. Those studies identified NFAT transcription factor signaling as playing a critical role in the expression of target genes critical to both inflammation and angiogenesis. Additionally, studies in immune cells had previously identified TNFα as an inducer of NFAT activity, as well as intracellular calcium flux, a key component of the NFAT signaling pathway. Based on this, we evaluated the effect of pharmacologic NFAT inhibition in TNFα-stimulated HRMEC via RNA-seq analysis.

The RNA-seq analysis served the dual role of characterizing the effects of TNFα-stimulation on HRMEC and evaluating the effect of NFAT inhibition in this experimental context. TNFα stimulation proved to be a powerful inducer of transcript expression in HRMEC, and pathway analysis revealed that this induction was largely related to inflammation, leukocyte recruitment, and leukocyte adhesion. These findings were predictable based on TNFα's reputation as a mediator of vascular and retinal inflammation, but still serve to confirm and add resolution to that relationship in HRMEC. The most significant finding to come out of the genomics study was that pharmacologic NFAT blockade inhibits the TNFα-induced expression of a small subset of transcripts, most of which are related to leukocyte chemoattraction and adhesion. This was the first insight into how NFAT-family transcription factors modulate TNFα signaling in the retinal endothelium, and strongly suggested a role for NFAT signaling in TNFα-induced retinal leukostasis.

To further evaluate that point, the functional effect of pharmacologic NFAT inhibition was evaluated in both *in vitro* and *in vivo* models of TNFα-induced leukostasis. The PPFC assay serves as an *in vitro* model for leukostasis, and in this experimental

context TNFα-treatment increases PBMC adhesion to endothelial cells through upregulation of leukocyte adhesion proteins such as E-selectin, ICAM1, VCAM1, and CX3CL1. All of these proteins have been shown to promote cell adhesion in similar flow models, and the expression of all of them was increased as a result of TNFα-stimulation in the RNA-seq study. Importantly, VCAM1 and CX3CL1 were also both inhibited by NFAT blockade, leading us to hypothesize that pharmacologic NFAT inhibition would reduce TNFα-induced PBMC adhesion under our experimental conditions. Accordingly, NFAT inhibition reduced PBMC adhesion to the endothelial monolayer, and the effect is largely attributed to NFAT inhibition of TNFα-induced VCAM1 and CX3CL1, as the other NFAT-dependent transcripts involved in leukostasis are chemoattractants, which serve no functional role in our PPFC model. Lastly, we evaluated the effect of pharmacologic NFAT inhibition in an *in vivo* model of TNFα-induced retinal leukostasis, and found that NFAT blockade significantly reduced TNFα-induced leukocyte adhesion to the retinal vasculature. Unlike in the PPFC assay, NFAT inhibition of additional TNFα-induced transcripts *CXCL10* and *CXCL11* may contribute to this effect as chemokines and leukocyte chemoattractants play a prominent role in this model by helping to recruit leukocytes to the retina.

Taken together, these initial studies identify a clear role for NFAT signaling in TNFα-induced retinal leukostasis. Which, given the importance of TNFα-signaling and retinal leukostasis in the progression of DR, suggests that NFAT signaling may represent an attractive target for therapeutics aimed at retinal leukostasis. Considering this, there are two logical extensions of this initial study. The first is an expansion of the *in vivo* studies to evaluate the effects of NFAT blockade on leukocyte adhesion and

subsequent pathologies in diabetic animals. The TNFα-induced retinal leukostasis model employed in these studies is an effective proof-of-principle study to evaluate the effects of pharmacologic NFAT inhibition in an acute inflammation context. Given the efficacy of NFAT blockade in this model, the next step is to look at the effect of NFAT inhibition in a chronic disease setting, and to expand the evaluation to include *in vivo* measurements of retinal cytokine production, vascular permeability, and endothelial apoptosis, all of which are lesions of DR that develop in diabetic animal models and have been tied to retinal leukostasis.

The second extension of these initial studies identifying NFAT signaling as a modulator of TNFα-induced retinal leukostasis, is a more thorough evaluation of the specific NFAT isoforms involved in this context. The inhibitor used in the previous studies, INCA-6, is NFAT-specific in that it binds to the discrete NFAT-binding site on CN preventing NFAT-dephosphorylation and activation without altering any other CN activity. However, it is also a general NFAT-inhibitor in that it is capable of blocking all CN-dependent NFAT isoforms through this mechanism. As a result, while these initial studies identified a clear role for NFAT signaling in TNFα-induced retinal leukostasis, they also revealed very little about the specific isoforms involved.

To address this gap in understanding, and to further characterize the involvement of NFAT signaling in TNFα-induced retinal leukostasis, we developed the techniques to target individual NFAT isoforms and utilized these techniques to evaluate the role of each isoform in TNFα-stimulated HRMEC. This study revealed unique roles for the individual isoforms in the regulation of TNFα-induced adhesion proteins and cytokines identified by the RNA-seq study, as well as identified additional NFAT gene targets that

had not previously been detected with pharmacologic inhibition (**Figures 12 & 13**). In short, NFATc2 siRNA inhibited TNFα-induced *CX3CL1*, *VCAM1*, *SELE*, and *ICAM1* expression while NFATc4 siRNA inhibited *SELE* expression as well as TNFα-induced increases in soluble CXCL10, CXCL11, and MCP-1. Conversely, NFATc1 siRNA increased TNFα-induced *ICAM1* expression and NFATc3 siRNA increased *CX3CL1* and *SELE* expression. This analysis was followed up with another PPFC study, looking at the role of individual NFAT isoforms in TNFα-induced leukocyte adhesion (**Figure 14**). In this context, NFATc2 and NFATc4 siRNA caused a decrease in TNFα-induced PBMC cell adhesion. Collectively, these studies highlight the unique contributions of individual NFAT isoforms in the response of HRMEC to TNFα, and identify NFATc2 and NFATc4 as potentially valuable therapeutic targets for the treatment of TNFα-induced retinal leukostasis.

The identification of NFATc2 and NFATc4 as regulators of TNFα-induced retinal leukostasis raises a number of additional questions suitable for investigation, most of which are related to mechanism of action. To date our studies have highlighted a clear role for NFAT signaling in TNFα-stimulated endothelial cells but have yet to identify a mechanism of action for these effects. TNFα is known to stimulate NFAT activity and intracellular Ca^{2+} flux, but the particulars of this activation have not been evaluated in HRMEC. Studies evaluating the effect of TNFα on intracellular Ca^{2+} are needed in order to fully understand how NFAT signaling comes into play downstream, and whether there is indeed direct activation of NFAT by TNFα. Initial efforts to address this later point using an NFAT-directed luciferase reporter indicate that TNFα does indeed induce

increased NFAT activity (**Appendix C**), though additional efforts to measure this activity in conjunction with isoform-specific siRNA knockdown have proved unreliable.

Another important question remaining is whether NFATc2 and NFATc4 act through direct binding and transcription of the target DNA sites. All of the targets evaluated here have been identified as NFAT target genes, but our analysis has not established whether there is direct transcription of these targets by NFAT. With the identification of NFATc2 and NFATc4, it is now considerably more feasible to do a ChIP-Seq assay to look at the direct binding of one or both of these isoforms to target gene sequences. Another aspect of target gene expression worthy of future investigation is the identification of NFAT transcriptional partners. Upon translocation to the nucleus, NFAT dimerizes with other transcription factors, and identification of those binding partners through co-immunoprecipitation would offer considerable insight into mechanism of action.

Lastly, a critical final step for evaluating the potential of NFATc2 and NFATc4 as therapeutic targets in DR would be to evaluate the effect of targeting one or both *in vivo*, using first the TNFα-induced leukostasis model and then ultimately a diabetic animal model. NFATc2 and NFATc4 knockout mice have both been generated, but have a number of confounding issues, including defects in immune cell production, a feature that would complicate their use in this context. Generation of conditional knockout mice is the most thorough way to evaluate the effect of these isoforms in the retinal endothelium under disease conditions. However, a more manageable approach might be to use intraocular injection of adeno-associated virus (AAV) transfection vectors to target individual isoforms via siRNA. This is not a technique that our lab currently

employs, so there would be considerable assay development and troubleshooting required, though the potential impact of the study is enticing. One thing to consider with regard to targeting individual NFAT isoforms *in vivo* is that there may be a beneficial effect of targeting both NFATc2 and NFATc4. The conserved nature of NFAT isoforms suggests that they play redundant roles in some contexts, so there may be an increased effect on a shared target such as E-selectin. Likewise, the fact that NFATc2 plays a role primarily in leukocyte adhesion protein expression while NFATc4 is prominently involved in the regulation of leukocyte recruitment proteins could result in a synergistic effect from targeting both *in vivo*. There may also be an increased effect on TNFα-induced PBMC adhesion in our PPFC assay, which would be relatively easy to evaluate before considering translation to the *in vivo* setting.

5.2 The role of NFAT signaling related to VEGF

The latter study presented herein focuses on the role of NFAT signaling in response to VEGF, another important signaling molecule in the development and progression of DR. VEGF, like TNFα, is able to induce microvascular complications and inflammation in the retina, and is known to both be present early in the progression of DR and contribute to the development of retinal leukostasis and vascular permeability in animal models of diabetes. VEGF also has a prominent well-established role in the development of retinal neovascularization, the critical pathology associated with PDR. In fact, anti-VEGF therapies including pegaptanib (Macugen®, Pfizer), bevacizumab (Avastin®, Genentech), and ranibizumab (Lucentis®, Genentech) have been proven highly efficacious in treating ocular neovascularization, and have recently become the primary means of addressing this pathology in PDR.[168,169] Despite their efficacy and

broadening use, a number of concerns about the continued and prolonged use of current therapies targeting this pathway remain. The requirement for frequent intravitreal injections and fluctuating levels of the antagonist in the eye between injections are both major therapeutic limitations, and there are concerns surrounding potential long-term effect of chronic treatment on retinal neurons that express the VEGF receptor and the potential for increased sensitivity to the growth factor in various ocular vascular beds. Endopthalmitis, inflammation of the intraocular cavity, is also a concern with the injection based treatment, occurring at a rate as high as 1.3% of patients per year in clinical studies, making morbidity and vision loss from treatment a rare but significant complication.[170] Lastly, anti-VEGF treatment doesn't work as effectively for everyone, and approximately 20% of patients have no response to treatment. Despite these concerns, VEGF antagonists have revolutionized the practice of ophthalmology, and clinical results clearly point to a continued need for ways to influence VEGF signaling in the context of ocular neovascularization.

With this backdrop, the final study presented herein focused on the role of NFAT signaling downstream of VEGF in both *in vitro* and *in vivo* models of retinal neovascularization. Prior to this work, the relationship between NFAT activity and VEGF signaling had not been examined in HRMEC, though VEGF had been described as an inducer of NFAT translocation and activity in a number of endothelial cell populations.[140,144,145] In these previous studies, VEGF was found to preferentially activate either NFATc1 or NFATc2 depending on the cell type, leading us to begin our evaluation by looking at the effect of VEGF treatment on NFAT isoform translocation in HRMEC (**Figure 15**). This study revealed that, similarly to human pulmonary valve

endothelial cells, VEGF treatment induces nuclear localization of NFATc1 in HRMEC.[144] Subsequent studies evaluated the role of pharmacologic NFAT blockade in *in vitro* angiogenic cell behavior assays, and found that INCA-6 treatment inhibited both VEGF- and serum-induced cell proliferation (**Figure 16**), as well as serum-induced tube formation (**Figure 17**). Based on these findings, we further evaluated the effect of pharmacologic NFAT blockade *in vivo* using both INCA-6 and the CN inhibitor FK-506 in a rat model of oxygen induced retinopathy (**Figure 18**). In this context, both INCA-6 and FK-506 significantly inhibited retinal neovascularization, without affecting normal intra-retinal vascular development. The efficacy obtained with FK-506 treatment is particularly interesting, as FK-506 marketed as Prograf® and Advagraf®, is approved for clinical use, both as an immunosuppressant to prevent organ rejection in organ and tissue transplant patients, and as a therapy for patients with severe refractory uveitis.[127-130] This feature could facilitate future translation to clinical use targeting retinal angiogenesis, but currently serves to highlight the efficacy and utility of targeting this pathway therapeutically.

Interestingly, the efficacy observed using either inhibitor in our *in vivo* model was greater than what might be predicted based on inhibition of HRMEC angiogenic behaviors in our *in vitro* experiments. One explanation might be that NFAT inhibition affects another, unrelated aspects of neovascularization. Indeed, preliminary studies in our lab (**Appendix D**) and in the context of corneal neovascularization, suggest a potential role for NFAT signaling in the regulation of retinal VEGF expression.[171] To test whether our CN/NFAT inhibitors achieved significant efficacy in part by inhibiting VEGF expression, we measured *in vivo* retinal VEGF protein levels after INCA-6 treatment as

well as the effect of INCA-6 on hypoxia-induced Müller cell VEGF production *in vitro* and found no effect (**Appendix E**). This suggests that the efficacy observed *in vivo* is largely due to inhibition of VEGF-stimulated NFAT signaling in HRMEC, though there could be additional, as yet unidentified, mechanisms that also contribute.

While the downstream targets of NFAT signaling were beyond the scope of this initial analysis, they are an intriguing avenue for further study. As was the case with our pharmacologic evaluation of NFAT signaling in the context of TNFα-induced activities, the logical extension of this VEGF study is to focus on the role of individual NFAT isoforms. The nuclear translocation analysis suggested that NFATc1 may be an important player in VEGF-signaling, and this can be confirmed using the tools developed in Chapter III to evaluate the effect of isoform-specific siRNA on HRMEC proliferation and tube formation. Based on this evaluation, the isoform, or isoforms, identified as critical regulators of these angiogenic cell behaviors in HRMEC should be further characterized in relation to VEGF signaling. The studies in Chapter II and III benefited greatly from having a restricted list of gene targets to characterize, and as a result a beneficial next step in this study would be an RNA-seq using VEGF and NFATc1 siRNA, or siRNA directed at another critical isoform, to identify VEGF-induced gene targets that are altered by this treatment. An alternative strategy would be to focus on the binding targets of the given isoform and conduct a ChIP-seq assay under VEGF-stimulated conditions to identify direct binding interactions associated with that particular isoform. From an *in vivo* perspective, targeting critical isoforms through use of AAV vectors as previously discussed, would be the ideal way to pair any isoform-specific effects identified *in vitro* with pathological effects *in vivo*.

Perhaps the most exciting future direction related to retinal VEGF and DR progression involves the further analysis of NFAT signaling in Müller glia as it relates to VEGF production. As previously discussed, VEGF plays a prominent role in early microvasculature complications and inflammation related to NPDR, and has been found elevated in vitreous prior to the onset of the PDR pathology looked at in Chapter IV. Interestingly, genetic disruption of Müller cell-derived VEGF in a mouse model of diabetes dramatically reduced inflammation-related features of DR, including leukostasis and vascular permeability, suggesting that Müller cell-derived VEGF drives pathogenic events occurring in NPDR.[172] Furthermore, high glucose has been reported to both increase intracellular Ca^{2+} levels and stimulate VEGF expression in Müller cells, suggesting a potential role for NFAT signaling in this context.[173-177] Our own preliminary studies investigating the link between hyperglycemia, NFAT signaling, and VEGF induction show that both high glucose and thapsigargin (a small molecule that increases cytosolic Ca^{2+} levels) induce VEGF, HIF-1a, and COX-2 expression in primary human Müller cells, and that NFAT blockade using FK-506 reduces high glucose-induced VEGF levels in culture media (**Appendix D**). This latter finding establishes a clear connection between NFAT-signaling and high glucose-induced Müller cell VEGF that is worthy of continued investigation. Use of the isoform specific siRNA identified in Chapter III in conjunction with a recently developed Müller cell specific transfection protocol, offer an established route toward identifying isoform-specific effects in this context and identification of one or more critical isoforms will allow for a more thorough analysis of mechanism of action. Notably, the potential role of NFAT signaling in Müller cells will be particularly important to keep in mind in the context of the proposed *in vivo*

studies involving diabetic animals, as hyperglycemia is the central driver of pathology in those models, and it will be difficult to attribute any particular effect to a given cell type using pharmacologic inhibition. While the interconnectedness of roles for NFAT in both the glial cells producing cytokines critical to DR pathology as well as the endothelial cells responding to them convolutes their study in complex *in vivo* systems, it also strengthens the case for therapeutics targeting NFAT as a treatment for DR.

CHAPTER VI

METHODS

5.1 Methods used in Chapter II

5.1.1 Retinal microvascular endothelial cell culture

Primary HRMEC (catalog #ACBRI 181) were purchased from Cell Systems (Kirkland, WA) and were cultured in flasks coated with attachment factor (Cell Signaling; Danvers, MA). Growth medium consisted of endothelial basal medium (EBM; Lonza; Walkersville, MD) supplemented with 10% FBS (Sigma Aldrich; St. Louis, MO) and endothelial cell growth supplements (EGM SingleQuots; Lonza). All cultures were incubated at 37°C, in 5% CO_2 and 95% relative humidity. Passage 3 cells were used for these experiments.

5.1.2 Treatment and RNA isolation

HRMEC were cultured to near confluence in 6-well dishes coated with attachment factor, before being serum starved (0.5% FBS in EBM) for 12hrs. Cells were then treated with TNFα (1ng/ml, Sigma-Aldrich) in the presence or absence of INCA-6 (1μM, Tocris; Minneapolis, MN). After 4hrs of treatment, cells were washed with cold Phosphate Buffered Saline (PBS; Invitrogen; Grand Island, NY) and total RNA was collected using an RNeasy kit (Qiagen; Valencia, CA, USA), according to the manufacturer's instructions.

5.1.3 RNA-seq and analysis

cDNA library preparation and sequencing

Total RNA samples were submitted to the Vanderbilt VANTAGE core for sequencing. RNA sample quality was confirmed using the 2100 Bioanalyzer (Agilent

Technologies; Santa Clara, CA). All RNA samples had an RNA integrity number > 9.0. Samples were prepared for sequencing using the TruSeq RNA Sample Prep Kit (Illumina; San Diego, CA) to enrich for mRNA and prepare cDNA libraries. Library quality was assessed using the 2100 Bioanalyzer. Sequencing was performed using a single read, 50 bp protocol on the Illumina HiSeq 2500 (Illumina). The sequence data can be found at the NCBI Short Read Archive with accession number SRP047271.

Alignment and differential expression

Sequence alignment and differential expression analyses were expedited using the Vanderbilt VANGARD core. Alignment to the UCSC human reference genome hg19 was performed using TopHat v2.0.9 with default parameters.[178] Mapped reads were then analyzed for differential expression using MultiRankSeq, which utilizes DESeq, edgeR, and baySeq algorithms.[179] Comparisons were made between the TNFα-treated group and the control group, and between the TNFα group and the TNFα plus INCA-6 group. Transcripts were filtered to those having a false discovery rate (FDR) < 0.05 in all three methods.

Pathway analysis

DAVID v6.7 was used for pathway enrichment analysis.[180,181] Lists of differentially expressed genes were submitted to the DAVID website and compared to a background of human reference genes. Pathway enrichment was determined using the KEGG Pathway annotation. Pathways were considered significantly enriched with $p<0.05$.

qRT-PCR validation

cDNA was reverse transcribed using the High-Capacity cDNA Archive Kit (Applied Biosystems; Carlsbad, CA) according to the manufacturer's instructions.

Quantitative real-time RT-PCR was performed by co-amplification of the gene of interest (*CXCL10*, *CXCL11*, *SELE*, *ICAM1*, or *VCAM1*) vs. *β-actin* (endogenous normalization control), using gene-specific TaqMan Gene Expression Assays (Applied Biosystems; **Table X**). Expression data was analyzed using the comparative Ct method. Analysis was done not only on the samples submitted for RNA-seq, but also on samples from additional biologically-independent experimental replicates.

Gene Target	Catalog No.
β-actin	Hs99999903_m1
CX3CL1	Hs00171086_m1
ICAM1	Hs00164932_m1
NFATc1	Hs00542678_m1
NFATc2	Hs00905451_m1
NFATc3	Hs00190046_m1
NFATc4	Hs00190037_m1
SELE	Hs00950401_m1
VCAM1	Hs01003372_m1

Table 7. Taqman gene expression assays used. All assays obtained from Applied Biosystems.

5.1.4 Parallel plate flow chamber assay

HRMEC were grown to confluence on attachment factor-coated glass slides, before being switched to 2% medium (2% FBS and EBM) for 8hrs. Monolayers were then stimulated for 4hrs with 2% medium, 2% medium plus TNFα (1ng/ml), or 2% medium plus TNFα and INCA-6 (1uM) in 2% medium. After treatment, slides were mounted in a rectangular parallel plate flow chamber (GlycoTech; Gaithersburg, MD) with a flow width of 1.00cm and chamber height of 0.005in. A syringe pump (World Precision Instruments; Sarasota, FL) was used to pull PBMC (Sanguine Biosciences;

Valencia, CA) suspended in Hank's Buffered Salt Solution (HBSS; Life Technologies; Carlsbad, CA) at a concentration of $2.5x10^5$ cells/ml, across HRMEC monolayers at a shear stress of 1dyn/cm^2 for 7min. Non-adherent cells were washed off with HBSS at 2dyn/cm^2 for 2min. Eight fields of view were captured from each slide using an IMT-2 inverted microscope (Olympus; Tokyo, Japan) and Q-Color3 digital camera (Olympus) at 20X magnification, then manually counted by two masked observers. Adherent cell counts of all the captured fields of a single slide were averaged and reported as adherent cells per mm^2.

5.1.5 Retinal leukostasis assay

All experiments were approved by the Vanderbilt University Institutional Animal Care and Use Committee and were performed in accordance with the ARVO Statement for the Use of Animals in Ophthalmic and Vision Research. Six-week old male C57BL/6 mice were procured from Charles Rivers (Wilmington, MA). Mice received a 2µl intravitreal injection of TNFα (50ng/ml) plus vehicle (0.1% DMSO in PBS) or INCA-6 (25µM). 6hrs later, mice were anesthetized with ketamine and xylazine and perfused with 0.9% saline, followed by FITC-conjugated concanavalin-A (40mg/ml in 2.5ml PBS). Residual non-adherent leukocytes were washed out using saline perfusion. Retinas were dissected in 4% paraformaldehyde, flat-mounted, and imaged with an AX70 upright scope (Olympus) and DP71 digital camera (Olympus) at 4X magnification, then manually counted by two masked observers. Retinal leukocyte counts for an entire retina were averaged and reported as retinal leukocytes per mm^2.

5.1.6 Statistical analyses

Data were analyzed with commercial software (JMP; SAS Institute, Cary, NC) using analysis of variance (ANOVA) and Dunnet's post hoc analyses with probability < 0.05 considered statistically significant.

5.2 Methods used in Chapter III

5.2.1 HRMEC culture and transfection

Primary HRMEC were cultured as described in 5.1.1. For transfection, cells were cultured in six-well dishes and 1ml of fresh media was added to each well 30min before treatment. For each well, 4µl of 10uM siRNA (**Table X**), 9µl Targefect Solution A (Targeting Systems, El Cajon, CA) and 18µl of Virofect (Targeting Systems) were added to 250ul Optimem (Life Technologies) in a separate tube and inverted 12 times between the addition of each reagent. Mixed reagents were incubated at 37°C for 25min and periodically inverted, before being added to each well.[182] Cells were incubated with transfection reagents for 12hrs, before being washed and treated with fresh media.

siRNA	Target Sequence	Company	Catalog No.
Control	5'-AATTCTCCGAACGTGTCACGT-3'	Qiagen	1022076
NFATc1	5'-CCGGGACCTGTGCAAGCCGAA-3'	Qiagen	SI03082422
	5'-TCCGACATTGAACTTCGGAAA-3'	Qiagen	SI00099512
NFATc2	5'-CTGGTCTATGGCGGCCAGCAA-3'	Qiagen	SI00099512
NFATc3	5'-CCGGGAGACTTCAATAGATGA-3'	Qiagen	SI00157997
NFATc4	5'-AAGGCTTACAGCACTATATGA-3'	Santa Cruz	sc-38115

Table 8. Selected siRNA oligos for individual NFAT isoforms. NFATc1 siRNA was a cocktail of the two oligos listed.

5.2.2 qRT-PCR analysis of transfected HRMEC

HRMEC were seeded in 6-well plates at 2 x 10^5 cells/well and maintained under growth conditions. At 75% confluence, HRMEC were transfected with Control, NFATc1,

NFATc2, NFATc3, or NFATc4 siRNA as described above. 12hrs post-transfection, cells were switched to 2% medium for 12hrs, before being placed in 0.5% medium for an additional 8hrs. Cells were then stimulated with 0.5% medium or 0.5% medium plus TNFα (1ng/ml) for 4hrs. After treatment, cells were washed with cold PBS and total RNA collected using an RNeasy kit. Total RNA was reverse transcribed and qRT-PCR was performed by co-amplification of the gene of interest (*NFATc1*, *NFATc2*, *NFATc3*, *NFATc4*, *CX3CL1, VCAM1, SELE, or ICAM1*) vs *β-actin*, using gene-specific TaqMan Gene Expression Assays (**Table 7)**. Expression data was analyzed using the comparative Ct method.

5.2.3 Soluble protein quantification

HRMEC were seeded in 6-well plates and grown to 75% confluence, before being transfected with Control, NFATc1, NFATc2, NFATc3, or NFATc4 siRNA as described above. 12hrs post-transfection, cells were switched to 2% medium for 12hrs, before being placed in 0.5% medium for an additional 6hrs. Cells were then stimulated with either 0.5% medium or 0.5% medium plus TNFα (1ng/ml) for 6hrs. After treatment, culture medium was collected and assayed for secreted CXCL10, CXCL11, MCP-1, and IL-6 protein concentrations using protein specific colorimetric sandwich ELISA kits (R&D Systems; Minneapolis, MN). Cells were washed with cold PBS and lysed using CellLytic lysis buffer (Sigma Aldrich), and the concentration of cell lysates was determined using a bicinchoninic acid assay (Pierce; Rockford, IL). Secreted protein concentrations were normalized to total protein of corresponding cell lysates and reported as pg/mg of total cellular protein.

5.2.4 Parallel plate flow chamber assay

HRMEC were grown to confluence on attachment factor-coated glass slides and transfected with Control, NFATc1, NFATc2, NFATc3, or NFATc4 siRNA as described above. 12hrs post-transfection, cells were switched to 2% medium for an additional 20hrs. Cells were then stimulated with fresh 2% medium or 2% medium plus TNFα (1ng/ml) for 4hrs. After treatment, slides were mounted into the parallel plate flow chamber and assayed as described in **5.1.7**.

5.2.5 Statistical analyses

Data were analyzed with JMP using ANOVA and Dunnet's post hoc analyses with $p<0.05$ considered statistically significant.

5.3 Methods used in Chapter IV

5.3.1 Immunocytochemistry

HRMEC were cultured on multi-well glass slides to near confluence, before being serum starved for 12hrs. Cells were then treated with VEGF (25ng/ml, Millipore; Billerica, MA) in the presence or absence INCA-6 (1.0μM). Thirty mins after treatment, cells were fixed with 4% paraformaldehyde and 1% Triton X-100 in PBS. Wells were then incubated with primary antibody (NFATc1: sc-13033; Santa Cruz Biotech) overnight at 4°C. After incubation, wells were washed and incubated with secondary antibody. Samples were viewed and imaged with a Zeiss LSM 510 inverted confocal microscope (Carl Zeiss Microscopy LLC; Thornwood, NY).

5.3.2 HRMEC proliferation assay

HRMEC were seeded at 3 X 10^3 cells/well in a 96-well plate containing standard growth medium for 8hrs to allow them to settle and attach. Cells were then serum-

starved for 12hrs before being treated with either 10% serum or VEGF (25ng/ml in medium containing 0.5% serum) in the presence or absence of the inhibitor INCA-6 (0.5, 1, or 2.5μM). After 24hrs of treatment, cells were labeled with BrdU labeling solution for an additional 12hrs, and BrdU incorporation was quantified using a colorimetric BrdU ELISA (Roche; Indianapolis, IN), according to the manufacturer's instructions. Absorbance values were normalized to the 0.5% serum control for each experiment.

5.3.3 HRMEC tube formation assay

24-well tissue culture plates were coated with 350μl of growth factor-reduced Matrigel® (Becton Dickenson, Franklin Lakes, NJ). HRMEC were seeded at 2.5 X 10^4 cells/well and treated with 10% serum in the presence or absence of INCA-6 (1 or 2.5μM). Tubes were imaged 12hrs after treatment, using a Nikon Eclipse Ti microscope (Nikon; Melville, NY, USA) and Nikon DS-Fi1 camera at 2X magnification. Image J software (NIH; Bethesda, MD, USA) was used to determine the mean tube length per unit area, and these values were normalized to a 0.5% serum control for each experiment.

5.3.4 Oxygen-induced retinopathy model

All animal procedures used in this study were approved by the Vanderbilt University Institutional Animal Care and Use Committee and were performed in accordance with the ARVO Statement for the Use of Animals in Ophthalmic and Vision Research. Within 8 hrs after birth, litters of Sprague-Dawley rat pups and their mothers (Charles Rivers) were transferred to oxygen exposure chambers in which they were

subjected to alternating 24hr periods of 50% and 10% oxygen for 14 days.[183] On postnatal day 14 [14(0)], the oxygen-exposed rats were removed to room air.

Intravitreal Injections

Rats were anesthetized by isoflurane (Butler Animal Health Supply; Dublin, OH) inhalation and a drop of 0.5% proparacaine (Allergan; Hormigueros, PR) was topically applied to the cornea before intravitreal injection. The globe was penetrated approximately 0.5 mm posterior to the ora ciliaris, using a 30-gauge needle with a 19° bevel and 10-µL syringe (Hamilton Co.; Reno, NV). The needle was advanced to the posterior vitreous at a steep angle to avoid contact with the lens. The injection bolus (5 µL) was delivered near the trunk of the hyaloid artery proximal to the posterior pole of the retina.[184-186] After injection, a topical antibiotic suspension (Vigamox; Alcon Laboratories; Fort Worth, TX) was applied. Non-injected eyes were also treated with topical proparacaine and antibiotic to control for the potential of these agents to influence retinal vessel growth. Subsets of oxygen-exposed rats were administered vehicle (0.1% DMSO in PBS) INCA-6 (2.5, 5, or 25µM) or FK-506 (2.5, 5, or 25µM; Tocris) by intravitreal injection on days 14(0) and 14(3). Non-injected animals were used as controls. Age matched room air pups, also received two injections of either vehicle, INCA-6 (25µM), or FK-506 (25µM) on days 14(0) and 14(3).

Quantification of Retinal Neovascularization

On day 14(6), all rats were sacrificed and their retinas dissected. After dissection, the retinal vasculature was stained for adenosine diphosphatase activity, according to well-established procedures.[183,184] Images of adenosine diphosphatase-stained retinas were digitized, and pre-retinal vessel tufts were measured by computer-assisted image

analysis. Data are reported in square millimeters. The data shown is normalized to neovascularization values from vehicle-treated eyes of each experimental group.

APPENDIX A

Sustained knockdown of *NFATc1* expression

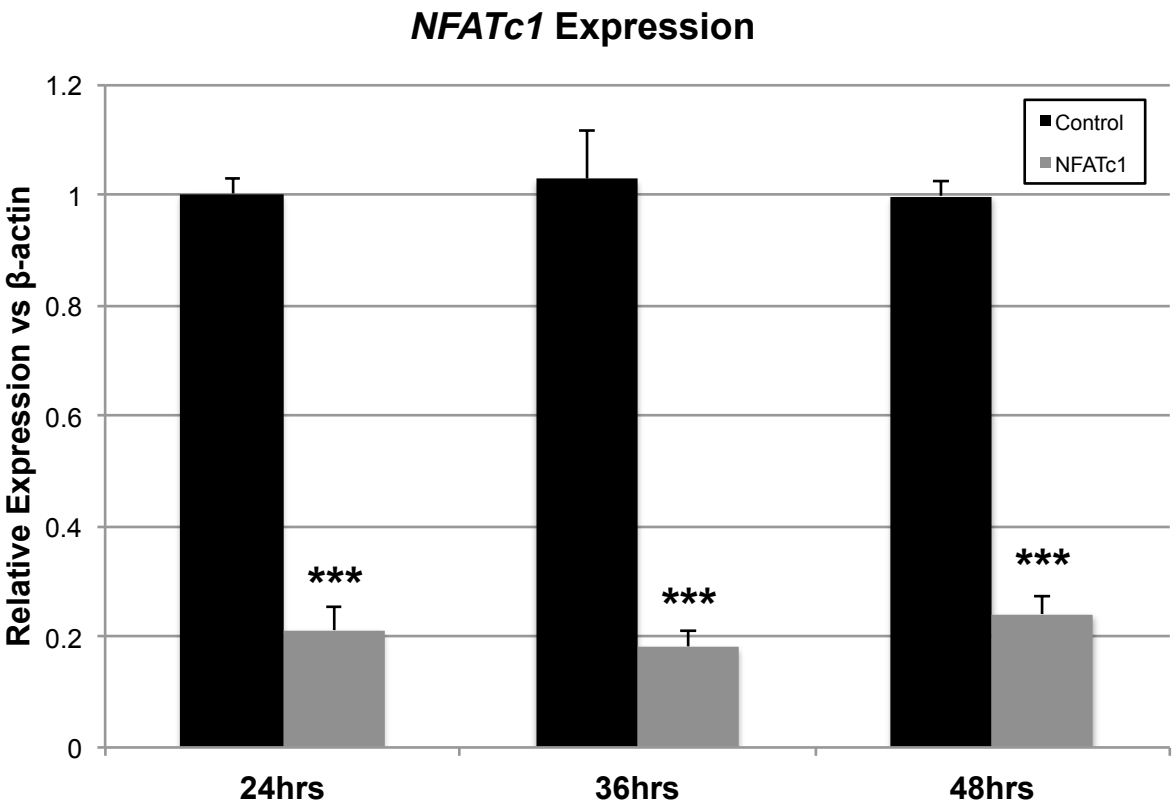

Sustained knockdown of *NFATc1* expression. HRMEC were transfected with control or NFATc1 siRNA for 24, 36, and 48hrs before collection and qRT-PCR analysis. *** = $p<0.001$

APPENDIX B

Effect of NFATc1 siRNA on VEGF-induced IL-6

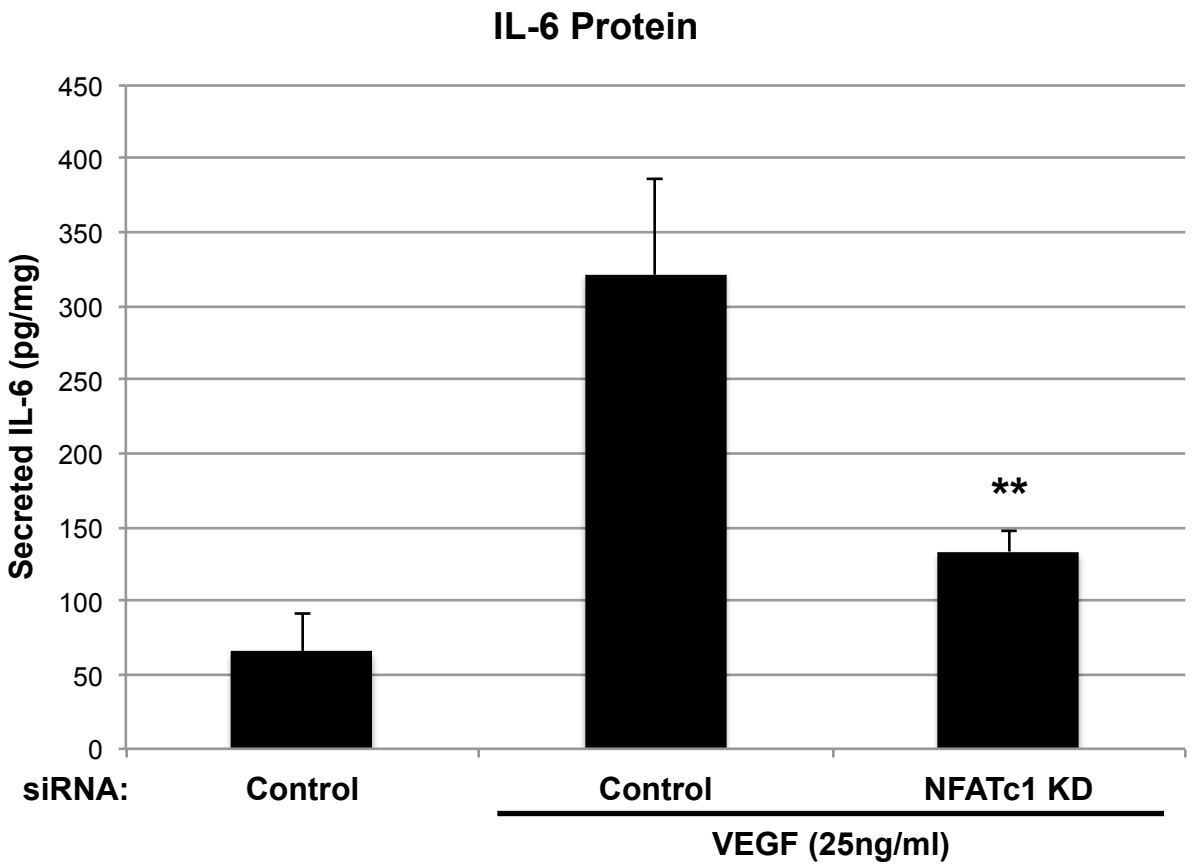

Effect of NFATc1 siRNA on VEGF-induced IL-6 production. HRMEC transfected with either control or NFATc1 siRNA were treated with VEGF (25ng/ml) for 12hrs. Conditioned media was then collected and analyzed for secreted Il-6 using ELISA. ** = $p<0.01$

APPENDIX C

Effect of TNFα treatment on NFAT-luciferase activity

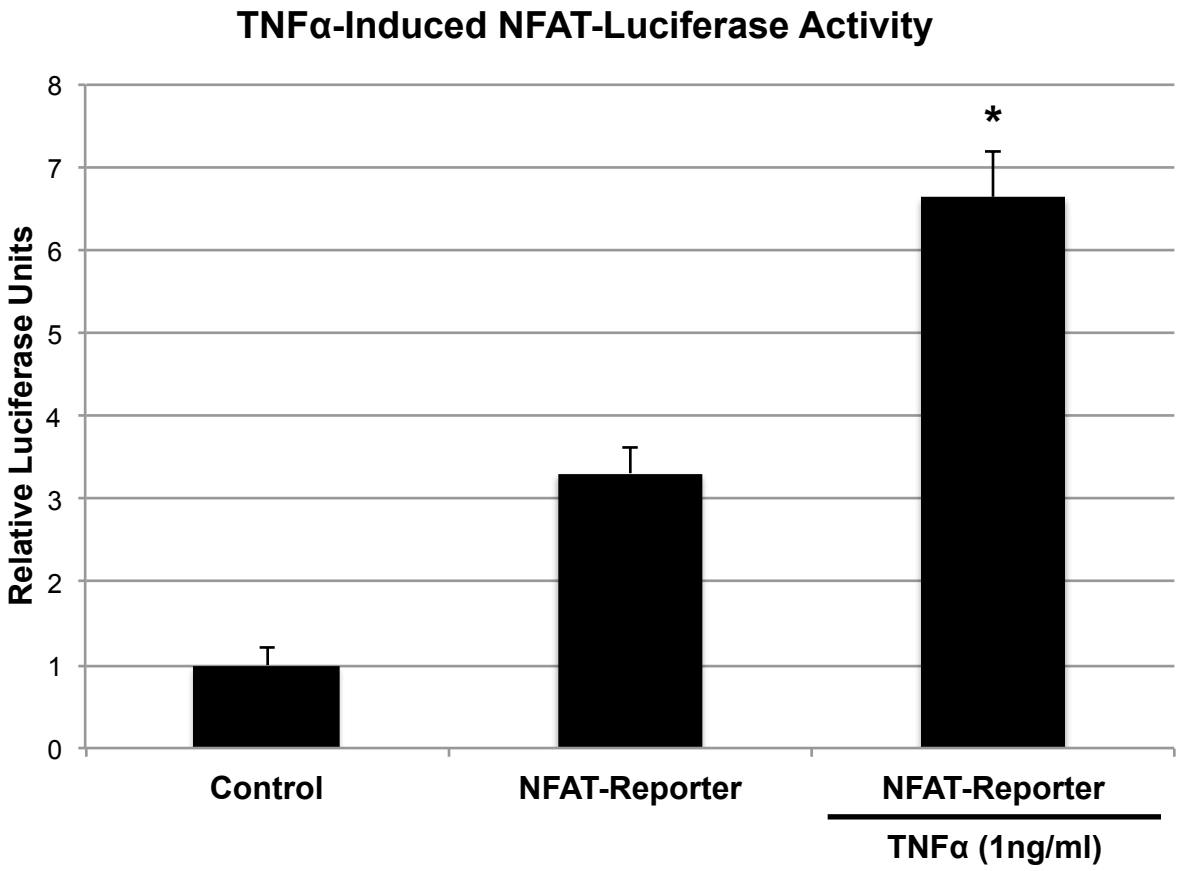

Effect of TNFα treatment on NFAT-luciferase activity. HRMEC were transfected with either a control or NFAT-luciferase reporter construct for 24hrs, after which cells were treated with TNFα (1ng/ml) for 4hrs then lysed and assayed for luciferase activity. * = $p<0.05$

APPENDIX D

Effect of pharmacologic NFAT inhibition on high-glucose induced VEGF production in Müller cells

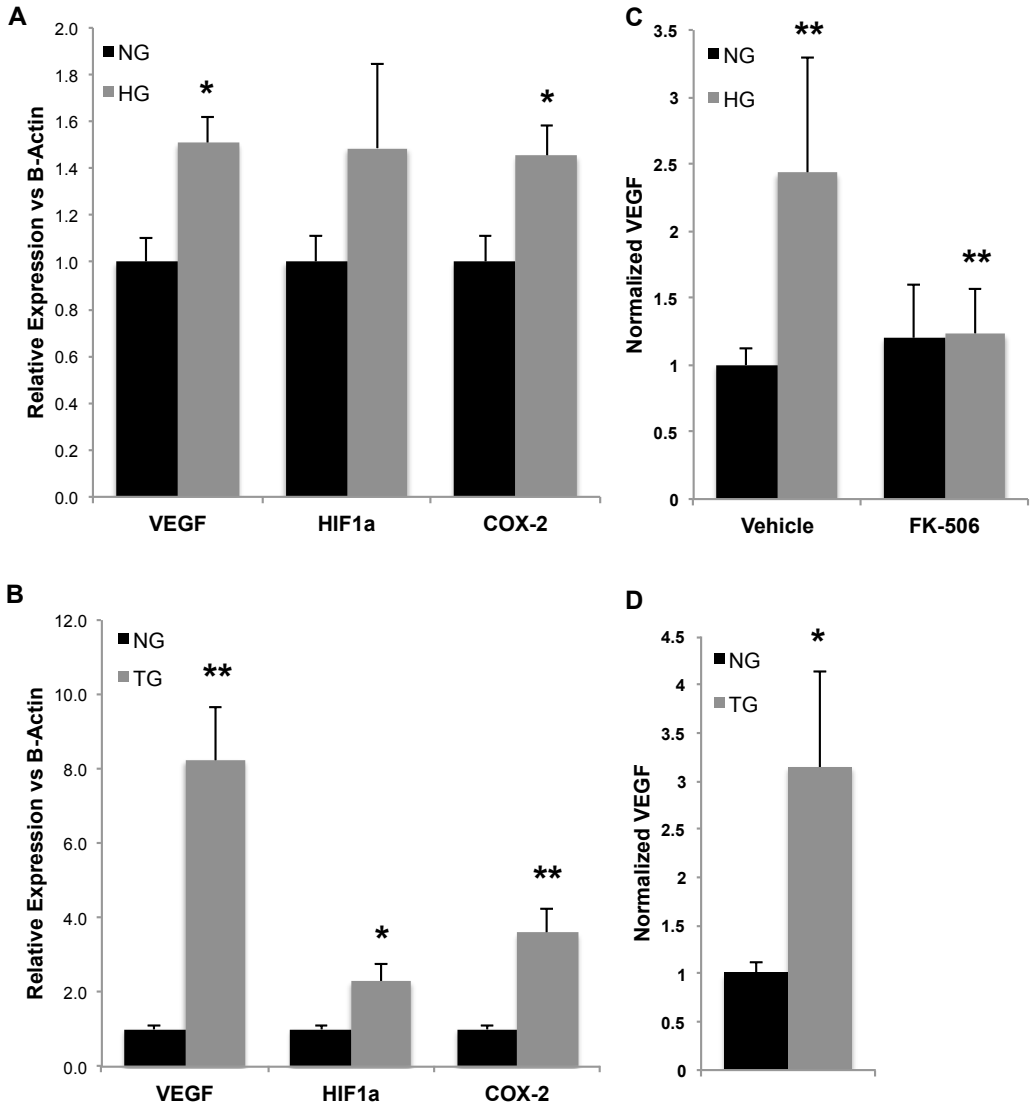

High glucose induction of VEGF in Müller cells is Ca^{2+}- and CN-dependent. A) Treatment of primary human Müller cells with glucose (25mM) for 24hrs induced expression of the target genes VEGF, HIF-1a, and COX-2, relative to normal glucose. **B)** This induction was mimicked by increasing intracellular calcium levels with TG (100nM) over the same time in normal glucose. **C)** High glucose treatment for 48hrs caused a 2.4-fold increase in secreted VEGF. This induction was eliminated by co-treatment with FK-506 (1μM). **D)** Treatment with 100nM thapsigargin for 24hrs caused a 3.2-fold increase in secreted VEGF. NG = normal glucose; HG = high glucose; TG = thapsigargin. * =p<0.05; ** =p<0.01

APPENDIX E

Effect of pharmacologic NFAT inhibition on hypoxia induced VEGF

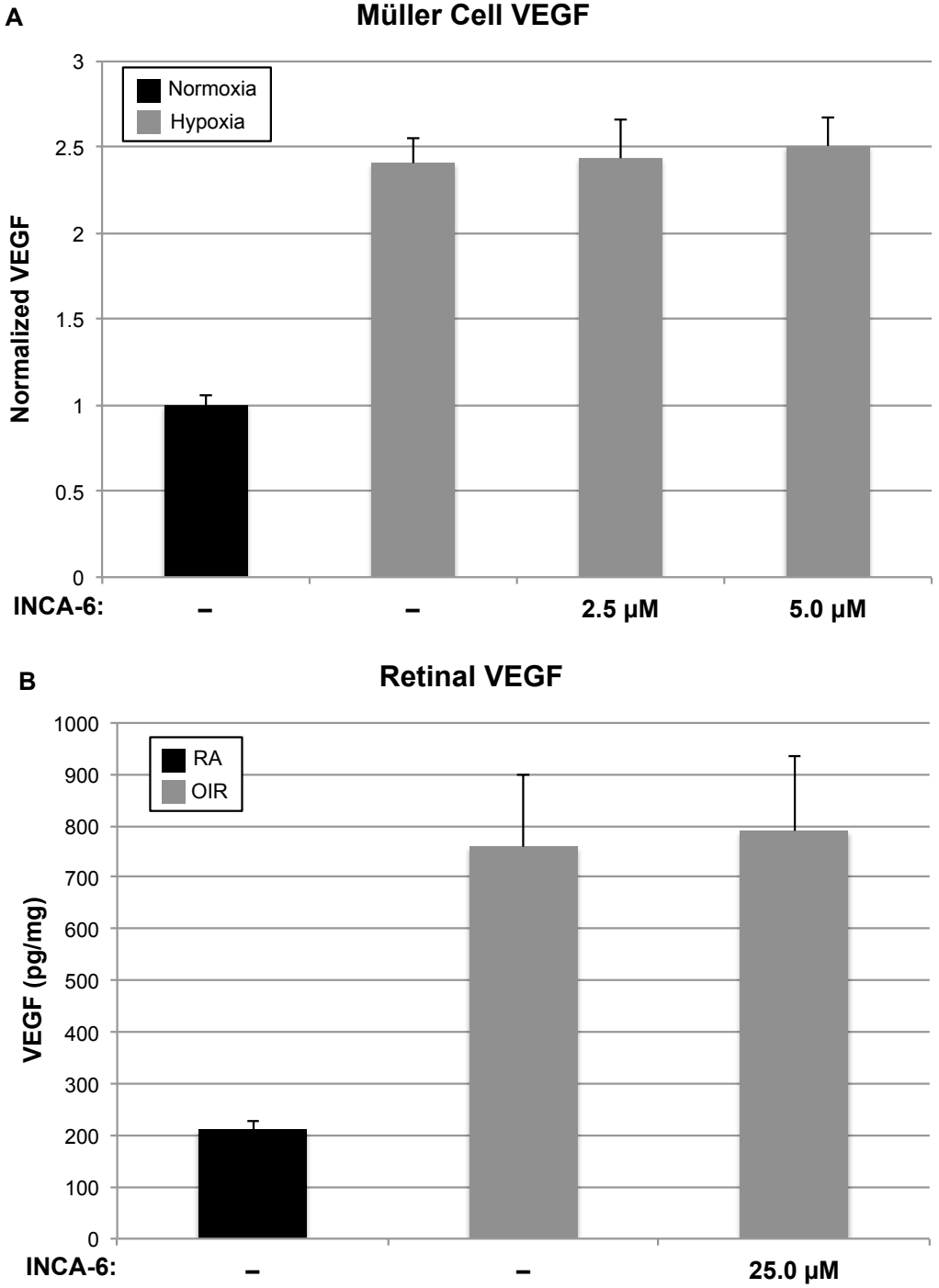

A) Effect of INCA-6 on hypoxia induced Müller cell VEGF. INCA-6 treatment did not significantly affect hypoxia induced VEGF production. Each bar represents the mean ± SEM (n=9). **B) Effect of INCA-6 on retinal VEGF levels in OIR retinas.** INCA-6 treatment did not significantly affect retinal VEGF protein levels following OIR treatment. Each bar represents the mean ± SEM (n=9).

REFERENCES

1. Brownlee M. The pathobiology of diabetic complications: a unifying mechanism. Diabetes. 2005;54(6):1615-25.

2. Atkinson MA. The pathogenesis and natural history of type 1 diabetes. Cold Spring Harbor perspectives in medicine. 2012;2(11). PMCID: PMC3543105.

3. Federation ID. IDF Diabetes Atlas, 6th edn. Brussels, Belgium: International Diabetes Federation; 2013.

4. Yau JW, Rogers SL, Kawasaki R, Lamoureux EL, Kowalski JW, Bek T, et al. Global prevalence and major risk factors of diabetic retinopathy. Diabetes care. 2012;35(3):556-64. PMCID: PMC3322721.

5. The effect of intensive treatment of diabetes on the development and progression of long-term complications in insulin-dependent diabetes mellitus. The Diabetes Control and Complications Trial Research Group. The New England journal of medicine. 1993;329(14):977-86.

6. Tight blood pressure control and risk of macrovascular and microvascular complications in type 2 diabetes: UKPDS 38. UK Prospective Diabetes Study Group. Bmj. 1998;317(7160):703-13. PMCID: PMC28659.

7. Kern TS. Contributions of inflammatory processes to the development of the early stages of diabetic retinopathy. Experimental diabetes research. 2007;2007:95103. PMCID: PMC2216058.

8. Stitt AW, Gardiner TA, Archer DB. Histological and ultrastructural investigation of retinal microaneurysm development in diabetic patients. The British journal of ophthalmology. 1995;79(4):362-7. PMCID: PMC505103.

9. Nunes S, Pires I, Rosa A, Duarte L, Bernardes R, Cunha-Vaz J. Microaneurysm turnover is a biomarker for diabetic retinopathy progression to clinically significant macular edema: findings for type 2 diabetics with nonproliferative retinopathy. Ophthalmologica Journal international d'ophtalmologie International journal of ophthalmology Zeitschrift fur Augenheilkunde. 2009;223(5):292-7.

10. Antonetti DA, Klein R, Gardner TW. Diabetic retinopathy. The New England journal of medicine. 2012;366(13):1227-39.

11. Newman DK. Surgical management of the late complications of proliferative diabetic retinopathy. Eye (Lond). 2010;24(3):441-9.

12. Antonetti DA, Lieth E, Barber AJ, Gardner TW. Molecular mechanisms of vascular permeability in diabetic retinopathy. Seminars in ophthalmology. 1999;14(4):240-8.

13. Muqit MM, Marcellino GR, Henson DB, Young LB, Patton N, Charles SJ, et al. Optos-guided pattern scan laser (Pascal)-targeted retinal photocoagulation in proliferative diabetic retinopathy. Acta ophthalmologica. 2013;91(3):251-8.

14. Maeshima K, Utsugi-Sutoh N, Otani T, Kishi S. Progressive enlargement of scattered photocoagulation scars in diabetic retinopathy. Retina. 2004;24(4):507-11.

15. Powell ED, Field RA. Diabetic Retinopathy and Rheumatoid Arthritis. Lancet. 1964;2(7349):17-8.

16. Kim SJ, Flach AJ, Jampol LM. Nonsteroidal anti-inflammatory drugs in ophthalmology. Survey of ophthalmology. 2010;55(2):108-33.

17. Effects of aspirin treatment on diabetic retinopathy. ETDRS report number 8. Early Treatment Diabetic Retinopathy Study Research Group. Ophthalmology. 1991;98(5 Suppl):757-65.

18. Kern TS, Miller CM, Du Y, Zheng L, Mohr S, Ball SL, et al. Topical administration of nepafenac inhibits diabetes-induced retinal microvascular disease and underlying abnormalities of retinal metabolism and physiology. Diabetes. 2007;56(2):373-9.

19. Tsilimbaris MK, Panagiotoglou TD, Charisis SK, Anastasakis A, Krikonis TS, Christodoulakis E. The use of intravitreal etanercept in diabetic macular oedema. Seminars in ophthalmology. 2007;22(2):75-9.

20. Sfikakis PP, Markomichelakis N, Theodossiadis GP, Grigoropoulos V, Katsilambros N, Theodossiadis PG. Regression of sight-threatening macular edema in type 2 diabetes following treatment with the anti-tumor necrosis factor monoclonal antibody infliximab. Diabetes care. 2005;28(2):445-7.

21. Joussen AM, Poulaki V, Mitsiades N, Kirchhof B, Koizumi K, Dohmen S, et al. Nonsteroidal anti-inflammatory drugs prevent early diabetic retinopathy via TNF-alpha suppression. Faseb J. 2002;16(3):438-40.

22. Stefanini FR, Arevalo JF, Maia M. Bevacizumab for the management of diabetic macular edema. World journal of diabetes. 2013;4(2):19-26. PMCID: PMC3627413.

23. Pacella E, La Torre G, Impallara D, Malarska K, Turchetti P, Brillante C, et al. Efficacy and safety of the intravitreal treatment of diabetic macular edema with pegaptanib: a 12-month follow-up. La Clinica terapeutica. 2013;164(2):e121-6.

24. Gragoudas ES, Adamis AP, Cunningham ET, Jr., Feinsod M, Guyer DR, Group VISiONCT. Pegaptanib for neovascular age-related macular degeneration. The New England journal of medicine. 2004;351(27):2805-16.

25. Nguyen QD, Shah SM, Khwaja AA, Channa R, Hatef E, Do DV, et al. Two-year outcomes of the ranibizumab for edema of the mAcula in diabetes (READ-2) study. Ophthalmology. 2010;117(11):2146-51.

26. Treatment for wet macular degeneration. FDA Consum. 2006;40(5):6.

27. Boyer DS, Hopkins JJ, Sorof J, Ehrlich JS. Anti-vascular endothelial growth factor therapy for diabetic macular edema. Therapeutic advances in endocrinology and metabolism. 2013;4(6):151-69. PMCID: PMC3855829.

28. Nguyen QD, Brown DM, Marcus DM, Boyer DS, Patel S, Feiner L, et al. Ranibizumab for diabetic macular edema: results from 2 phase III randomized trials: RISE and RIDE. Ophthalmology. 2012;119(4):789-801.

29. Sang DN, D'Amore PA. Is blockade of vascular endothelial growth factor beneficial for all types of diabetic retinopathy? Diabetologia. 2008;51(9):1570-3.

30. Wirostko B, Wong TY, Simo R. Vascular endothelial growth factor and diabetic complications. Prog Retin Eye Res. 2008;27(6):608-21.

31. Antonetti DA, Barber AJ, Bronson SK, Freeman WM, Gardner TW, Jefferson LS, et al. Diabetic retinopathy: seeing beyond glucose-induced microvascular disease. Diabetes. 2006;55(9):2401-11.

32. Adamis AP, Berman AJ. Immunological mechanisms in the pathogenesis of diabetic retinopathy. Seminars in immunopathology. 2008;30(2):65-84.

33. Gardner TW, Antonetti DA, Barber AJ, LaNoue KF, Levison SW. Diabetic retinopathy: more than meets the eye. Survey of ophthalmology. 2002;47 Suppl 2:S253-62.

34. Joussen AM, Poulaki V, Le ML, Koizumi K, Esser C, Janicki H, et al. A central role for inflammation in the pathogenesis of diabetic retinopathy. Faseb J. 2004;18(12):1450-2.

35. Giacco F, Brownlee M. Oxidative stress and diabetic complications. Circulation research. 2010;107(9):1058-70. PMCID: PMC2996922.

36. Vlassara H, Striker GE. Advanced glycation endproducts in diabetes and diabetic complications. Endocrinology and metabolism clinics of North America. 2013;42(4):697-719.

37. Curtis TM, Scholfield CN. The role of lipids and protein kinase Cs in the pathogenesis of diabetic retinopathy. Diabetes/metabolism research and reviews. 2004;20(1):28-43.

38. Bhagat N, Grigorian RA, Tutela A, Zarbin MA. Diabetic macular edema: pathogenesis and treatment. Survey of ophthalmology. 2009;54(1):1-32.

39. Murugeswari P, Shukla D, Rajendran A, Kim R, Namperumalsamy P, Muthukkaruppan V. Proinflammatory cytokines and angiogenic and anti-angiogenic factors in vitreous of patients with proliferative diabetic retinopathy and eales' disease. Retina. 2008;28(6):817-24.

40. Demircan N, Safran BG, Soylu M, Ozcan AA, Sizmaz S. Determination of vitreous interleukin-1 (IL-1) and tumour necrosis factor (TNF) levels in proliferative diabetic retinopathy. Eye (Lond). 2006;20(12):1366-9.

41. Tang J, Kern TS. Inflammation in diabetic retinopathy. Progress in retinal and eye research. 2011;30(5):343-58. PMCID: PMC3433044.

42. Gustavsson C, Agardh E, Bengtsson B, Agardh CD. TNF-alpha is an independent serum marker for proliferative retinopathy in type 1 diabetic patients. Journal of diabetes and its complications. 2008;22(5):309-16.

43. Funatsu H, Yamashita H, Noma H, Mimura T, Nakamura S, Sakata K, et al. Aqueous humor levels of cytokines are related to vitreous levels and progression of diabetic retinopathy in diabetic patients. Graefe's archive for clinical and experimental ophthalmology = Albrecht von Graefes Archiv fur klinische und experimentelle Ophthalmologie. 2005;243(1):3-8.

44. Aiello LP, Avery RL, Arrigg PG, Keyt BA, Jampel HD, Shah ST, et al. Vascular endothelial growth factor in ocular fluid of patients with diabetic retinopathy and other retinal disorders. The New England journal of medicine. 1994;331(22):1480-7.

45. Boulton M, Foreman D, Williams G, McLeod D. VEGF localisation in diabetic retinopathy. The British journal of ophthalmology. 1998;82(5):561-8. PMCID: PMC1722605.

46. Amin RH, Frank RN, Kennedy A, Eliott D, Puklin JE, Abrams GW. Vascular endothelial growth factor is present in glial cells of the retina and optic nerve of human subjects with nonproliferative diabetic retinopathy. Investigative ophthalmology & visual science. 1997;38(1):36-47.

47. Joussen AM, Doehmen S, Le ML, Koizumi K, Radetzky S, Krohne TU, et al. TNF-alpha mediated apoptosis plays an important role in the development of early diabetic retinopathy and long-term histopathological alterations. Molecular vision. 2009;15:1418-28. PMCID: PMC2716944.

48. Abcouwer SF. Angiogenic Factors and Cytokines in Diabetic Retinopathy. Journal of clinical & cellular immunology. 2013;Suppl 1(11). PMCID: PMC3852182.

49. Aveleira CA, Lin CM, Abcouwer SF, Ambrosio AF, Antonetti DA. TNF-alpha signals through PKCzeta/NF-kappaB to alter the tight junction complex and increase retinal endothelial cell permeability. Diabetes. 2010;59(11):2872-82. PMCID: PMC2963546.

50. Harhaj NS, Felinski EA, Wolpert EB, Sundstrom JM, Gardner TW, Antonetti DA. VEGF activation of protein kinase C stimulates occludin phosphorylation and contributes to endothelial permeability. Investigative ophthalmology & visual science. 2006;47(11):5106-15.

51. Desai TR, Leeper NJ, Hynes KL, Gewertz BL. Interleukin-6 causes endothelial barrier dysfunction via the protein kinase C pathway. The Journal of surgical research. 2002;104(2):118-23.

52. Huang H, Gandhi JK, Zhong X, Wei Y, Gong J, Duh EJ, et al. TNFαlpha is required for late BRB breakdown in diabetic retinopathy, and its inhibition prevents leukostasis and protects vessels and neurons from apoptosis. Investigative ophthalmology & visual science. 2011;52(3):1336-44. PMCID: PMC3101693.

53. Lutty GA, Cao J, McLeod DS. Relationship of polymorphonuclear leukocytes to capillary dropout in the human diabetic choroid. The American journal of pathology. 1997;151(3):707-14. PMCID: PMC1857840.

54. Kim SY, Johnson MA, McLeod DS, Alexander T, Hansen BC, Lutty GA. Neutrophils are associated with capillary closure in spontaneously diabetic monkey retinas. Diabetes. 2005;54(5):1534-42.

55. Tang S, Luo Y, Hu J, Lin S. [Activated T lymphocytes in epiretinal membranes from eyes of patients with proliferative diabetic retinopathy]. Yan ke xue bao = Eye science / "Yan ke xue bao" bian ji bu. 1999;15(4):229-32.

56. Miyamoto K, Khosrof S, Bursell SE, Rohan R, Murata T, Clermont AC, et al. Prevention of leukostasis and vascular leakage in streptozotocin-induced diabetic retinopathy via intercellular adhesion molecule-1 inhibition. Proceedings of the National Academy of Sciences of the United States of America. 1999;96(19):10836-41. PMCID: PMC17969.

57. Ley K. Functions of selectins. Results and problems in cell differentiation. 2001;33:177-200.

58. Asa D, Raycroft L, Ma L, Aeed PA, Kaytes PS, Elhammer AP, et al. The P-selectin glycoprotein ligand functions as a common human leukocyte ligand for P- and E-selectins. The Journal of biological chemistry. 1995;270(19):11662-70.

59. McEver RP. Selectins: lectins that initiate cell adhesion under flow. Current opinion in cell biology. 2002;14(5):581-6.

60. Noda K, Nakao S, Ishida S, Ishibashi T. Leukocyte adhesion molecules in diabetic retinopathy. Journal of ophthalmology. 2012;2012:279037. PMCID: PMC3216271.

61. Ulbrich H, Eriksson EE, Lindbom L. Leukocyte and endothelial cell adhesion molecules as targets for therapeutic interventions in inflammatory disease. Trends in pharmacological sciences. 2003;24(12):640-7.

62. Hogg N, Patzak I, Willenbrock F. The insider's guide to leukocyte integrin signalling and function. Nature reviews Immunology. 2011;11(6):416-26.

63. Umehara H, Bloom ET, Okazaki T, Nagano Y, Yoshie O, Imai T. Fractalkine in vascular biology: from basic research to clinical disease. Arteriosclerosis, thrombosis, and vascular biology. 2004;24(1):34-40.

64. Fong AM, Robinson LA, Steeber DA, Tedder TF, Yoshie O, Imai T, et al. Fractalkine and CX3CR1 mediate a novel mechanism of leukocyte capture, firm adhesion, and activation under

physiologic flow. The Journal of experimental medicine. 1998;188(8):1413-9. PMCID: PMC2213407.

65. Haskell CA, Cleary MD, Charo IF. Molecular uncoupling of fractalkine-mediated cell adhesion and signal transduction. Rapid flow arrest of CX3CR1-expressing cells is independent of G-protein activation. The Journal of biological chemistry. 1999;274(15):10053-8.

66. Bazan JF, Bacon KB, Hardiman G, Wang W, Soo K, Rossi D, et al. A new class of membrane-bound chemokine with a CX3C motif. Nature. 1997;385(6617):640-4.

67. Almulki L, Noda K, Nakao S, Hisatomi T, Thomas KL, Hafezi-Moghadam A. Localization of vascular adhesion protein-1 (VAP-1) in the human eye. Experimental eye research. 2010;90(1):26-32. PMCID: PMC2826198.

68. Soedamah-Muthu SS, Chaturvedi N, Schalkwijk CG, Stehouwer CD, Ebeling P, Fuller JH, et al. Soluble vascular cell adhesion molecule-1 and soluble E-selectin are associated with micro- and macrovascular complications in Type 1 diabetic patients. Journal of diabetes and its complications. 2006;20(3):188-95.

69. Nowak M, Wielkoszynski T, Marek B, Kos-Kudla B, Swietochowska E, Sieminska L, et al. Blood serum levels of vascular cell adhesion molecule (sVCAM-1), intercellular adhesion molecule (sICAM-1) and endothelial leucocyte adhesion molecule-1 (ELAM-1) in diabetic retinopathy. Clinical and experimental medicine. 2008;8(3):159-64.

70. Adamiec-Mroczek J, Oficjalska-Mlynczak J, Misiuk-Hojlo M. Proliferative diabetic retinopathy-The influence of diabetes control on the activation of the intraocular molecule system. Diabetes research and clinical practice. 2009;84(1):46-50.

71. Limb GA, Hickman-Casey J, Hollifield RD, Chignell AH. Vascular adhesion molecules in vitreous from eyes with proliferative diabetic retinopathy. Investigative ophthalmology & visual science. 1999;40(10):2453-7.

72. McLeod DS, Lefer DJ, Merges C, Lutty GA. Enhanced expression of intracellular adhesion molecule-1 and P-selectin in the diabetic human retina and choroid. The American journal of pathology. 1995;147(3):642-53. PMCID: PMC1870979.

73. Joussen AM, Murata T, Tsujikawa A, Kirchhof B, Bursell SE, Adamis AP. Leukocyte-mediated endothelial cell injury and death in the diabetic retina. The American journal of pathology. 2001;158(1):147-52. PMCID: PMC1850259.

74. Gustavsson C, Agardh CD, Zetterqvist AV, Nilsson J, Agardh E, Gomez MF. Vascular cellular adhesion molecule-1 (VCAM-1) expression in mice retinal vessels is affected by both hyperglycemia and hyperlipidemia. PloS one. 2010;5(9):e12699. PMCID: PMC2938334.

75. Imaizumi T, Matsumiya T, Fujimoto K, Okamoto K, Cui X, Ohtaki U, et al. Interferon-gamma stimulates the expression of CX3CL1/fractalkine in cultured human endothelial cells. The Tohoku journal of experimental medicine. 2000;192(2):127-39.

76. You JJ, Yang CH, Huang JS, Chen MS, Yang CM. Fractalkine, a CX3C chemokine, as a mediator of ocular angiogenesis. Investigative ophthalmology & visual science. 2007;48(11):5290-8.

77. Jones BA, Beamer M, Ahmed S. Fractalkine/CX3CL1: a potential new target for inflammatory diseases. Molecular interventions. 2010;10(5):263-70. PMCID: PMC3002219.

78. Schroder S, Palinski W, Schmid-Schonbein GW. Activated monocytes and granulocytes, capillary nonperfusion, and neovascularization in diabetic retinopathy. The American journal of pathology. 1991;139(1):81-100. PMCID: PMC1886150.

79. Taub DD, Lloyd AR, Conlon K, Wang JM, Ortaldo JR, Harada A, et al. Recombinant human interferon-inducible protein 10 is a chemoattractant for human monocytes and T lymphocytes and promotes T cell adhesion to endothelial cells. The Journal of experimental medicine. 1993;177(6):1809-14. PMCID: PMC2191047.

80. Charo IF, Taubman MB. Chemokines in the pathogenesis of vascular disease. Circulation research. 2004;95(9):858-66.

81. Porter JC, Falzon M, Hall A. Polarized localization of epithelial CXCL11 in chronic obstructive pulmonary disease and mechanisms of T cell egression. Journal of immunology. 2008;180(3):1866-77. PMCID: PMC2274894.

82. Nawaz MI, Van Raemdonck K, Mohammad G, Kangave D, Van Damme J, Abu El-Asrar AM, et al. Autocrine CCL2, CXCL4, CXCL9 and CXCL10 signal in retinal endothelial cells and are enhanced in diabetic retinopathy. Experimental eye research. 2013;109:67-76.

83. Elner SG, Elner VM, Jaffe GJ, Stuart A, Kunkel SL, Strieter RM. Cytokines in proliferative diabetic retinopathy and proliferative vitreoretinopathy. Curr Eye Res. 1995;14(11):1045-53.

84. Mitamura Y, Takeuchi S, Yamamoto S, Yamamoto T, Tsukahara I, Matsuda A, et al. Monocyte chemotactic protein-1 levels in the vitreous of patients with proliferative vitreoretinopathy. Japanese journal of ophthalmology. 2002;46(2):218-21.

85. He P. Leucocyte/endothelium interactions and microvessel permeability: coupled or uncoupled? Cardiovasc Res. 2010;87(2):281-90. PMCID: PMC2895544.

86. Ozaki H, Seo MS, Ozaki K, Yamada H, Yamada E, Okamoto N, et al. Blockade of vascular endothelial cell growth factor receptor signaling is sufficient to completely prevent retinal neovascularization. The American journal of pathology. 2000;156(2):697-707. PMCID: PMC1850054.

87. Penn JS, Madan A, Caldwell RB, Bartoli M, Caldwell RW, Hartnett ME. Vascular endothelial growth factor in eye disease. Progress in retinal and eye research. 2008;27(4):331-71. PMCID: PMC3682685.

88. Adamis AP, Miller JW, Bernal MT, D'Amico DJ, Folkman J, Yeo TK, et al. Increased vascular endothelial growth factor levels in the vitreous of eyes with proliferative diabetic retinopathy. American journal of ophthalmology. 1994;118(4):445-50.

89. Clermont AC, Aiello LP, Mori F, Aiello LM, Bursell SE. Vascular endothelial growth factor and severity of nonproliferative diabetic retinopathy mediate retinal hemodynamics in vivo: a potential role for vascular endothelial growth factor in the progression of nonproliferative diabetic retinopathy. American journal of ophthalmology. 1997;124(4):433-46.

90. Graef IA, Gastier JM, Francke U, Crabtree GR. Evolutionary relationships among Rel domains indicate functional diversification by recombination. Proceedings of the National Academy of Sciences of the United States of America. 2001;98(10):5740-5. PMCID: PMC33283.

91. Rao A, Luo C, Hogan PG. Transcription factors of the NFAT family: regulation and function. Annual review of immunology. 1997;15:707-47.

92. Cheung CY, Ko BC. NFAT5 in cellular adaptation to hypertonic stress - regulations and functional significance. Journal of molecular signaling. 2013;8(1):5. PMCID: PMC3655004.

93. Graef IA, Chen F, Chen L, Kuo A, Crabtree GR. Signals transduced by Ca(2+)/calcineurin and NFATc3/c4 pattern the developing vasculature. Cell. 2001;105(7):863-75.

94. Chen L, Glover JN, Hogan PG, Rao A, Harrison SC. Structure of the DNA-binding domains from NFAT, Fos and Jun bound specifically to DNA. Nature. 1998;392(6671):42-8.

95. Okamura H, Aramburu J, Garcia-Rodriguez C, Viola JP, Raghavan A, Tahiliani M, et al. Concerted dephosphorylation of the transcription factor NFAT1 induces a conformational switch that regulates transcriptional activity. Molecular cell. 2000;6(3):539-50.

96. Hogan PG, Chen L, Nardone J, Rao A. Transcriptional regulation by calcium, calcineurin, and NFAT. Genes & development. 2003;17(18):2205-32.

97. Shibasaki F, Price ER, Milan D, McKeon F. Role of kinases and the phosphatase calcineurin in the nuclear shuttling of transcription factor NF-AT4. Nature. 1996;382(6589):370-3.

98. Gwack Y, Feske S, Srikanth S, Hogan PG, Rao A. Signalling to transcription: store-operated Ca2+ entry and NFAT activation in lymphocytes. Cell Calcium. 2007;42(2):145-56.

99. Graef IA, Mermelstein PG, Stankunas K, Neilson JR, Deisseroth K, Tsien RW, et al. L-type calcium channels and GSK-3 regulate the activity of NF-ATc4 in hippocampal neurons. Nature. 1999;401(6754):703-8.

100. Boss V, Abbott KL, Wang XF, Pavlath GK, Murphy TJ. The cyclosporin A-sensitive nuclear factor of activated T cells (NFAT) proteins are expressed in vascular smooth muscle cells. Differential localization of NFAT isoforms and induction of NFAT-mediated transcription by phospholipase C-coupled cell surface receptors. The Journal of biological chemistry. 1998;273(31):19664-71.

101. Boss V, Talpade DJ, Murphy TJ. Induction of NFAT-mediated transcription by Gq-coupled receptors in lymphoid and non-lymphoid cells. The Journal of biological chemistry. 1996;271(18):10429-32.

102. Gomez MF, Stevenson AS, Bonev AD, Hill-Eubanks DC, Nelson MT. Opposing actions of inositol 1,4,5-trisphosphate and ryanodine receptors on nuclear factor of activated T-cells regulation in smooth muscle. The Journal of biological chemistry. 2002;277(40):37756-64.

103. Cockerill GW, Bert AG, Ryan GR, Gamble JR, Vadas MA, Cockerill PN. Regulation of granulocyte-macrophage colony-stimulating factor and E-selectin expression in endothelial cells by cyclosporin A and the T-cell transcription factor NFAT. Blood. 1995;86(7):2689-98.

104. Nilsson J, Nilsson LM, Chen YW, Molkentin JD, Erlinge D, Gomez MF. High glucose activates nuclear factor of activated T cells in native vascular smooth muscle. Arteriosclerosis, thrombosis, and vascular biology. 2006;26(4):794-800.

105. D'Angelo G, Struman I, Martial J, Weiner RI. Activation of mitogen-activated protein kinases by vascular endothelial growth factor and basic fibroblast growth factor in capillary endothelial cells is inhibited by the antiangiogenic factor 16-kDa N-terminal fragment of prolactin. Proceedings of the National Academy of Sciences of the United States of America. 1995;92(14):6374-8. PMCID: PMC41520.

106. Dawson NS, Zawieja DC, Wu MH, Granger HJ. Signaling pathways mediating VEGF165-induced calcium transients and membrane depolarization in human endothelial cells. Faseb J. 2006;20(7):991-3.

107. Merat DL, Cheung WY. Calmodulin-dependent protein phosphatase: isolation of subunits and reconstitution to holoenzyme. Methods in enzymology. 1987;139:79-87.

108. Crabtree GR, Olson EN. NFAT signaling: choreographing the social lives of cells. Cell. 2002;109 Suppl:S67-79.

109. Zhu J, Shibasaki F, Price R, Guillemot JC, Yano T, Dotsch V, et al. Intramolecular masking of nuclear import signal on NF-AT4 by casein kinase I and MEKK1. Cell. 1998;93(5):851-61.

110. Liu J, Farmer JD, Jr., Lane WS, Friedman J, Weissman I, Schreiber SL. Calcineurin is a common target of cyclophilin-cyclosporin A and FKBP-FK506 complexes. Cell. 1991;66(4):807-15.

111. Clipstone NA, Fiorentino DF, Crabtree GR. Molecular analysis of the interaction of calcineurin with drug-immunophilin complexes. The Journal of biological chemistry. 1994;269(42):26431-7.

112. Kino T, Hatanaka H, Miyata S, Inamura N, Nishiyama M, Yajima T, et al. FK-506, a novel immunosuppressant isolated from a Streptomyces. II. Immunosuppressive effect of FK-506 in vitro. The Journal of antibiotics. 1987;40(9):1256-65.

113. Flanagan WM, Corthesy B, Bram RJ, Crabtree GR. Nuclear association of a T-cell transcription factor blocked by FK-506 and cyclosporin A. Nature. 1991;352(6338):803-7.

114. Roehrl MH, Kang S, Aramburu J, Wagner G, Rao A, Hogan PG. Selective inhibition of calcineurin-NFAT signaling by blocking protein-protein interaction with small organic molecules. Proceedings of the National Academy of Sciences of the United States of America. 2004;101(20):7554-9. PMCID: PMC419644.

115. Kang S, Li H, Rao A, Hogan PG. Inhibition of the calcineurin-NFAT interaction by small organic molecules reflects binding at an allosteric site. The Journal of biological chemistry. 2005;280(45):37698-706.

116. Macian F, Lopez-Rodriguez C, Rao A. Partners in transcription: NFAT and AP-1. Oncogene. 2001;20(19):2476-89.

117. Wu H, Naya FJ, McKinsey TA, Mercer B, Shelton JM, Chin ER, et al. MEF2 responds to multiple calcium-regulated signals in the control of skeletal muscle fiber type. The EMBO journal. 2000;19(9):1963-73. PMCID: PMC305686.

118. Molkentin JD, Lu JR, Antos CL, Markham B, Richardson J, Robbins J, et al. A calcineurin-dependent transcriptional pathway for cardiac hypertrophy. Cell. 1998;93(2):215-28.

119. Liu Q, Chen Y, Auger-Messier M, Molkentin JD. Interaction between NFkappaB and NFAT coordinates cardiac hypertrophy and pathological remodeling. Circulation research. 2012;110(8):1077-86. PMCID: PMC3341669.

120. Beals CR, Sheridan CM, Turck CW, Gardner P, Crabtree GR. Nuclear export of NF-ATc enhanced by glycogen synthase kinase-3. Science. 1997;275(5308):1930-4.

121. Arron JR, Winslow MM, Polleri A, Chang CP, Wu H, Gao X, et al. NFAT dysregulation by increased dosage of DSCR1 and DYRK1A on chromosome 21. Nature. 2006;441(7093):595-600.

122. Shaw JP, Utz PJ, Durand DB, Toole JJ, Emmel EA, Crabtree GR. Identification of a putative regulator of early T cell activation genes. Science. 1988;241(4862):202-5.

123. Schulz RA, Yutzey KE. Calcineurin signaling and NFAT activation in cardiovascular and skeletal muscle development. Developmental biology. 2004;266(1):1-16.

124. Graef IA, Chen F, Crabtree GR. NFAT signaling in vertebrate development. Current opinion in genetics & development. 2001;11(5):505-12.

125. Macian F. NFAT proteins: key regulators of T-cell development and function. Nature reviews Immunology. 2005;5(6):472-84.

126. Serfling E, Berberich-Siebelt F, Chuvpilo S, Jankevics E, Klein-Hessling S, Twardzik T, et al. The role of NF-AT transcription factors in T cell activation and differentiation. Biochimica et biophysica acta. 2000;1498(1):1-18.

127. Todo S, Fung JJ, Starzl TE, Tzakis A, Demetris AJ, Kormos R, et al. Liver, kidney, and thoracic organ transplantation under FK 506. Annals of surgery. 1990;212(3):295-305; discussion 6-7. PMCID: PMC1358160.

128. Szekeres T, Haushofer A. Clinical pharmacogenetics of immunosuppressive drugs in organ transplantation. Pharmacogenomics. 2005;6(2):163-8.

129. Sloper CM, Powell RJ, Dua HS. Tacrolimus (FK506) in the treatment of posterior uveitis refractory to cyclosporine. Ophthalmology. 1999;106(4):723-8.

130. Hogan AC, McAvoy CE, Dick AD, Lee RW. Long-term efficacy and tolerance of tacrolimus for the treatment of uveitis. Ophthalmology. 2007;114(5):1000-6.

131. Faralli JA, Clark RW, Filla MS, Peters DM. NFATc1 activity regulates the expression of myocilin induced by dexamethasone. Experimental eye research. 2015;130:9-16. PMCID: PMC4276455.

132. Xu Y, Yang L, Yu S, Shu Q, Yang C, Wang J, et al. Spatiotemporal changes in NFATc4 expression of retinal ganglion cells after light-induced damage. Journal of molecular neuroscience : MN. 2014;53(1):69-77.

133. Bretz CA, Savage S, Capozzi M, Penn JS. The role of the NFAT signaling pathway in retinal neovascularization. Investigative ophthalmology & visual science. 2013;54(10):7020-7. PMCID: PMC3809948.

134. Savage SR, Bretz CA, Penn JS. RNA-Seq Reveals a Role for NFAT-Signaling in Human Retinal Microvascular Endothelial Cells Treated with TNFαlpha. PloS one. 2015;10(1):e0116941. PMCID: PMC4305319.

135. Bishara NB, Ding H. Glucose enhances expression of TRPC1 and calcium entry in endothelial cells. Am J Physiol Heart Circ Physiol. 2010;298(1):H171-8.

136. Lawrence MC, Bhatt HS, Easom RA. NFAT regulates insulin gene promoter activity in response to synergistic pathways induced by glucose and glucagon-like peptide-1. Diabetes. 2002;51(3):691-8.

137. Yarilina A, Xu K, Chen J, Ivashkiv LB. TNF activates calcium-nuclear factor of activated T cells (NFAT)c1 signaling pathways in human macrophages. Proceedings of the National Academy of Sciences of the United States of America. 2011;108(4):1573-8. PMCID: PMC3029683.

138. Chen CC, Sun YT, Chen JJ, Chiu KT. TNF-alpha-induced cyclooxygenase-2 expression in human lung epithelial cells: involvement of the phospholipase C-gamma 2, protein kinase C-alpha, tyrosine kinase, NF-kappa B-inducing kinase, and I-kappa B kinase 1/2 pathway. Journal of immunology. 2000;165(5):2719-28.

139. Wang YR, Li ZG, Fu JL, Wang ZH, Wen Y, Liu P. TNFαlpha-induced IP3R1 expression through TNFR1/PC-PLC/PKCalpha and TNFR2 signalling pathways in human mesangial cell. Nephrology, dialysis, transplantation : official publication of the European Dialysis and Transplant Association - European Renal Association. 2011;26(1):75-83.

140. Armesilla AL, Lorenzo E, Gomez del Arco P, Martinez-Martinez S, Alfranca A, Redondo JM. Vascular endothelial growth factor activates nuclear factor of activated T cells in human endothelial cells: a role for tissue factor gene expression. Molecular and cellular biology. 1999;19(3):2032-43. PMCID: PMC83996.

141. Mancini M, Toker A. NFAT proteins: emerging roles in cancer progression. Nat Rev Cancer. 2009;9(11):810-20. PMCID: PMC2866640.

142. Schabbauer G, Schweighofer B, Mechtcheriakova D, Lucerna M, Binder BR, Hofer E. Nuclear factor of activated T cells and early growth response-1 cooperate to mediate tissue factor gene induction by vascular endothelial growth factor in endothelial cells. Thromb Haemost. 2007;97(6):988-97. PMCID: PMC2879320.

143. Ferrara N, Gerber HP, LeCouter J. The biology of VEGF and its receptors. Nature medicine. 2003;9(6):669-76.

144. Johnson EN, Lee YM, Sander TL, Rabkin E, Schoen FJ, Kaushal S, et al. NFATc1 mediates vascular endothelial growth factor-induced proliferation of human pulmonary valve endothelial cells. The Journal of biological chemistry. 2003;278(3):1686-92. PMCID: PMC2813494.

145. Rafiee P, Heidemann J, Ogawa H, Johnson NA, Fisher PJ, Li MS, et al. Cyclosporin A differentially inhibits multiple steps in VEGF induced angiogenesis in human microvascular endothelial cells through altered intracellular signaling. Cell communication and signaling : CCS. 2004;2(1):3. PMCID: PMC441414.

146. Rinne A, Banach K, Blatter LA. Regulation of nuclear factor of activated T cells (NFAT) in vascular endothelial cells. J Mol Cell Cardiol. 2009;47(3):400-10. PMCID: PMC2779755.

147. Schweighofer B, Testori J, Sturtzel C, Sattler S, Mayer H, Wagner O, et al. The VEGF-induced transcriptional response comprises gene clusters at the crossroad of angiogenesis and inflammation. Thromb Haemost. 2009;102(3):544-54. PMCID: PMC2886966.

148. Xue J, Thippegowda PB, Hu G, Bachmaier K, Christman JW, Malik AB, et al. NF-kappaB regulates thrombin-induced ICAM-1 gene expression in cooperation with NFAT by binding to the intronic NF-kappaB site in the ICAM-1 gene. Physiol Genomics. 2009;38(1):42-53. PMCID: PMC2696150.

149. Orr AW, Lee MY, Lemmon JA, Yurdagul A, Jr., Gomez MF, Bortz PD, et al. Molecular mechanisms of collagen isotype-specific modulation of smooth muscle cell phenotype. Arteriosclerosis, thrombosis, and vascular biology. 2009;29(2):225-31. PMCID: PMC2692987.

150. Nilsson LM, Sun ZW, Nilsson J, Nordstrom I, Chen YW, Molkentin JD, et al. Novel blocker of NFAT activation inhibits IL-6 production in human myometrial arteries and reduces vascular smooth muscle cell proliferation. Am J Physiol Cell Physiol. 2007;292(3):C1167-78.

151. Gerlach K, Daniel C, Lehr HA, Nikolaev A, Gerlach T, Atreya R, et al. Transcription Factor NFATc2 Controls the Emergence of Colon Cancer Associated with IL-6-Dependent Colitis. Cancer research. 2012;72(17):4340-50.

152. Boss V, Wang X, Koppelman LF, Xu K, Murphy TJ. Histamine induces nuclear factor of activated T cell-mediated transcription and cyclosporin A-sensitive interleukin-8 mRNA expression in human umbilical vein endothelial cells. Molecular pharmacology. 1998;54(2):264-72.

153. Shiratori M, Tozaki-Saitoh H, Yoshitake M, Tsuda M, Inoue K. P2X7 receptor activation induces CXCL2 production in microglia through NFAT and PKC/MAPK pathways. Journal of neurochemistry. 2010;114(3):810-9.

154. Bochkov VN, Mechtcheriakova D, Lucerna M, Huber J, Malli R, Graier WF, et al. Oxidized phospholipids stimulate tissue factor expression in human endothelial cells via activation of ERK/EGR-1 and Ca(++)/NFAT. Blood. 2002;99(1):199-206.

155. Hesser BA, Liang XH, Camenisch G, Yang S, Lewin DA, Scheller R, et al. Down syndrome critical region protein 1 (DSCR1), a novel VEGF target gene that regulates expression of inflammatory markers on activated endothelial cells. Blood. 2004;104(1):149-58.

156. Minami T, Miura M, Aird WC, Kodama T. Thrombin-induced autoinhibitory factor, Down syndrome critical region-1, attenuates NFAT-dependent vascular cell adhesion molecule-1 expression and inflammation in the endothelium. The Journal of biological chemistry. 2006;281(29):20503-20.

157. Minami T, Horiuchi K, Miura M, Abid MR, Takabe W, Noguchi N, et al. Vascular endothelial growth factor- and thrombin-induced termination factor, Down syndrome critical region-1, attenuates endothelial cell proliferation and angiogenesis. The Journal of biological chemistry. 2004;279(48):50537-54.

158. Barreiro O, Martin P, Gonzalez-Amaro R, Sanchez-Madrid F. Molecular cues guiding inflammatory responses. Cardiovasc Res. 2010;86(2):174-82.

159. Bittner S, Ruck T, Schuhmann MK, Herrmann AM, Moha ou Maati H, Bobak N, et al. Endothelial TWIK-related potassium channel-1 (TREK1) regulates immune-cell trafficking into the CNS. Nature medicine. 2013;19(9):1161-5.

160. Patel KD. Mechanisms of selective leukocyte recruitment from whole blood on cytokine-activated endothelial cells under flow conditions. Journal of immunology. 1999;162(10):6209-16.

161. Zhang Q, Jiang Y, Toutounchian JJ, Soderland C, Yates CR, Steinle JJ. Insulin-like growth factor binding protein-3 inhibits monocyte adhesion to retinal endothelial cells in high glucose conditions. Molecular vision. 2013;19:796-803. PMCID: PMC3626378.

162. Arndt H, Bolanowski MA, Granger DN. Role of interleukin 8 on leucocyte-endothelial cell adhesion in intestinal inflammation. Gut. 1996;38(6):911-5. PMCID: PMC1383201.

163. Kaminuma O, Kitamura F, Kitamura N, Hiroi T, Miyoshi H, Miyawaki A, et al. Differential contribution of NFATc2 and NFATc1 to TNF-alpha gene expression in T cells. Journal of immunology. 2008;180(1):319-26.

164. Lawrence MC, Naziruddin B, Levy MF, Jackson A, McGlynn K. Calcineurin/nuclear factor of activated T cells and MAPK signaling induce TNF-{alpha} gene expression in pancreatic islet endocrine cells. The Journal of biological chemistry. 2011;286(2):1025-36. PMCID: PMC3020709.

165. Zhang J, Patel JM. Role of the CX3CL1-CX3CR1 axis in chronic inflammatory lung diseases. International journal of clinical and experimental medicine. 2010;3(3):233-44. PMCID: PMC2929949.

166. Li JH, Kirkiles-Smith NC, McNiff JM, Pober JS. TRAIL induces apoptosis and inflammatory gene expression in human endothelial cells. Journal of immunology. 2003;171(3):1526-33.

167. Zetterqvist AV, Berglund LM, Blanco F, Garcia-Vaz E, Wigren M, Duner P, et al. Inhibition of nuclear factor of activated T-cells (NFAT) suppresses accelerated atherosclerosis in diabetic mice. PloS one. 2014;8(6):e65020. PMCID: PMC3670844.

168. Cook HL, Patel PJ, Tufail A. Age-related macular degeneration: diagnosis and management. Br Med Bull. 2008;85:127-49.

169. Gaudreault J, Fei D, Rusit J, Suboc P, Shiu V. Preclinical pharmacokinetics of Ranibizumab (rhuFabV2) after a single intravitreal administration. Invest Ophthalmol Vis Sci. 2005;46(2):726-33.

170. Jonas JB, Spandau UH, Rensch F, Von Baltz S, Schlichtenbrede F. Infectious and noninfectious endophthalmitis after intravitreal bevacizumab. J Ocul Pharmacol Ther. 2007;23(3):240-2.

171. Turgut B, Guler M, Akpolat N, Demir T, Celiker U. The impact of tacrolimus on vascular endothelial growth factor in experimental corneal neovascularization. Current eye research. 2011;36(1):34-40.

172. Wang J, Xu X, Elliott MH, Zhu M, Le YZ. Muller cell-derived VEGF is essential for diabetes-induced retinal inflammation and vascular leakage. Diabetes. 2010;59(9):2297-305. PMCID: PMC2927953.

173. Li J, Zhao SZ, Wang PP, Yu SP, Zheng Z, Xu X. Calcium mediates high glucose-induced HIF-1alpha and VEGF expression in cultured rat retinal Muller cells through CaMKII-CREB pathway. Acta pharmacologica Sinica. 2012;33(8):1030-6.

174. Pereira Tde O, da Costa GN, Santiago AR, Ambrosio AF, dos Santos PF. High glucose enhances intracellular Ca2+ responses triggered by purinergic stimulation in retinal neurons and microglia. Brain research. 2010;1316:129-38.

175. Ye X, Ren H, Zhang M, Sun Z, Jiang AC, Xu G. ERK1/2 signaling pathway in the release of VEGF from Muller cells in diabetes. Investigative ophthalmology & visual science. 2012;53(7):3481-9.

176. Mu H, Zhang XM, Liu JJ, Dong L, Feng ZL. Effect of high glucose concentration on VEGF and PEDF expression in cultured retinal Muller cells. Molecular biology reports. 2009;36(8):2147-51.

177. Swiatek-De Lange M, Stampfl A, Hauck SM, Zischka H, Gloeckner CJ, Deeg CA, et al. Membrane-initiated effects of progesterone on calcium dependent signaling and activation of VEGF gene expression in retinal glial cells. Glia. 2007;55(10):1061-73.

178. Kim D, Pertea G, Trapnell C, Pimentel H, Kelley R, Salzberg SL. TopHat2: accurate alignment of transcriptomes in the presence of insertions, deletions and gene fusions. Genome biology. 2013;14(4):R36. PMCID: PMC4053844.

179. Guo Y, Zhao S, Ye F, Sheng Q, Shyr Y. MultiRankSeq: multiperspective approach for RNAseq differential expression analysis and quality control. BioMed research international. 2014;2014:248090. PMCID: PMC4058234.

180. Huang da W, Sherman BT, Lempicki RA. Systematic and integrative analysis of large gene lists using DAVID bioinformatics resources. Nature protocols. 2009;4(1):44-57.

181. Huang da W, Sherman BT, Lempicki RA. Bioinformatics enrichment tools: paths toward the comprehensive functional analysis of large gene lists. Nucleic acids research. 2009;37(1):1-13. PMCID: PMC2615629.

182. Suarez S, McCollum GW, Bretz CA, Yang R, Capozzi ME, Penn JS. Modulation of VEGF-Induced Retinal Vascular Permeability by Peroxisome Proliferator-Activated Receptor-beta/delta. Investigative ophthalmology & visual science. 2014;55(12):8232-40. PMCID: PMC4271638.

183. Penn JS, Henry MM, Tolman BL. Exposure to alternating hypoxia and hyperoxia causes severe proliferative retinopathy in the newborn rat. Pediatric research. 1994;36(6):724-31.

184. Barnett JM, McCollum GW, Penn JS. Role of cytosolic phospholipase A(2) in retinal neovascularization. Investigative ophthalmology & visual science. 2010;51(2):1136-42. PMCID: PMC2868444.

185. Yanni SE, Barnett JM, Clark ML, Penn JS. The role of PGE2 receptor EP4 in pathologic ocular angiogenesis. Investigative ophthalmology & visual science. 2009;50(11):5479-86. PMCID: PMC4071769.

186. Penn JS, Rajaratnam VS, Collier RJ, Clark AF. The effect of an angiostatic steroid on neovascularization in a rat model of retinopathy of prematurity. Investigative ophthalmology & visual science. 2001;42(1):283-90.